DTIC FILE COPY

AD-A222 795

DISTRIBUTION STATEMENT A
Approved for public release;
Distribution Unlimited

DTIC
ELECTE
JUN 21 1990
S D
E

DEPARTMENT OF THE AIR FORCE
AIR UNIVERSITY

AIR FORCE INSTITUTE OF TECHNOLOGY

Wright-Patterson Air Force Base, Ohio

90 06 20 063

AFIT/GAE/ENY/89D-30

ROBUSTNESS EVALUATION OF H2 AND H∞ CONTROL THEORY AS APPLIED TO A TRANSPORT AIRCRAFT

THESIS

Randy L. Robinson
Captain, USAF

AFIT/GAE/ENY/89D-30

DTIC
ELECTE
JUN 21 1990
S D
E

Approved for public release; distribution unlimited

AFIT/GAE/ENY/89D-30

ROBUSTNESS EVALUATION OF H2 AND H∞ CONTROL THEORY AS APPLIED TO A TRANSPORT AIRCRAFT

THESIS

Presented to the Faculty of the School of Engineering
of the Air Force Institute of Technology
Air University
In Partial Fulfillment of the
Requirements for the Degree of
Master of Science in Aeronautical Engineering

Randy L. Robinson, M.S.
Captain, USAF

March 1990

Approved for public release; distribution unlimited

Acknowledgements

I'd like to thank my advisor, Captain D. Brett Ridgely, for his help and guidance in doing this thesis. Without the special seminar class on H2 and H∞ control theory and other helpful advise, this thesis would not have been possible. I'd also like to thank Captain Curtis Mracek and Dr Robert Calico for their patience while I completed this work. Also, I wish to thank Captain Randy Riddle for the the many informative discussions concerning our related work. Not to be forgotten are my sponsors in the Control Analysis Group at the Flight Dynamics Laboratory. I wish to extend my appreciation to them for their help. Last and certainly not least, I'd like to thank my wife Melanie for her encouragement and support while completing this thesis.

Accession For
NTIS GRA&I
DTIC TAB
Unannounced
Justification
By
Distribution/
Availability Codes
Dist | Avail and/or Special
A-1

DTIC COPY INSPECTED

Table of Contents

List of Figures

List of Tables

Abstract

The purpose of this study was to evaluate the performance and stability robustness of a lateral autopilot designed for a transport aircraft using H2 and H∞ control theory. The intent was to design a controller that met performance and robustness specifications over a range of flight conditions. First, a control structure to be used in designing the autopilot was developed. Once this was accomplished, it was formulated into the small gain problem. Controllers were then developed using H2 and H∞ control theory. The final task involved evaluating the controllers developed in a closed loop simulation.

ROBUSTNESS EVALUATION OF H2 AND Hω CONTROL THEORY AS APPLIED TO A TRANSPORT AIRCRAFT

I. Introduction

1.1 Background

In June of 1989, the results of a design challenge were presented at the American Control Conference(1:585-620). The focus of the challenge was to design a lateral autopilot for a transport aircraft. Several papers were presented utilizing different design techniques. These included classical control, a model-matching approach, LQG/LTR, and Hω control theory.

The state space equations for fourteen flight conditions were provided. In addition, a list of design requirements were given.

One objective of the design challenge was to design a controller that would satisfy the design requirements for all fourteen flight conditions without the need for gain scheduling. Many of the autopilots in aircraft and missiles today were designed using single-input single-output (SISO) design techniques at specific flight conditions. This requires a large number of gains for the flight envelope. Design techniques such as regulator theory that handle multiple-input multiple-output (MIMO) systems lack the

robustness to handle parameter variations and sensor noise.

The H2 control theory and the more recent H∞ control theory are designed to be robust in the face of design uncertainties. H2 control theory handles structured uncertainties such as parameter variations effectively. The H∞ control theory is very effective against unstructured uncertainties which include unmodelled dynamics and sensor noise.

The above features of H2 and H∞ control theories yield controllers that are robust. This allows controllers to be designed that reduce or eliminate the need for gain scheduling over a given range of flight conditions.

1.2 Purpose

The purpose of this thesis is to use H2 and H∞ control theory to design a lateral autopilot for a transport aircraft using the data from the design challenge at the 1989 American Control Conference. The state space representations for the fourteen flight conditions will be used in an attempt to develop a controller that will satisfy the given design requirements. The problem will be formulated into the small gain or standard problem as defined in Doyle et. al. (2:831). A detailed analysis of the problem setup and formulation will be covered.

The controllers developed will be tested to see if they are robust enough to handle the parameter variations of the

fourteen flight conditions. The H2 and H∞ controllers will be compared.

1.3 Overview

In Chapter 2, aspects of multivariable control theory are discussed as well as H2 and H∞ theory. Chapter 3 covers the problem description and characterization of the open-loop data. The formulation of the standard problem is contained in Chapter 4. In Chapter 5, the procedure and analysis techniques required to develop the H2 and H∞ controllers are discussed. In Chapter 6, the results obtained from running the controllers in a closed loop simulation are presented. Chapter 7 contains a summary and conclusions followed by recommendations for further study.

The software package PC-MATLAB was used for this thesis. This included the basic program along with the Control System Toolbox.

II. H2 and H∞ Control Theory

2.1 Singular Values and Loop Shaping

Before H2 and H∞ control theory are covered, it is important to discuss a few fundamentals of multivariable control design. One of these is singular values.

Singular values of a matrix A are the non-negative square roots of the eigenvalues of A^*A as given by

$$\sigma_i(A) = [\lambda_i(A^*A)]^{1/2} \qquad (2.1)$$

where $A \in C^{m \times n}$ and A^* is the complex conjugate transpose of the matrix A. The largest singular value, σ_{max}, is denoted $\bar{\sigma}$. The smallest singular value, σ_{min}, is denoted $\underline{\sigma}$.

For a transfer function $G(j\omega)$, $\bar{\sigma}[G]$ and $\underline{\sigma}[G]$ can be computed. These two quantities are frequency dependent and give a measure of the size of the transfer function matrix. In SISO systems, the Bode magnitude plot shows the magnitude of a transfer function as a function of frequency. The singular value plot is the MIMO analog of the Bode magnitude plot (4:4-11).

The idea of loop shaping is also important. Figure 2.1 shows a typical MIMO system. The concepts of a good loop shape carry over to the MIMO system. In SISO systems, to have good command following and disturbance rejection, the loop gain must be large at low frequency. A small loop gain is required for attenuation of modelling errors at high

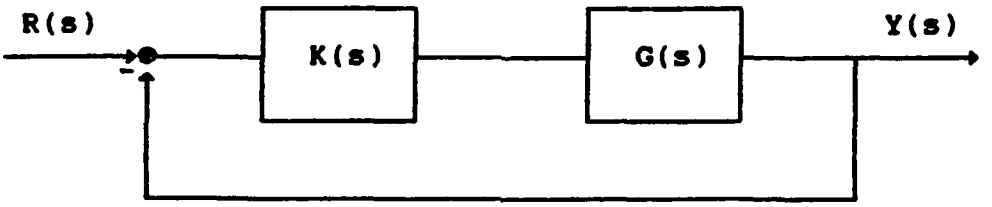

Fig. 2.1 MIMO System Block Diagram

frequency. To avoid sensor noise, which is a high frequency phenomenon, the loop gain must be small. Therefore, a good loop shape is as shown in Figure 2.2. A detailed discussion of loop shaping is covered by Ridgely and Banda (4:4-1:4-10).

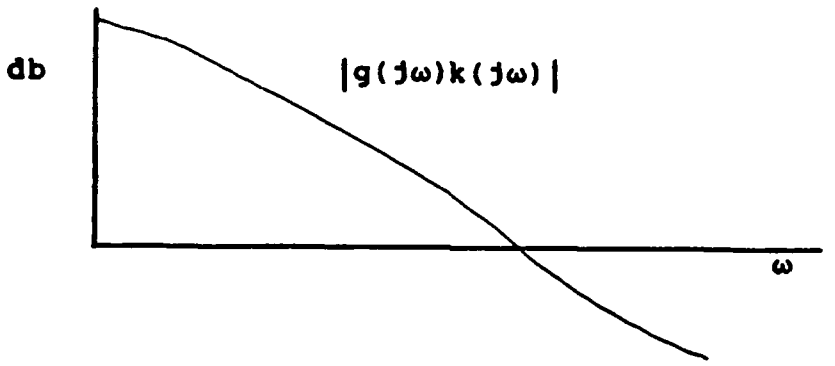

Fig. 2.2 Good Loop Shape (SISO)

As mentioned, the singular value plot is the equivalent of the Bode magnitude plot. The $\bar{\sigma}[GK]$ and $\underline{\sigma}[GK]$ give information concerning the loop gain and bandwidth of the system. The loop shape of Figure 2.2 for the SISO system equates to Figure 2.3 for the MIMO system. At low frequency, $\underline{\sigma}[GK]$ must be large to ensure performance and $\bar{\sigma}[GK]$ must be

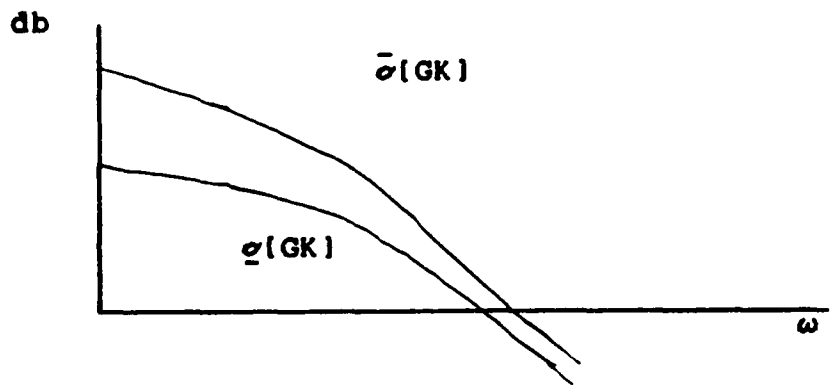

Fig. 2.3 Good Loop Shape (MIMO)

small at high frequency to give desirable robustness.

These ideas will be used in designing the controller for the lateral autopilot.

2.2 H2 and H∞ Control Theory

The standard problem, as discussed in Francis (3:Chap 3), is shown by Figure 2.4. All signals can be vector

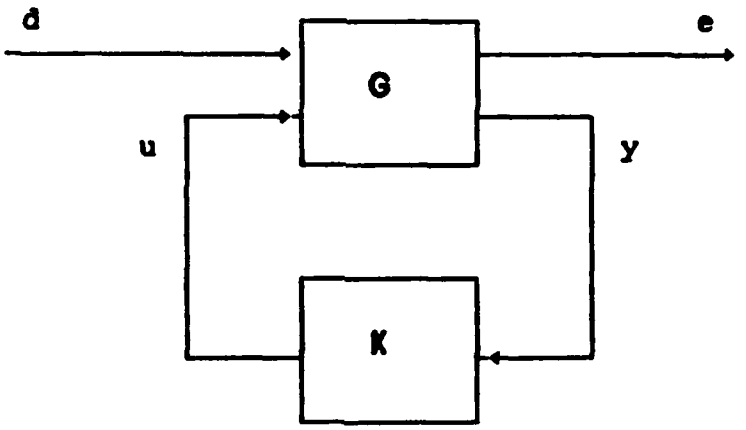

Fig. 2.4 Standard Problem Block Diagram

quantities. The exogenous inputs, d, to the plant, G, are tracking signals or disturbances. The regulated output of the system is denoted e. The measured output fed back through the controller, K, is y. The control inputs to the system are denoted u. The plant can be partitioned as

$$G = \begin{bmatrix} G11 & G12 \\ G21 & G22 \end{bmatrix} \tag{2.2}$$

which yields the equations

$$e = G11d + G12u \tag{2.3}$$

$$y = G21d + G22u \tag{2.4}$$

$$u = Ky \tag{2.5}$$

The equivalent state space form is

$$\dot{x} = Ax + B1d + B2u \tag{2.6}$$

$$e = C1x + D11d + D12u \tag{2.7}$$

$$y = C2x + D21d + D22u \tag{2.8}$$

Given the above, the standard problem is to find a

real-rational proper K to minimize either the H2 or the H∞ norm of T_{ed}, under the constraint that K stabilizes G. T_{ed} is the transfer function from e to d in Figure 2.4. K stabilizes G if the states of G and K tend to zero for every initial condition and can be thought of as a simple definition of internal stability. The H2 norm is given by (2:831)

$$\|G\|_2 = \left(\frac{1}{2\pi}\int_{-\infty}^{+\infty} tr[G(j\omega)^* G(j\omega))]d\omega\right)^{1/2} \qquad (2.9)$$

The H∞ norm is given by (2:831)

$$\|G\|_\infty = \sup_\omega \sigma_{max}[G(jw)] \qquad (2.10)$$

The standard problem will be solved using the Doyle/Glover parameterization(2). In the case of H2 optimization, the following is required:

1) D11 = 0 and D22 = 0

2) $D12^T * D12 = I$ and $D21 * D21^T = I$

3) (A,B1) stabilizable and (C1,A) detectable

4) (A,B2) stabilizable and (C2,A) detectable

To use the Doyle/Glover parameterization, the plant input and output must be scaled as shown in Figure 2.5.

The following equation development is taken from a summary of the Doyle/Glover parameterization(2) by Ridgely(5:1-8). The resulting equations from the scaling are

$$u = S_u^{-1}\,\tilde{u} \qquad (2.11)$$

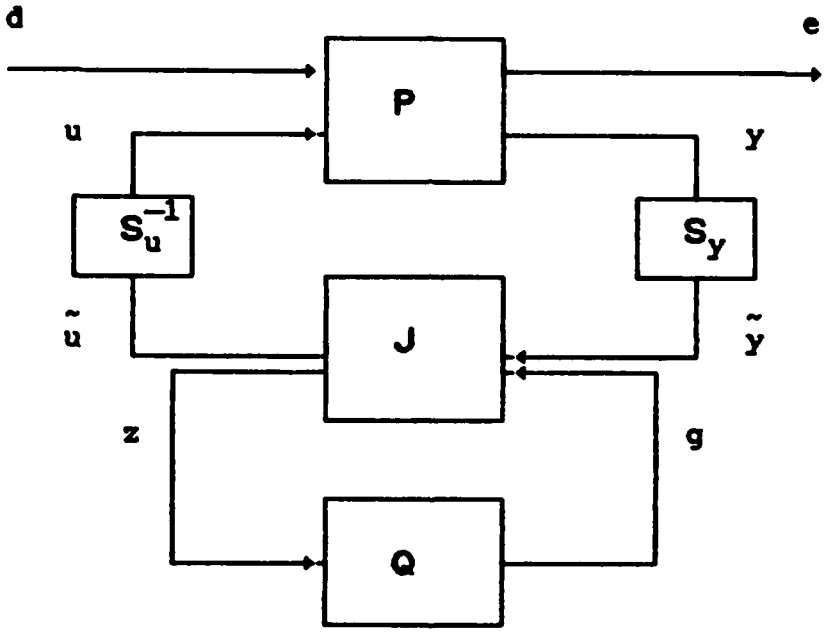

Fig. 2.5 Scaled Standard Block Diagram for H2 Optimization

$$\tilde{y} = S_y\, y \tag{2.12}$$

The scale factors are found using a Cholesky decomposition of the right hand side of the equations

$$S_u{}^T S_u = D_{12}{}^T D_{12} \tag{2.13}$$

$$S_y{}^{-1}\,(S_y{}^{-1})^T = D_{21} D_{21}{}^T \tag{2.14}$$

The plant equations now become

$$\dot{x} = Ax + B_1 d + \tilde{B}_2 \tilde{u} \tag{2.15}$$

$$e = C_1 x + \tilde{D}_{12} \tilde{u} \tag{2.16}$$

$$\tilde{y} = \tilde{C}_2 x + \tilde{D}_{21} d \tag{2.17}$$

where

$$\tilde{B}_2 = B_2 S_u{}^{-1} \tag{2.18}$$

$$\tilde{C}_2 = S_y C_2 \tag{2.19}$$

$$\tilde{D}_{12} = D_{22} S_u{}^{-1} \tag{2.20}$$

$$\tilde{D}_{21} = S_y D_{21} \tag{2.21}$$

The family of all H2 compensators is given by

$$T_{ed} = F_\ell(P,K) \tag{2.22}$$

$$K = F_\ell(J,Q) \tag{2.23}$$

$$J = C_j (sI - A_j)^{-1} B_j + D_j \tag{2.24}$$

$$A_j = A - K_f \tilde{C}_2 - \tilde{B}_2 K_c \tag{2.25}$$

$$B_j = [K_f \quad K_{f1}] \tag{2.26}$$

$$C_j = \begin{bmatrix} -K_c \\ K_{c1} \end{bmatrix} \tag{2.27}$$

$$D_j = \begin{bmatrix} 0 & I \\ I & 0 \end{bmatrix} \tag{2.28}$$

$$K_c = \tilde{B}_2^T X_2 + \tilde{D}_{12}^T C_1 \tag{2.29}$$

$$K_{c1} = -(\tilde{D}_{21} B_1^T X_2 + \tilde{C}_2) \tag{2.30}$$

$$K_f = Y_2 \tilde{C}_2^T + B_1 \tilde{D}_{21}^T \tag{2.31}$$

$$K_{f1} = Y_2 C_1^T \tilde{D}_{12} + \tilde{B}_2 \tag{2.32}$$

where X_2 and Y_2 are the solutions to the Ricatti equations

$$(A-\tilde{B}_2\tilde{D}_{12}^T C_1)^T X_2 + X_2(A-\tilde{B}_2\tilde{D}_{12}^T C_1) - X_2\tilde{B}_2\tilde{B}_2^T X_2 + \hat{C}_1^T\hat{C}_1 = 0 \tag{2.33}$$

$$(A-\tilde{B}_1\tilde{D}_{21}^T C_2)Y_2 + Y_2(A-\tilde{B}_1\tilde{D}_{21}^T C_2)^T - Y_2\tilde{C}_2^T\tilde{C}_2 Y_2 + \hat{B}_1\hat{B}_1^T = 0 \tag{2.34}$$

where

$$\hat{C}_1 = (I - \tilde{D}_{12}\tilde{D}_{12}^T)C_1 \tag{2.35}$$

$$\hat{B}_1 = B_1(I - \tilde{D}_{21}^T\tilde{D}_{21}) \tag{2.36}$$

and Q is any stable, strictly proper, transfer function such that

$$\|Q\|_2^2 \leq \gamma^2 - \gamma_{opt}^2 \tag{2.37}$$

γ_{opt} is the optimal 2 norm solution, which is obtained when Q is chosen equal to zero. A suboptimal solution is obtained for Q not equal to zero.

In the Doyle/Glover parameterization for H∞

optimization, the following conditions must be satisfied:

1) D11 = 0 and D22 = 0

2) $D12^T * D12 = I$ and $D21 * D21^T = I$

3) (A,B1) controllable and (C1,A) observable

4) (A,B2) stabilizable and (C2,A) detectable

In addition, the parameterization for H∞ optimization also requires scaling on d and e as shown in Figure 2.6. The scale factors are given by

$$\tilde{d} = \sqrt{\gamma}\, d \tag{2.38}$$

$$e = \sqrt{\gamma}\, \tilde{e} \tag{2.39}$$

$$\tilde{y} = S_y\, y \tag{2.40}$$

$$u = S_u^{-1}\, \tilde{u} \tag{2.41}$$

where again S_u and S_y are found using a Cholesky decomposition of the right hand side of

$$S_u^T S_u = \frac{1}{\gamma} D_{12}^T D_{12} \tag{2.42}$$

and

$$S_y^{-1}(S_y^{-1})^T = \frac{1}{\gamma} D_{21} D_{21}^T \tag{2.43}$$

The plant equations become

$$\dot{x} = Ax + \tilde{B}_1 d + \tilde{B}_2 \tilde{u} \tag{2.44}$$

$$e = \tilde{C}_1 x + \tilde{D}_{12} \tilde{u} \tag{2.45}$$

$$y = \tilde{C}_2 x + \tilde{D}_{21} \tilde{d} \tag{2.46}$$

where

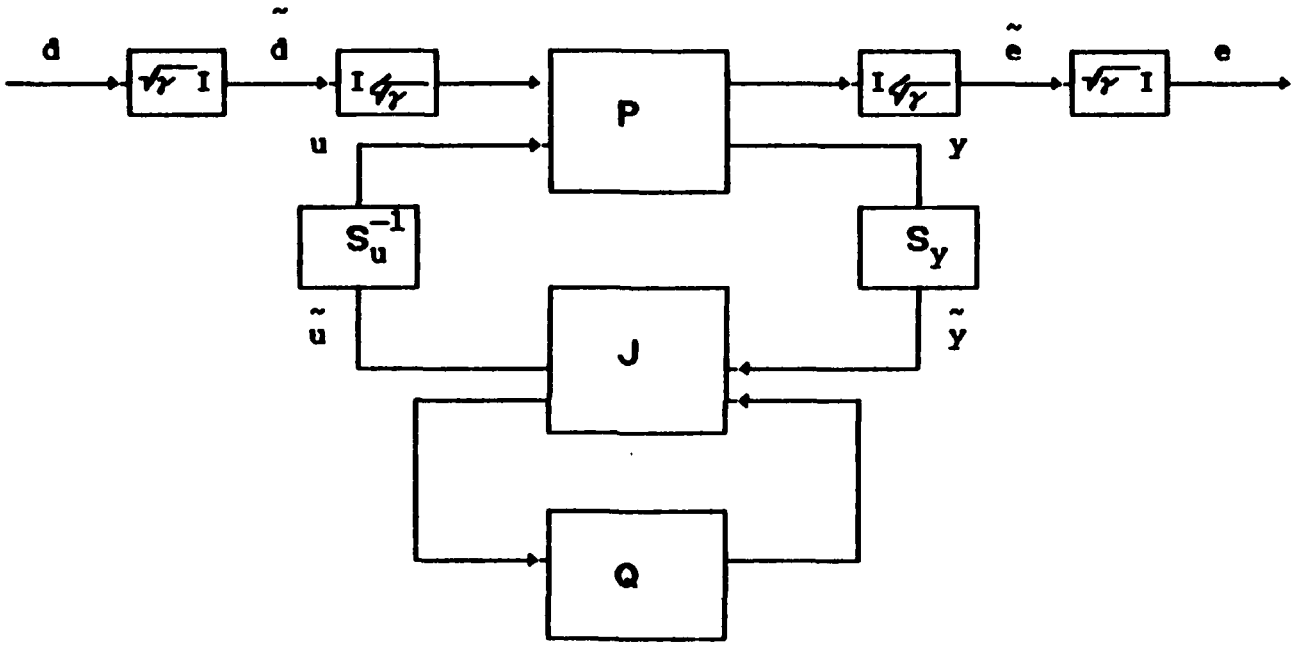

Fig. 2.6 Scaled Standard Block Diagram for H∞ Optimization

$$\tilde{B}_1 = \sqrt{1/\gamma}\, B_1 \tag{2.47}$$

$$\tilde{B}_2 = B_2 S_u^{-1} \tag{2.48}$$

$$\tilde{C}_1 = \sqrt{1/\gamma}\, C_1 \tag{2.49}$$

$$\tilde{C}_2 = \tilde{S}_y C_2 \tag{2.50}$$

$$\tilde{D}_{12} = \sqrt{1/\gamma}\, D_{12} S_u^{-1} \tag{2.51}$$

$$\tilde{D}_{21} = \sqrt{1/\gamma}\, S_y D_{21} \tag{2.52}$$

The family of all stabilizing compensators such that

$$\|T_{\tilde{e}\tilde{d}}\|_\infty \leq 1 \tag{2.53}$$

is given by

$$T_{\tilde{e}\tilde{d}} = F_\ell(P,K) \tag{2.54}$$

$$K = F_\ell(J,Q) \tag{2.55}$$

$$J = C_j(sI - A_j)^{-1}B_j + D_j \tag{2.56}$$

$$A_j = A - K_f\tilde{C}_2 - \tilde{B}_2K_2 + Y_\infty\tilde{C}_1^T(\tilde{C}_1 - D_{12}K_c) \tag{2.57}$$

$$B_j = [K_f \quad K_{f1}] \tag{2.58}$$

$$C_j = \begin{bmatrix} -K_c \\ K_{c1} \end{bmatrix} \tag{2.59}$$

$$D_j = \begin{bmatrix} 0 & I \\ I & 0 \end{bmatrix} \tag{2.60}$$

$$K_c = (\tilde{B}_2^T X_\infty + \tilde{D}_{12}^T\tilde{C}_1)(I - Y_\infty X_\infty)^{-1} \tag{2.61}$$

$$K_{c1} = -(\tilde{D}_{21}B_1^T X_\infty + \tilde{C}_2)(I - Y_\infty X_\infty)^{-1} \tag{2.62}$$

$$K_f = Y_\infty\tilde{C}_2^T + B_1\tilde{D}_{21}^T \tag{2.63}$$

$$K_{f1} = Y_\infty C_1^T \tilde{D}_{12} + \tilde{B}_2 \tag{2.64}$$

where X_∞ and Y_∞ are solutions of the algebraic Ricatti equations

$$(A-\tilde{B}_2\tilde{D}_{12}^T C_1)^T X_\infty + X_\infty (A-\tilde{B}_2\tilde{D}_{12}^T C_1) - X_\infty \tilde{B}_2\tilde{B}_2^T X_\infty + \hat{C}_1^T\hat{C}_1 = 0 \tag{2.65}$$

and

$$(A-\tilde{B}_1\tilde{D}_{21}^T C_2) Y_\infty + Y_\infty (A-\tilde{B}_1\tilde{D}_{21}^T C_2)^T - Y_\infty \tilde{C}_2^T\tilde{C}_2 Y_\infty + \hat{B}_1\hat{B}_1^T = 0 \tag{2.66}$$

where

$$\hat{C}_1 = (I - \tilde{D}_{12}\tilde{D}_{12}^T)C_1 \tag{2.67}$$

$$\hat{B}_1 = B_1(I - \tilde{D}_{21}^T\tilde{D}_{21}) \tag{2.68}$$

and Q is any stable, proper transfer function such that

$$\|Q\|_\infty < 1 \tag{2.69}$$

These equations are solved by what is known as gamma iteration. The H∞ optimal solution is not unique. To be valid, X_∞ and Y_∞ must have solutions that are elements of the Ricatti domain and positive semidefinite. The reasons for this are covered in the Doyle/Glover development(2:833). The product $Y_\infty X_\infty$ must also have a spectral radius less than one, where the spectral radius of a matrix A is given by

$$\rho(A) = \max_i |\lambda_i(A)| \tag{2.70}$$

The above equations were solved using PC-MATLAB routines.

III. Problem Description

3.1 General Description

The aim of the design was to develop a lateral autopilot that met the design requirements. The autopilot had to meet performance, robustness, control activity, and gust response requirements over a range of fourteen flight conditions.

The autopilot is to operate in two modes: heading hold mode, and localizer capture and track mode. In the heading control mode, the autopilot is to track a pilot-commanded heading angle. In the localizer capture and track mode, it must drive the cross track error to zero and align the aircraft velocity vector with the runway heading. Figure 3.1 shows a diagram of the approach geometry.

In this thesis, only the localizer capture and track autopilot will be designed. The localizer capture and track autopilot is more difficult to design since it must track two signals.

3.2 Plant Description

The state space representation for the fourteen flight conditions was provided. These are in the form

$$\dot{x} = Ax + Bu \tag{3.1}$$

$$y = Cx + Du \tag{3.2}$$

The state space representations are for the lateral dynamics of the aircraft. The states are

$$\dot{x} = [\ \beta\ p\ \phi\ r\ \psi\ y\ ]^T \tag{3.3}$$

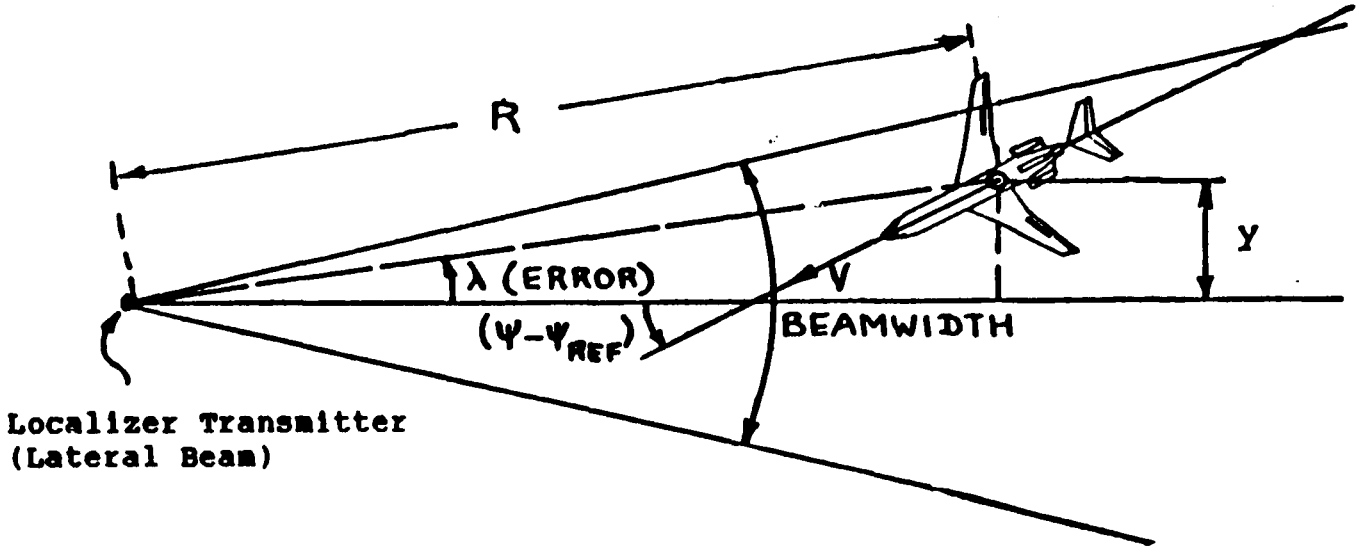

Fig. 3.1 Approach Geometry

where

β - side slip angle (deg)

p - roll rate (deg/sec)

ϕ - roll angle (deg)

r - yaw rate (deg/sec)

ψ - heading angle (deg)

y - cross track error (ft)

The outputs are

$$y = [\ \dot{\beta}\quad n_y\quad \dot{r}\quad \psi_{gt}\ ]^T \tag{3.4}$$

where

$\dot{\beta}$ - side slip angular rate (deg/sec)

n_y - side acceleration (g's)

$\dot{r}$ - yaw acceleration (deg/sec^2)

ψ_{gt} - ground track heading angle

The control inputs are

$$u = [\ \delta a\quad \delta r\ ]^T \tag{3.5}$$

where

δa = aileron deflection angle (deg)

δr = rudder deflection angle (deg)

The disturbance input was

βg = beta gust (deg)

The numbering for the flight conditions is not sequential since they were taken from a larger data base of linearized flight conditions. The flight conditions provided are 001, 004, 017, 020, 033, 036, 049, 052, 065, 068, 081, 084, 097, and 100. The state space representations for these are in Appendix A.

3.3 Design Requirements

The design requirements include specifications on performance, robustness, control activity, and gust response.

The performance specifications required zero time domain overshoot and zero steady state tracking error. The bank angle could not exceed 30 degrees. The lateral acceleration during aircraft maneuvers was to remain below 0.05 g's. The bandwidth requirements are just stated as to maximize response bandwidths while remaining within limitations on overshoot and control surface activity.

The robustness requirements are stated in terms of the eigenvalues or pole placement. A minimum damping ratio of 0.4 is required for all modes. The minimum damping ratio on the dominant mode is required to be 0.6. Stability margins of 4 db and 40 degrees simultaneously are required for all inputs and outputs.

The control surface activity for the ailerons and rudder must remain within $\pm$ 15 degrees. The control surface rates must remain below $\pm$ 30 deg/sec.

There were additional requirements placed on the response to a 1 ft/sec RMS Dryden gust. The heading and sideslip angular positions are to remain below 0.5 degrees. The angular rates for these two states must remain below 0.5 deg/sec. The control surface activity for the gust response is to be less than 2 degrees in position and 5 deg/sec in rate for the ailerons and rudder.

3.4 Open Loop Plant Description

The flight conditions given are for various phases of the approach, including different aircraft configurations. The data can be broken down into two groups based on velocity. Flight Conditions 001, 017, 033, 049, 065, 081, and 097 are for a slow approach. Flight Conditions 004, 020, 036, 052, 068, 084, and 100 are for a fast approach. Table I list the aircraft parameters.

The typical lateral dynamics include the spiral, roll, and Dutch roll modes. The spiral and roll modes have real roots and the Dutch roll is a complex conjugate pair. The roots for the three modes for Flight Condition 084 are

spiral: $\lambda_1 = -0.0107$ ($\tau_1 = 93.5$ sec)
roll: $\lambda_2 = -3.4824$ ($\tau_2 = 0.287$ sec)
Dutch roll: $\lambda_{3,4} = -0.1278 \pm 1.5028$

The Dutch roll has a natural frequency, wn, of 1.508 rad/sec and is very lightly damped with a damping ratio of 0.085. All flight conditions, with the exceptions of 065 and 097, have stable roots. The characteristics modes are given in Table II.

The heading and cross track error states were added for the localizer capture and track mode. These two states introduced two poles at the origin. The heading angle is given by

$$\psi = \frac{1}{s} r \qquad (3.6)$$

and the cross track by

Table I Flight Condition Parameters

Flight Cond #	Flap Setting Deg	Mach	Alpha Deg	Airspeed Ft/Sec	Dynamic Press Lbs/FT^2	Indicated Airspeed Knots	Gear 0-up 1-down
001	1	0.209	11.25	232.9	65.2	138	0
004	1	0.318	3.74	354.4	153.1	210	0
017	5	0.197	10.79	219.4	57.8	130	0
020	5	0.318	2.42	354.4	153.1	210	0
033	10	0.189	11.03	211.0	53.4	125	0
036	10	0.318	1.78	354.4	153.1	210	0
049	15	0.184	10.35	205.9	50.8	122	0
052	15	0.298	1.29	329.1	131.6	195	0
065	25	0.178	9.77	199.2	47.5	118	0
068	25	0.287	-0.07	320.7	124.8	190	0
081	30	0.175	7.99	195.8	45.9	116	1
084	30	0.280	-2.02	312.2	118.2	185	1
097	40	0.171	6.33	190.7	43.5	113	1
100	40	0.257	-2.48	286.9	99.5	170	1

Table II Characteristic Modes

Flight Cond #	Dutch Roll Mode		Spiral Mode(s)	Roll Mode(s)
	ω_n - rad/s	ζ		
001	1.307	0.181	120.5	0.532
004	1.732	0.126	61.3	0.321
017	1.245	0.169	192.3	0.538
020	1.712	0.113	70.9	0.297
033	1.182	0.191	166.7	0.496
036	1.693	0.115	112.4	0.261
049	1.150	0.184	137.0	0.453
052	1.596	0.115	100.0	0.261
065*	1.172	0.164	(212.8)	0.487
068	1.603	0.096	1099.8	0.282
081	1.145	0.138	185.2	0.481
084	1.508	0.085	93.5	0.287
097*	1.154	0.107	(476.2)	0.474
100	1.441	0.054	93.5	0.315

* Unstable mode

$$y = \frac{1}{s} V\sin(\psi + \beta - \phi\sin\alpha) \qquad (3.7)$$

where

V - aircraft velocity (ft/sec)
α - angle of attack (deg)

An explanation of the localizer capture and track mode is given in Roskam (6:1198-1207).

To evaluate the open-loop frequency domain characteristics, the open-loop singular values were plotted. The singular value plot for flight conditions 001 and 004 are shown in Figures 3.2 - 3.3. The general trends are that the plant has widely separated singular values at low frequency. The plant doesn't exhibit integral action. The $\underline{\sigma}$ has very low gain at low frequency. This will need to be corrected for good performance and steady state tracking accuracies. The plant, as given, is proper and doesn't roll off at high frequency. This will need to be changed for robustness, and to be able to use H2 and H∞ optimization.

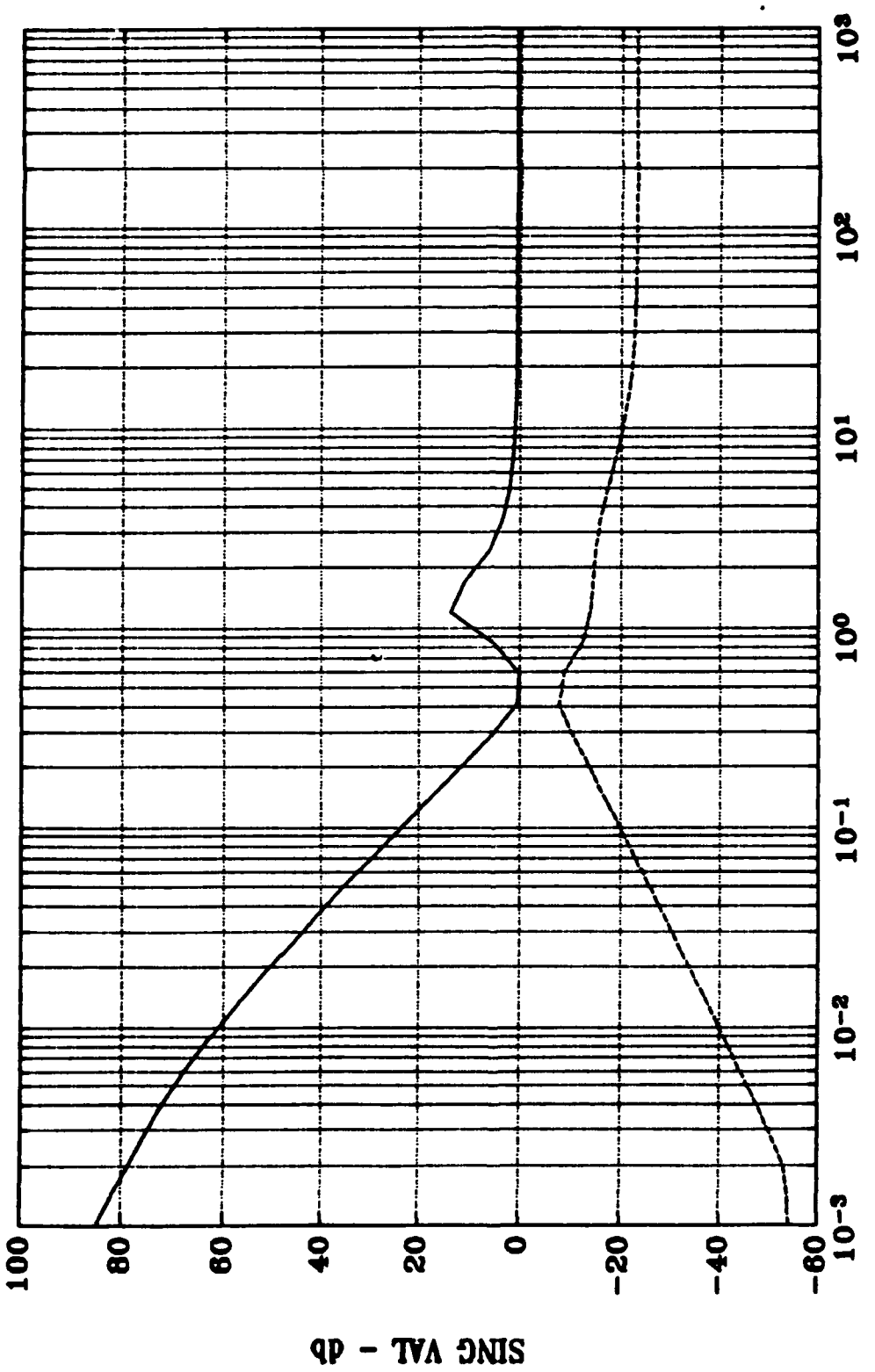

Fig. 3.2 Flight Condition 001 Open Loop Singular Value Plot

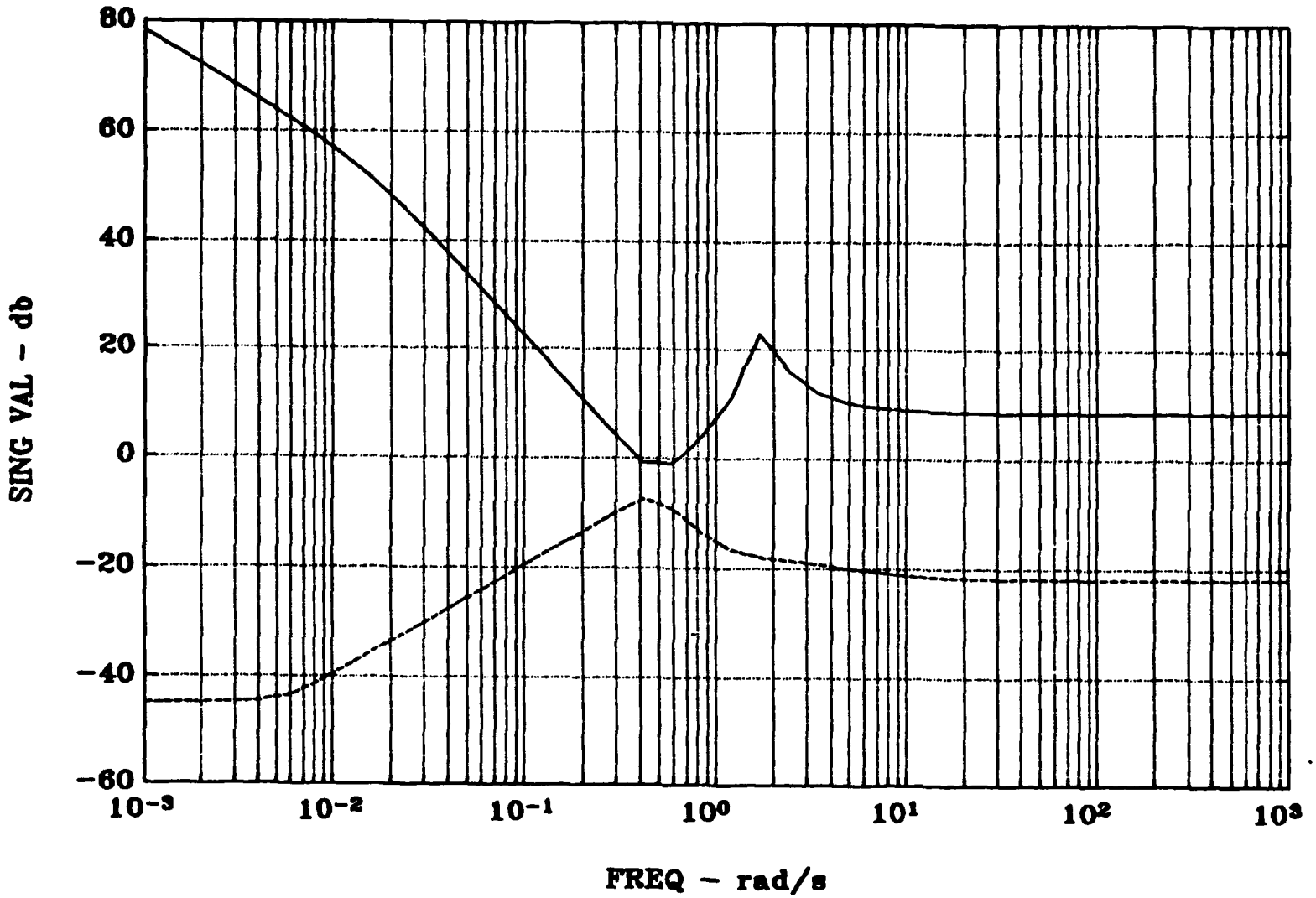

Fig. 3.3 Flight Condition 004 Open Loop Singular Value Plot

IV. Problem Synthesis

4.1 Modification of the Plant

The state space description of the plant as given is not strictly proper. One of the requirements of H2 and H∞ theory is that the D22 matrix of equation (2.8) be zero. This means that the plant can have no feedforward elements. In order to satisfy this requirement, actuator dynamics were augmented into the plant. The actuators for the aileron and rudder were represented by

$$\delta a(s) = \delta r(s) = \frac{15}{s+15} \tag{4.1}$$

The state space representation of the actuators is given by

$$\dot{\delta} = A\delta + B\delta_c \tag{4.2}$$

and

$$y = C\delta \tag{4.3}$$

where

$$A = \begin{bmatrix} -15 & 0 \\ 0 & -15 \end{bmatrix} \quad B = \begin{bmatrix} 1 & 0 \\ 0 & 1 \end{bmatrix} \quad C = \begin{bmatrix} 15 & 0 \\ 0 & 15 \end{bmatrix}$$

The actuator dynamics were augmented into the plant by cascading the two systems together as shown in Figure 4.1.

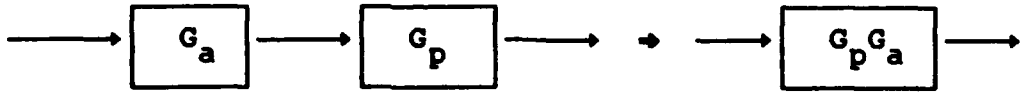

Fig. 4.1 Cascaded Systems

This yields a new state space representation with eight states. The singular values were replotted for flight conditions 001 and 004, and as expected for a strictly proper

system, the singular values rolled off at 20 db/decade at high frequency as shown in Figures 4.2 and 4.3.

In addition to augmenting the actuator dynamics, the cross track error was scaled by 100 to normalize outputs.

Now the system could be formulated into the standard problem shown in Figure 2.4.

4.2 Small Gain Problem Formulation

In order to formulate the control design into the standard problem, a suitable block diagram was needed. The block diagram in Figure 4.4 was used.

The system has exogenous inputs, d, of tracking signals, gust input, and sensor noise. These are labeled d1, d2, and d3 respectively. The tracking signals for the localizer capture and hold autopilot are the heading angle and cross track error. The only disturbance is the gust input.

The outputs of the system as given were

$$v = [\ \dot{\beta}\ \ n_y\ \ \dot{r}\ \ \psi_{gt}\ ]^T \tag{4.4}$$

These were modified to

$$v = [\ \dot{\beta}\ \ n_y\ \ \psi_{gt}\ \ y\ ]^T \tag{4.5}$$

The output of the cross track error was added since the error signal for this state is desired. The yaw acceleration was deleted since it was not needed.

The d1 vector was made the same as v to keep the number of inputs and outputs equal. This was done in order to formulate the problem with a tracking error signal of r-v as is done in the tracking problem setup in Francis (3:3.4-3.5).

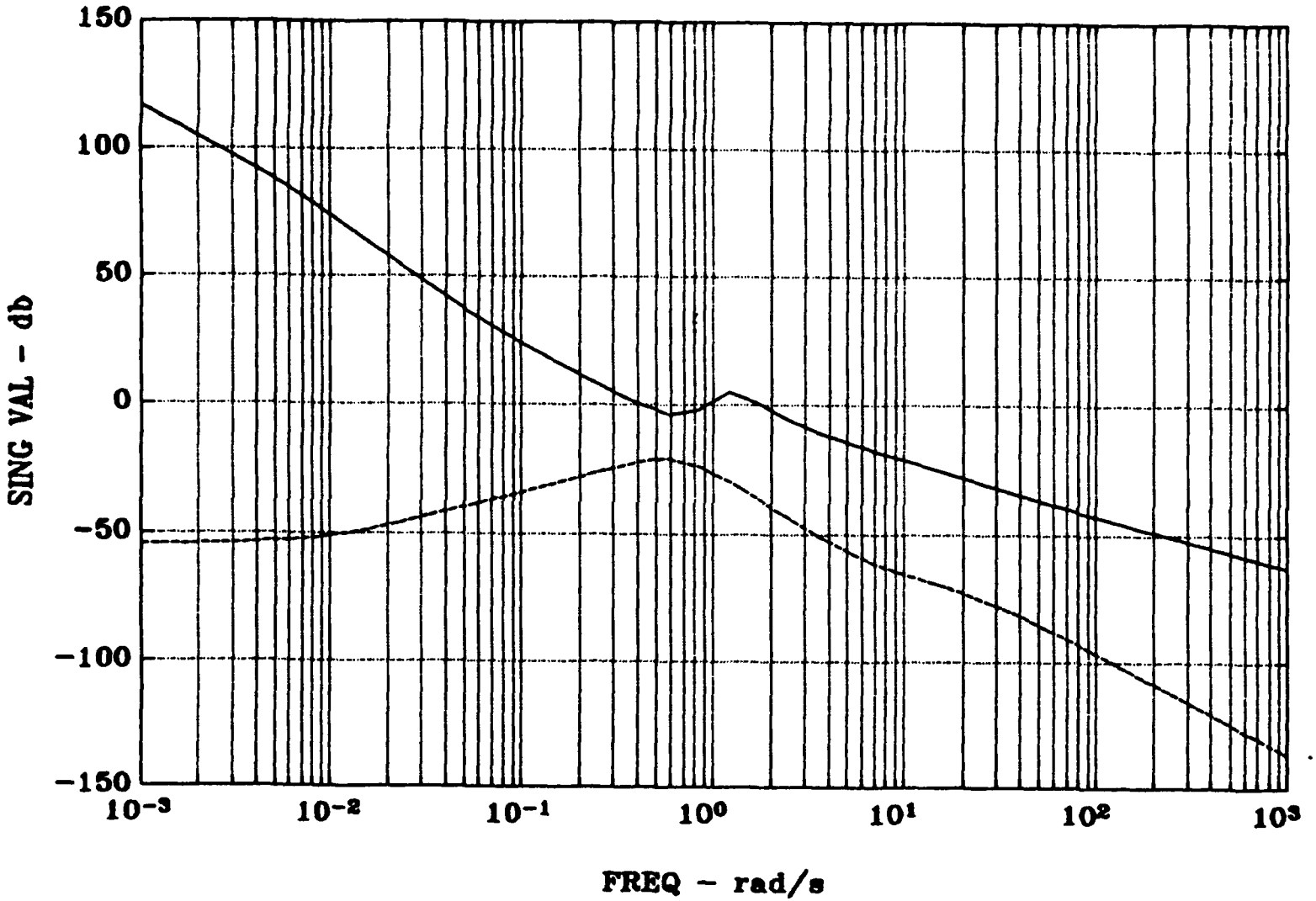

Fig. 4.2 Flight Cond. 001 Open Sing. Val - Augmented Plant

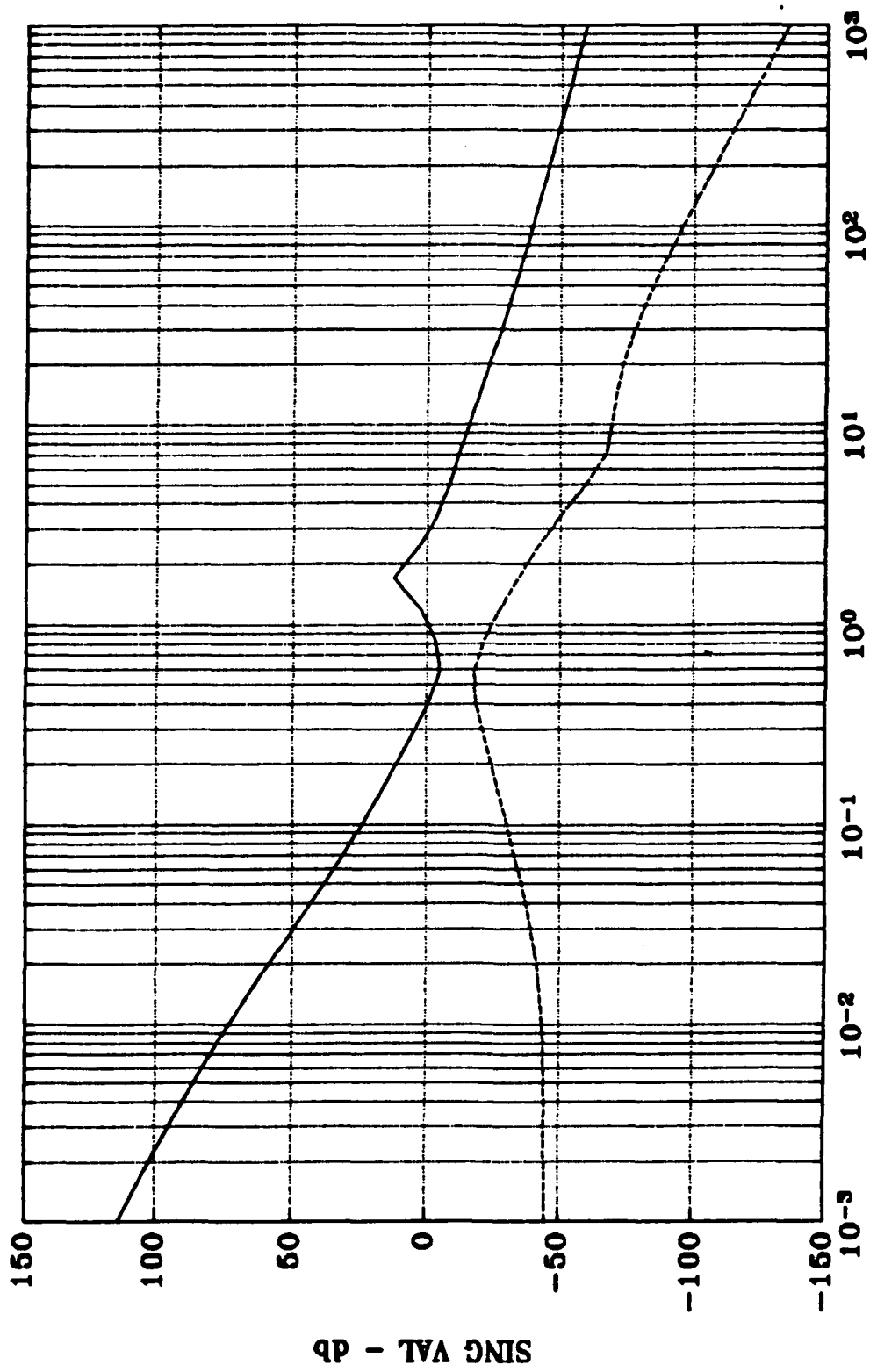

Fig. 4.3 Flight Cond. 004 Open Sing. Val - Augmented Plant

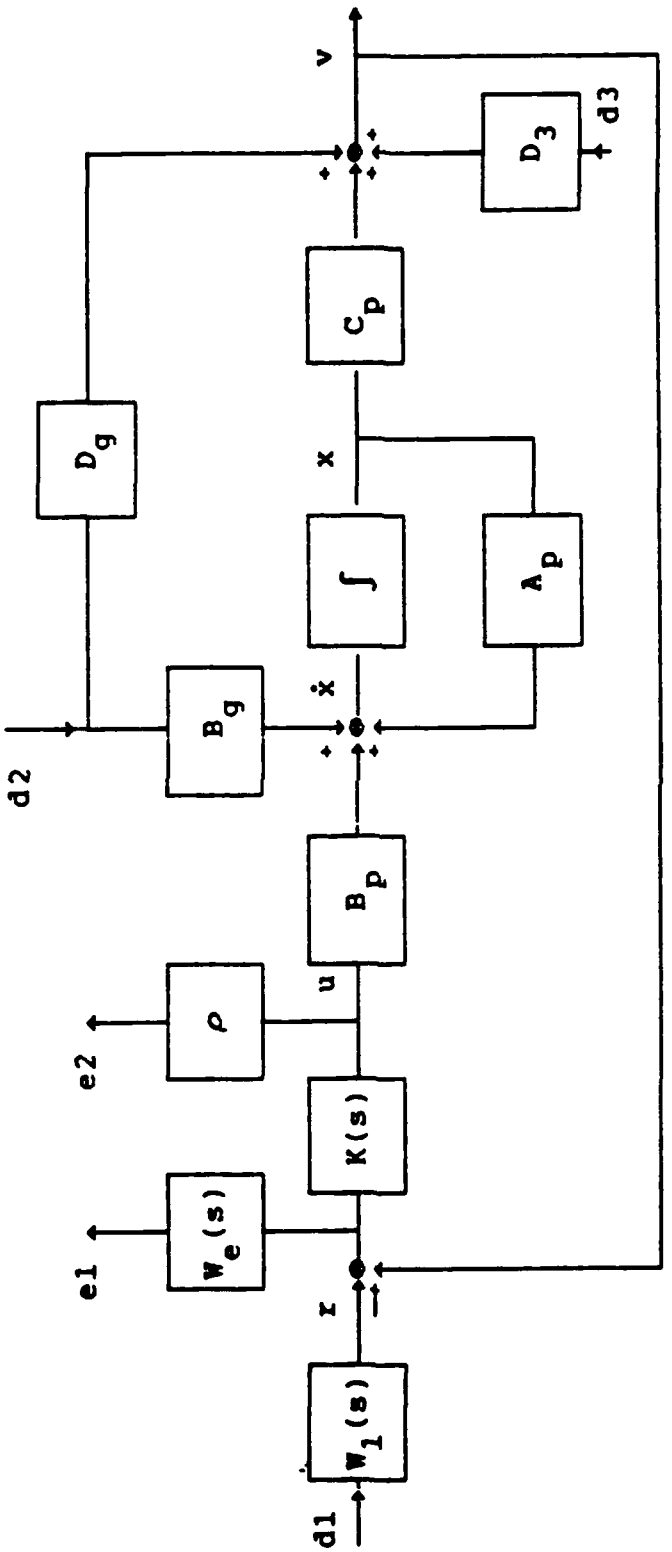

Fig. 4.4 System Block Diagram

The control input is also included in the cost function

$$\left(\| r-v \|_2^2 + \| \rho u \|_2^2 \right)^{1/2} \tag{4.6}$$

where ρ is a weighting factor to penalize the amount of control power used.

Weights were put on the incoming signal, d1, and the error signal, e1. These were added to make the system tunable when designing the compensators and to satisfy the H2 and H∞ requirements.

The system block diagram in Figure 4.4 is a hybrid of the plant state space representation and the transfer functions of the weights that have been added. To put the system in the form of equations (2.6)-(2.8), the weights need to be written in a state space form. These, along with the plant state space representation, are then substituted into equations (2.6)-(2.8).

The weight on d1, W1, can be written as

$$\dot{x}_1 = A_1 x_1 + B_1 d_1 \tag{4.7}$$

$$r = C_1 x_1 + D_1 d_1 \tag{4.8}$$

The weight on the error, We, can be written as

$$\dot{x}_e = A_e x_e + B_e (r-v) \tag{4.9}$$

$$e_1 = C_e x_e + D_e (r-v) \tag{4.10}$$

The weight on the control input is a diagonal scale factor given by

$$e_2 = \rho \tag{4.11}$$

Now using Figure 4.2,

$$\dot{x}_p = A_p x_p + B_g d_2 + B_p u \tag{4.12}$$

$$y = C_p x_p \tag{4.13}$$

$$v = C_p x_p + D_g d_2 + D_3 d_3 \tag{4.14}$$

These equations can be used to write

$$\dot{x}_e = A_e x_e + B_e C_1 x_1 + B_e D_1 d_1 - B_e C_p x_p - B_e D_g d_2 - B_e D_3 d_3 \tag{4.15}$$

$$e_1 = C_e x_e + D_e C_1 x_1 + D_e D_1 d_1 - D_e C_p x_p - D_e D_g d_2 - D_e D_3 d_3 \tag{4.16}$$

The standard problem state space form can now be written for Figure 4.4 as

$$\begin{bmatrix} \dot{x}_p \\ \dot{x}_1 \\ \dot{x}_e \end{bmatrix} = \begin{bmatrix} A_p & 0 & 0 \\ 0 & A_1 & 0 \\ -B_e C_p & B_e C_1 & A_e \end{bmatrix} \begin{bmatrix} x_p \\ x_1 \\ x_e \end{bmatrix} + \begin{bmatrix} 0 & B_g & 0 \\ B_1 & 0 & 0 \\ B_e D_1 & -B_e D_g & -B_e D_3 \end{bmatrix} \begin{bmatrix} d_1 \\ d_2 \\ d_3 \end{bmatrix} + \begin{bmatrix} B_p \\ 0 \\ 0 \end{bmatrix} [u] \tag{4.17}$$

$$\begin{bmatrix} e_1 \\ e_2 \end{bmatrix} = \begin{bmatrix} -D_e C_p & D_e C_1 & C_e \\ 0 & 0 & 0 \end{bmatrix} \begin{bmatrix} x_p \\ x_1 \\ x_e \end{bmatrix} + \begin{bmatrix} D_e D_1 & -D_e D_g & -D_e D_3 \\ 0 & 0 & 0 \end{bmatrix} \begin{bmatrix} d_1 \\ d_2 \\ d_3 \end{bmatrix} + \begin{bmatrix} 0 \\ \rho \end{bmatrix} [u] \tag{4.18}$$

$$[y] = \begin{bmatrix} -C_p & C_1 & 0 \end{bmatrix} \begin{bmatrix} x_p \\ x_1 \\ x_e \end{bmatrix} + \begin{bmatrix} D_1 & -D_g & -D_3 \end{bmatrix} \begin{bmatrix} d_1 \\ d_2 \\ d_3 \end{bmatrix} + [0][u] \tag{4.19}$$

The conditions for the Doyle/Glover parameterization require D11 and D22 to be zero. D22 has already been taken care of. D11 is made equal to zero by choosing the weights properly. From equation (4.18), it can be seen that D_e must be zero. This says that the weight on the error signal must be strictly proper.

The other conditions are that $D12^T D12$ and $D21 D21^T$ be

similar to I. The first condition is satisfied, in that

$$D12^T D12 = \rho^2 \tag{4.20}$$

which is chosen to be a full rank diagonal matrix. The later is satisfied by

$$D21D21^T = D_1 D_1^T + D_g D_g^T + D_3 D_3^T \tag{4.21}$$

where D_3 is a 4 by 4 identity matrix added for inputing measurement noise, D_g is a 4 by 1 vector the gust disturbance enters the output of the system through, and D1 is a 4 by 4 matrix since W1 is proper. This guarantees that equations (4.20) and (4.21) have full rank.

The open loop plant is both controllable and observable. The augmented system is stabilizable and detectable. Condition 3 for H∞ requires that (A,B1) be controllable and (A,C1) be observable. These conditions are not truly met, as the condition numbers of the controllability and observability matrices are very large. The condition number is the ratio of the maximum and minimum singular values. A large condition number is indicative of a nearly singular matrix. This will probably cause numerical problems in the computation of the H∞ controllers. This problem will be addressed later in the discussion section.

The system equations can be modified now that the form of the weights has been specified. The new equations are

$$\begin{bmatrix} x_p \\ \dot{x}_1 \\ \dot{x}_e \end{bmatrix} = \begin{bmatrix} A_p & 0 & 0 \\ 0 & A_1 & 0 \\ -B_e C_p & B_e C_1 & A_e \end{bmatrix} \begin{bmatrix} x_p \\ x_1 \\ x_e \end{bmatrix} + \begin{bmatrix} 0 & B_g & 0 \\ B_1 & 0 & 0 \\ B_e D_1 & -B_e D_g & -B_e D_3 \end{bmatrix} \begin{bmatrix} d_1 \\ d_2 \\ d_3 \end{bmatrix} + \begin{bmatrix} B_p \\ 0 \\ 0 \end{bmatrix} [u] \tag{4.22}$$

$$\begin{bmatrix} e_1 \\ e_2 \end{bmatrix} = \begin{bmatrix} 0 & 0 & C_e \\ 0 & 0 & 0 \end{bmatrix} \begin{bmatrix} x_p \\ x_1 \\ x_e \end{bmatrix} + \begin{bmatrix} 0 & 0 & 0 \\ 0 & 0 & 0 \end{bmatrix} \begin{bmatrix} d_1 \\ d_2 \\ d_3 \end{bmatrix} + \begin{bmatrix} 0 \\ \rho I \end{bmatrix} [u] \quad (4.23)$$

$$[\, y \,] = [-C_p \quad C_1 \quad 0\,] \begin{bmatrix} x_p \\ x_1 \\ x_e \end{bmatrix} + [\, D_1 \quad -D_g \quad -D_3\,] \begin{bmatrix} d_1 \\ d_2 \\ d_3 \end{bmatrix} + [0\,][u] \quad (4.24)$$

The problem synthesis is complete. These equations will now be used in the H2 and H∞ routines to design two controllers for the aircraft's lateral autopilot.

V. Analysis

5.1 General Approach

The goal of this thesis was to design one controller that meets all the design requirements for all flight conditions. It was determined that one controller would not meet the specifications for all flight conditions after a controller designed for a nominal case for all fourteen flight conditions yielded poor results in closed loop simulation runs. The flight conditions were then broken down into the slow and fast conditions. A nominal condition was picked for which the design was based on. Once these controllers were designed, they were used in the closed loop simulation to evaluate the performance. A controller was obtained using H2 and H∞ control theory for both the slow and fast approach flight conditions.

The techniques used to design each controller was a mix of trying to shape the singular value plots of the loop gain, the sensitivity function, and the complementary sensitivity function combined with evaluating the time domain response characteristics. The weights on the input signal, W1, and on the error signal, We, were varied in trying to obtain the desired response. In addition to these, the scale parameter, ρ, on the control inputs was also varied.

The program PCMATLAB was used for this thesis. Many programs were written using the PCMATLAB-based software. The Control System Toolbox was also used.

Routines to build the matrices in equations (4.22)-(4.24) were written. DOABCD formulated the A, B1, B2, C1, C2, D11, D12, D21, and the D22 matrices for input into the code to solve for the H2 and the H∞ controllers. These programs returned the H2 and H∞ controllers.

Routines to build the state space matrices for the weights were also written. These routines, DOW1 and DOWE, returned the A1, B1, C1, D1, Ae, Be, and Ce matrices used in equations (4.22)-(4.24).

The routine CLOSE formed the closed loop matrices which consisted of the original plant and the controller. The PCMATLAB routine LSIM was used to simulate the closed loop system.

Other utility routines were written. The routines RUNH2 and RUNHI used the above mentioned routines to do the design form start to finish. Several routines to plot simulation data and singular value plots were also written. The user written code is listed in Appendix B.

5.2 Nominal Controller Design and Analysis

The flight condition chosen for the nominal controller design for the fast approach data was Flight Condition 084. Flight Condition 033 was chosen for the nominal controller design for the slow approach data. The data is a sampling of the most extreme conditions for the landing profile.

The weights used in the design were based on the classical control ideas of bandwidths and gains. The

response could be altered significantly with the weights.

Weighting strategies of trying to shape the singular value plots were also used. This entailed knowing what the sensitivity of the system should look like and using a weight which gave the desired sensitivity. The sensitivity should be low at low frequency since the loop gain is large. The sensitivity function is given by

$$S = (I + GK)^{-1} \tag{5.1}$$

On a Bode plot, the sensitivity goes to 0 db at high frequency since GK is small. The weights were also chosen in an effort to achieve high loop gains at low frequency.

The Bode magnitude plot of W1, the weight on the inputs, is shown in Figure 5.1. This weight is on the ground track heading angle and the cross track error. The other inputs were just passed through with unity gain since they were mainly there to achieve an equal number of inputs to the number of outputs.

The W1 weights were chosen to shape the inputs of the system as a step. Moving the bandwidths had significant effect on the system response, as did changing the DC gains.

The error weights, We, were just as effective. The error weights were thought of in terms of penalizing a particular signal. A good example of this is the lightly damped pole from the Dutch roll mode around 1.5 rad/sec. This pole had a damping ratio of 0.08, for Flight Condition 084, and was increased to 0.52 by penalizing the sideslip angular rate

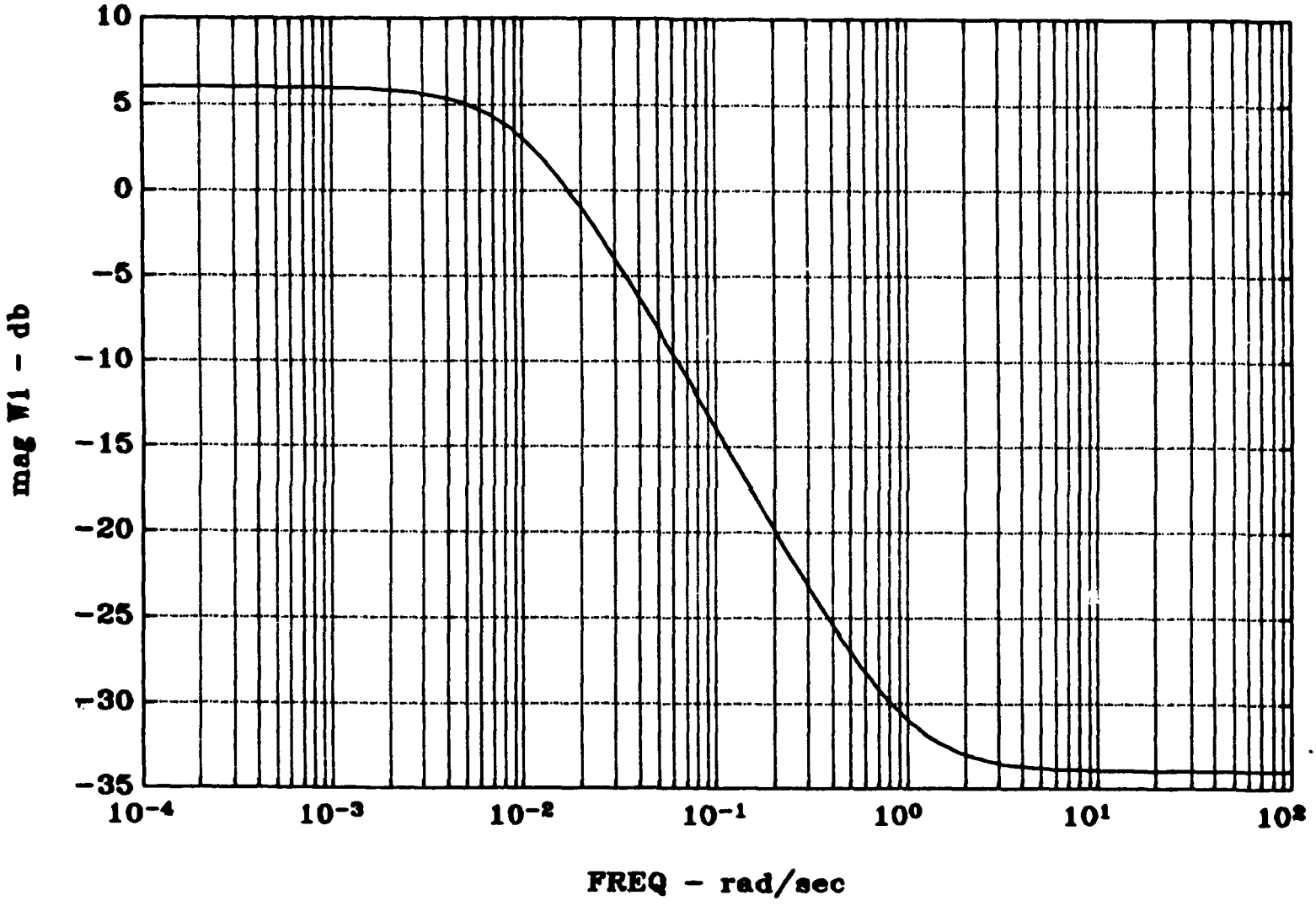

Fig. 5.1 Weight on Inputs

error, $\dot{\beta}_e$. The Bode plots of the weights for the four error outputs are shown in Figures 5.2-5.5. The weights on $\dot{\beta}$ and n_y each added one state to the compensator. The choice of weights on the ground track heading error, ψ_{gt} , and cross track error, y_e, were made in terms of adjusting the gains for steady state accuracy and moving the bandwidths for damping the response.

The flexibility of the weights gave enormous amounts of tuning control. Unfortunately, it also gives an enormous amount of possible combinations of weighting. As mentioned, several weighting strategies were used. The resultant strategy was somewhat of a combination of all of them.

The success of shaping the singular value loop shapes was minimal. The minimum singular value of the loop gain was very low. This caused problems in obtaining the desired steady state accuracy in both channels.

When the weights were finalized for the nominal controllers, the response for the closed loop system was run for all flight conditions. This will be discussed in the next section. The closed loop system was formed by writing the controller in its state space form, given by

$$\dot{x}_k = A_k x_k + B_k(r-v) \tag{5.2}$$

$$u = C_k x_k \tag{5.3}$$

Closing the loop yielded the equations

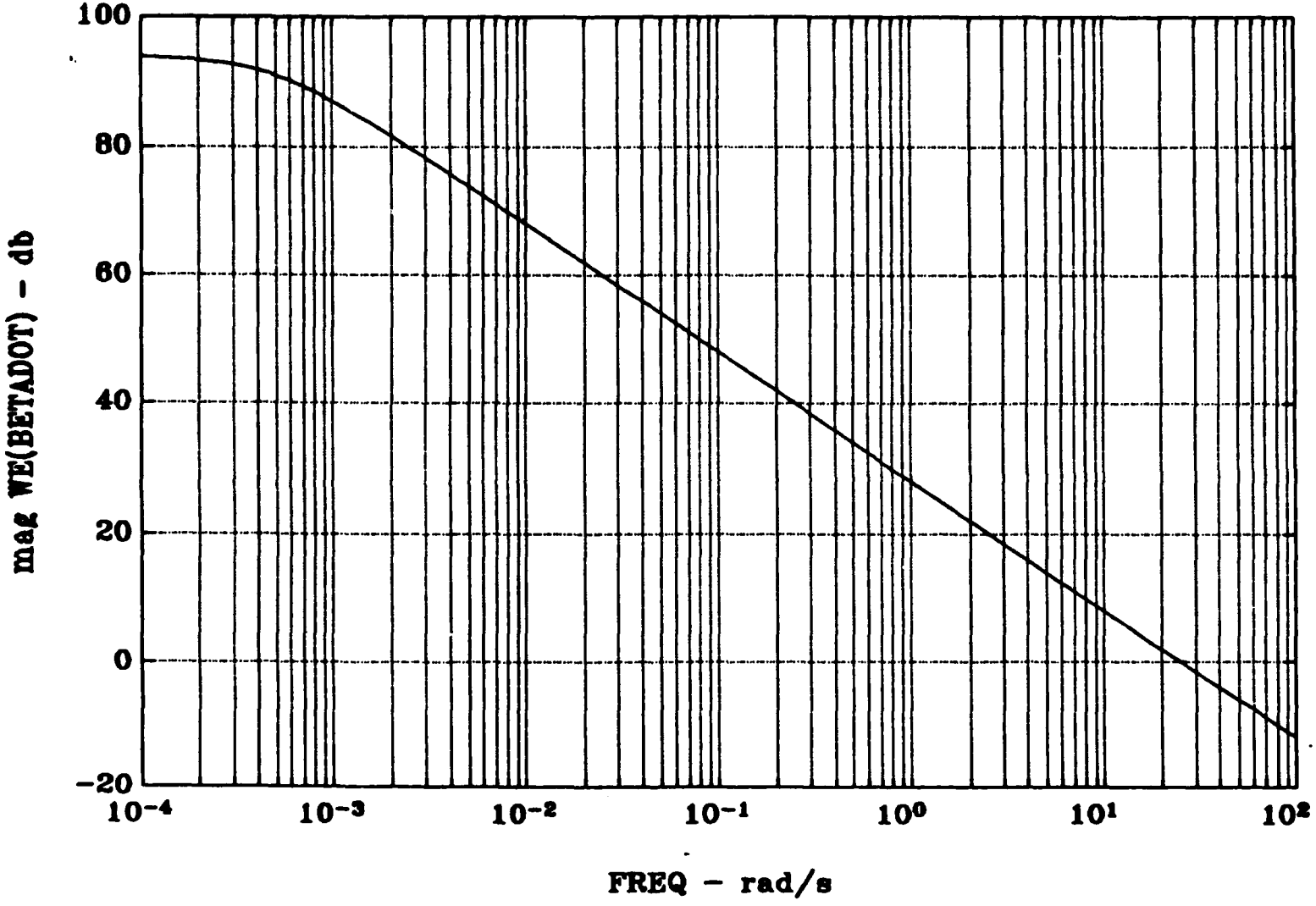

Fig. 5.2 Weight on Betadot Error Output

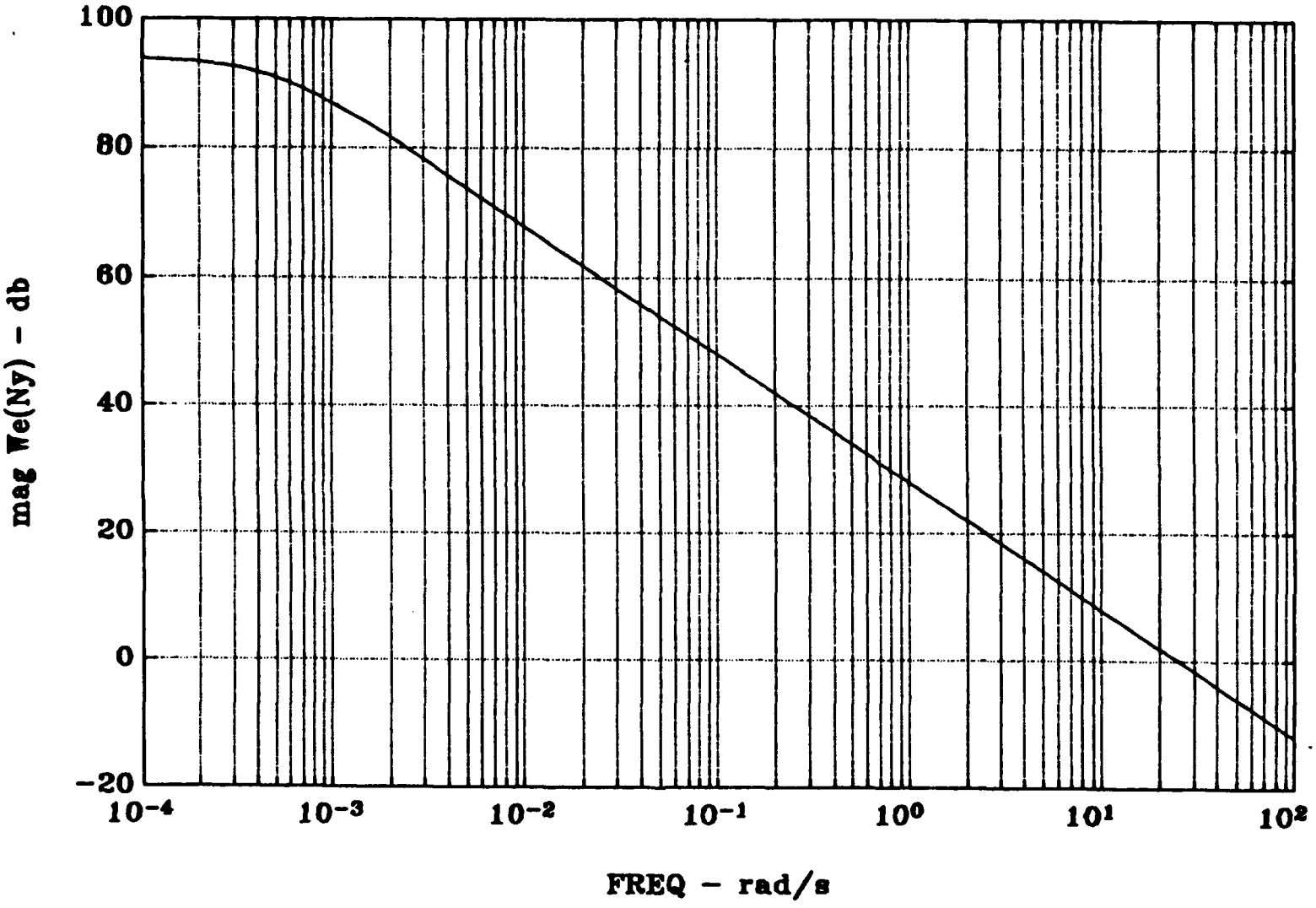

Fig. 5.3 Weight on Normal Acceleration Error Output

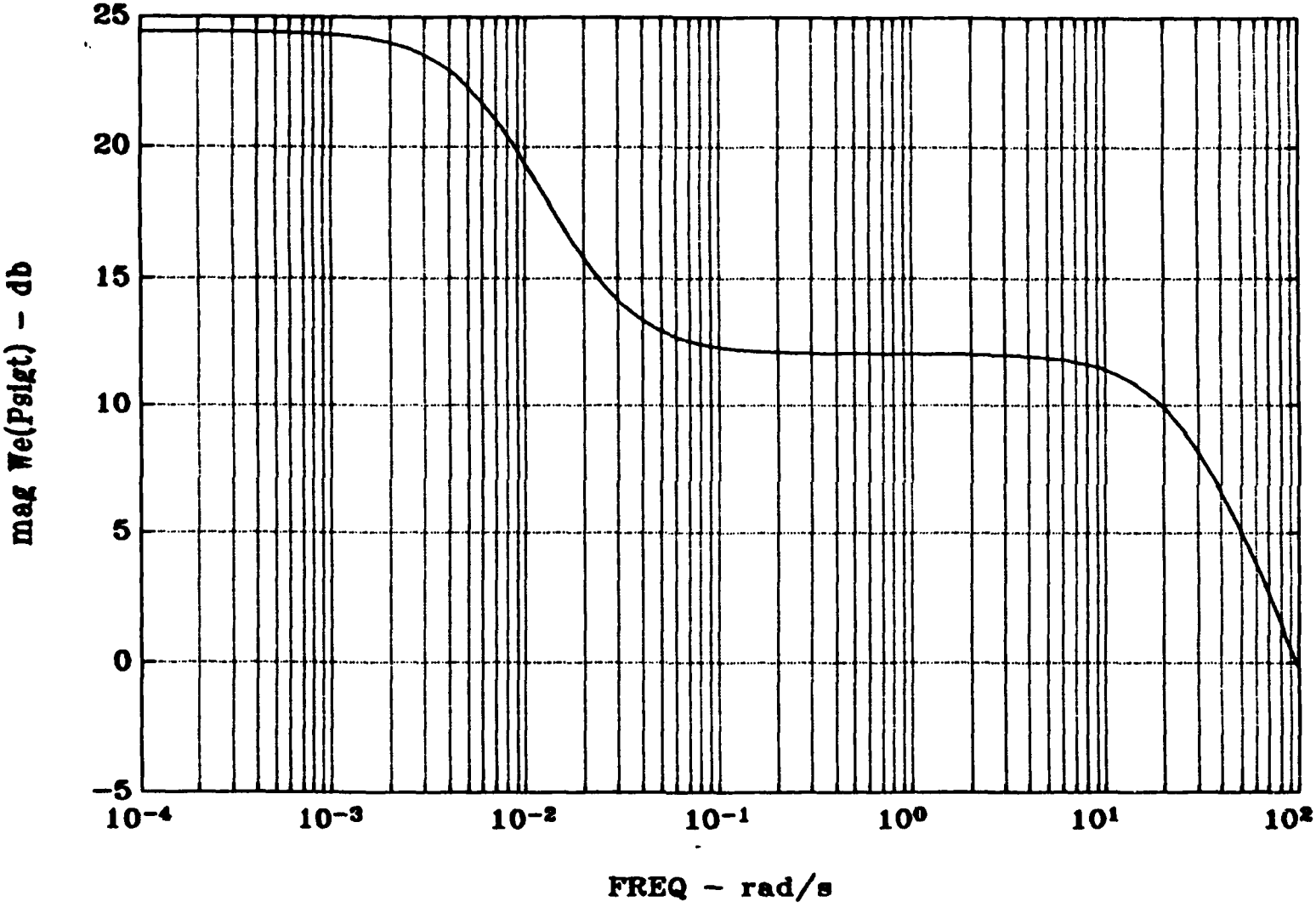

Fig. 5.4 Weight on Ground Track Heading Angle Error Output

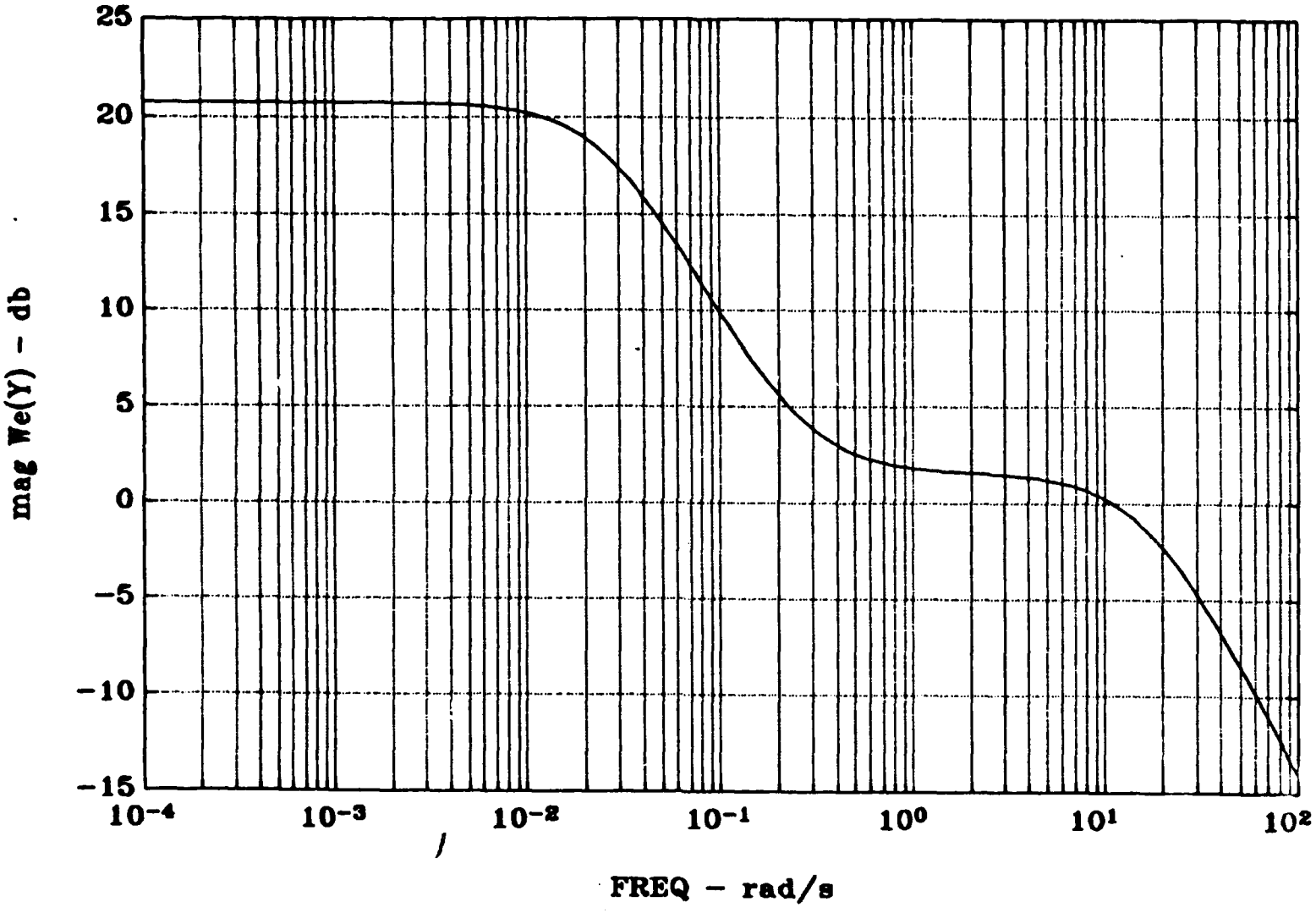

Fig. 5.5 Weight on Cross Track Error Error Output

$$\begin{bmatrix} \dot{x}_p \\ \dot{x}_k \end{bmatrix} = \begin{bmatrix} A & BC_k \\ -B_k C_p & A_k \end{bmatrix} \begin{bmatrix} x_p \\ x_k \end{bmatrix} + \begin{bmatrix} 0 & B_g & 0 \\ B_k & -B_k D_g & -B_k D_3 \end{bmatrix} \begin{bmatrix} d_1 \\ d_2 \\ d_3 \end{bmatrix} \qquad (5.$$

$$\begin{bmatrix} y \end{bmatrix} = \begin{bmatrix} C & 0 \end{bmatrix} \begin{bmatrix} x_p \\ x_k \end{bmatrix} + \begin{bmatrix} 0 & D_g & D_3 \end{bmatrix} \begin{bmatrix} d_1 \\ d_2 \\ d_3 \end{bmatrix} \qquad (5.5)$$

The controller returned by the H2 and H∞ calculations has the number of states equal to the original plant plus the number of the states associated with the weighting filters. The final controller has 16 states.

The initial conditions input to the simulation were an initial cross track error offset of 2500 feet. This corresponded to intercepting a 2.5 degree localizer beam at 9.5 nautical miles from the transmitter. The initial heading angle was aligned with the runway heading angle which was 0 degrees.

The response obtained for the nominal system for the H2 controller designed using Flight Condition 084 and 033 are shown in Figures 5.6 and 5.7. The response for these controllers met all the specifications. All poles had a damping ratio greater than the required 0.4 and the dominant pole was greater than 0.6. The steady state tracking for the cross track error and ground track heading angle also met the specifications. The control surface angular positions and rates were within the allowable values.

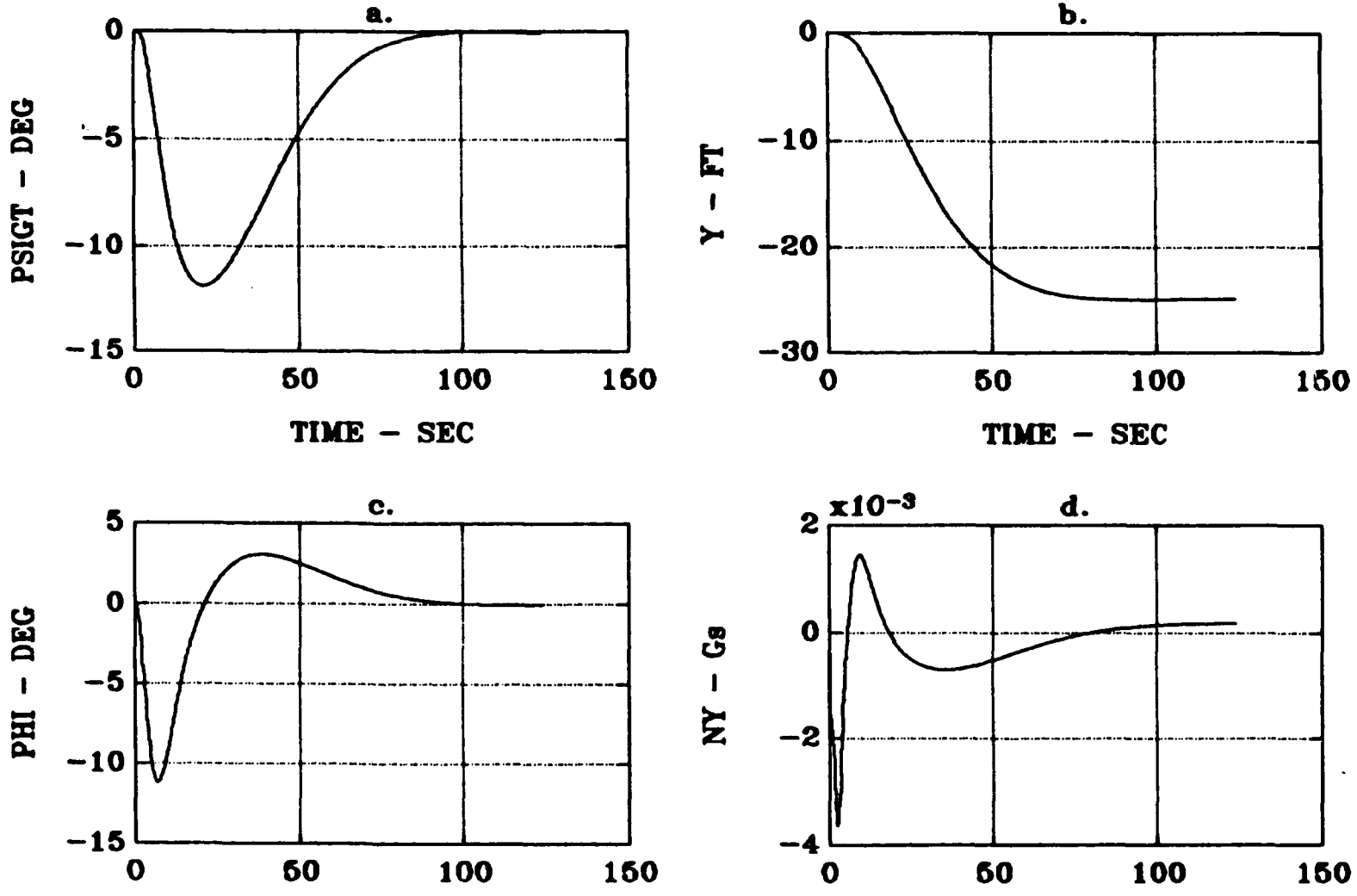

Fig. 5.6a.- d. Flt Cond 084 Time Response for H2 Ctrl

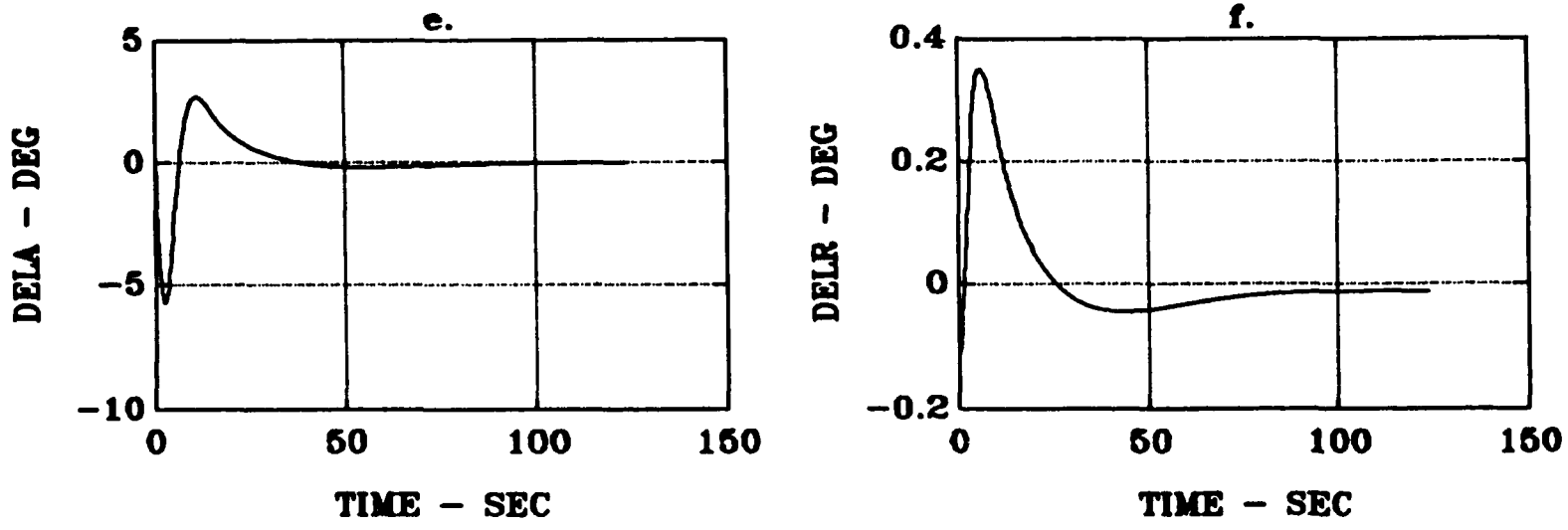

Fig. 5.6e.- f. Flt Cond 084 Time Response for H2 Ctrl

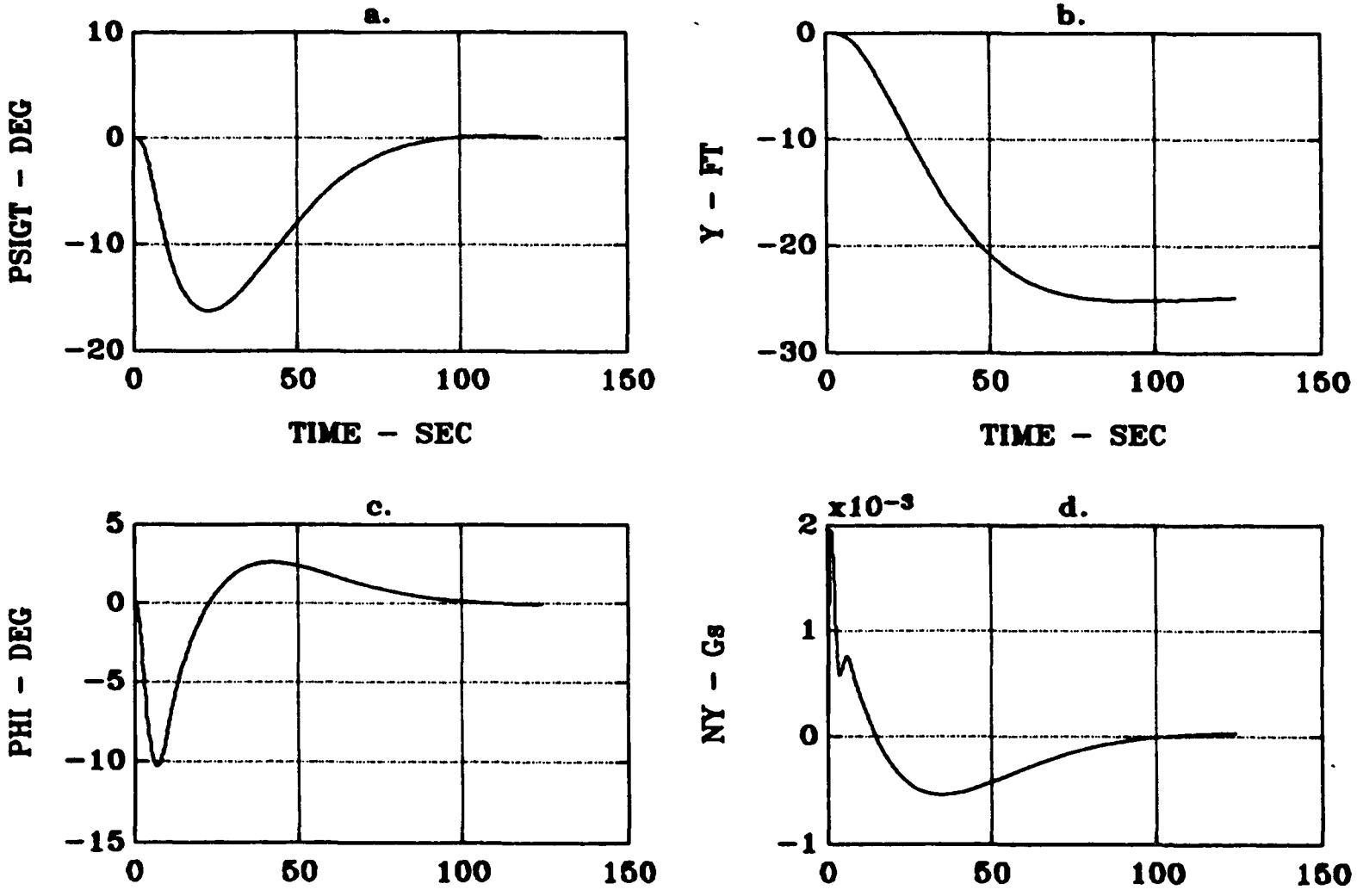

Fig. 5.7a.- d. Flt Cond 033 Time Response for H2 Ctrl

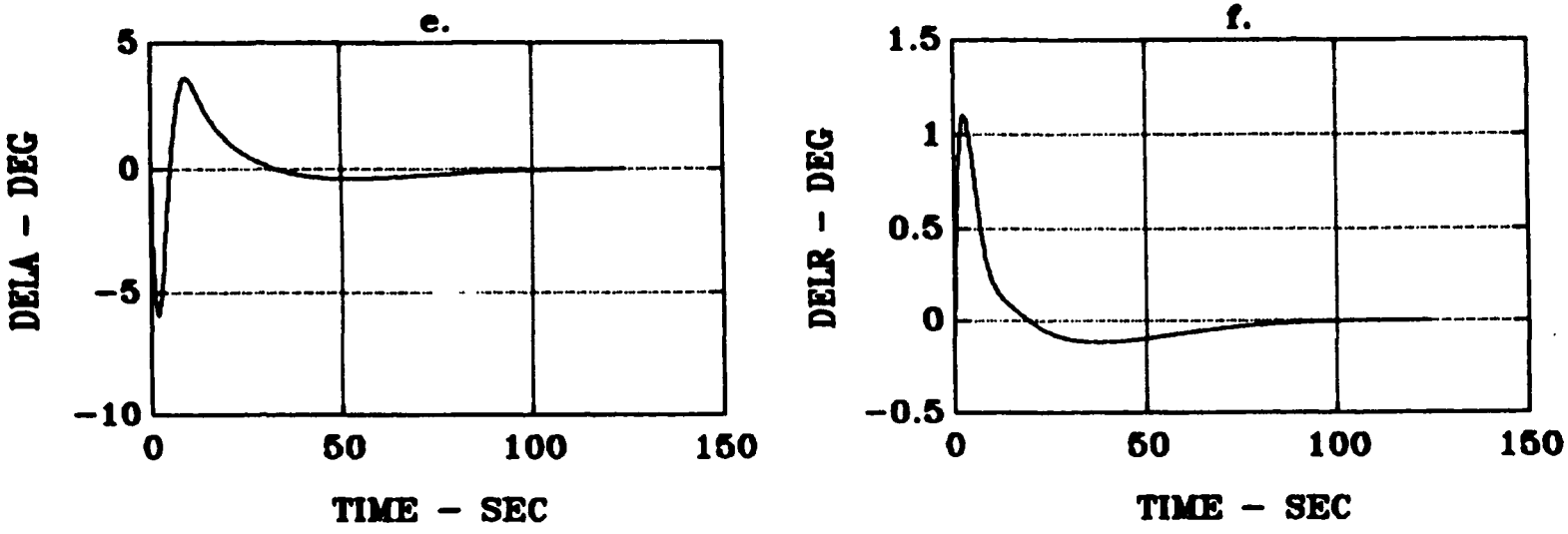

Fig. 5.7e.- f. Flt Cond 033 Time Response for H2 Ctrl

The singular value plots for Flight Condition 084 and 033 are shown in Figures 5.8 - 5.9. The loop gain for both cases is not high enough for good performance robustness. This will be addressed in the next section when these two controllers are used for the off nominal conditions. The maximum singular value of the closed loop or complementary sensitive function for both cases indicates adequate stability margins.

The approach for the H∞ controller design was basically the same as for the H2 controller except for the addition of the gamma iteration. Gamma, the scale factor shown in Figure 2.6, must be chosen close to the optimum H∞ norm. This is necessary since the H∞ optimal controller can only be approached and not calculated directly as in H2 optimization. The weights used for the H2 controller design required modifications to allow the H∞ computations to achieve reasonable results. By this, it is meant that initially the controller developed using H∞ control theory and Flight Condition 084 destabilized the closed loop system. The reason for the destabilizing controllers was numerical error. The controllability and observability conditions required for (A,B1) and (C1,A) in H∞ control theory were not met.

The initial value of gamma used to achieve a solution was 170. This was improved upon by bringing the separation of the poles and zeros in the weights closer together. The final controller designed for the fast approach data using

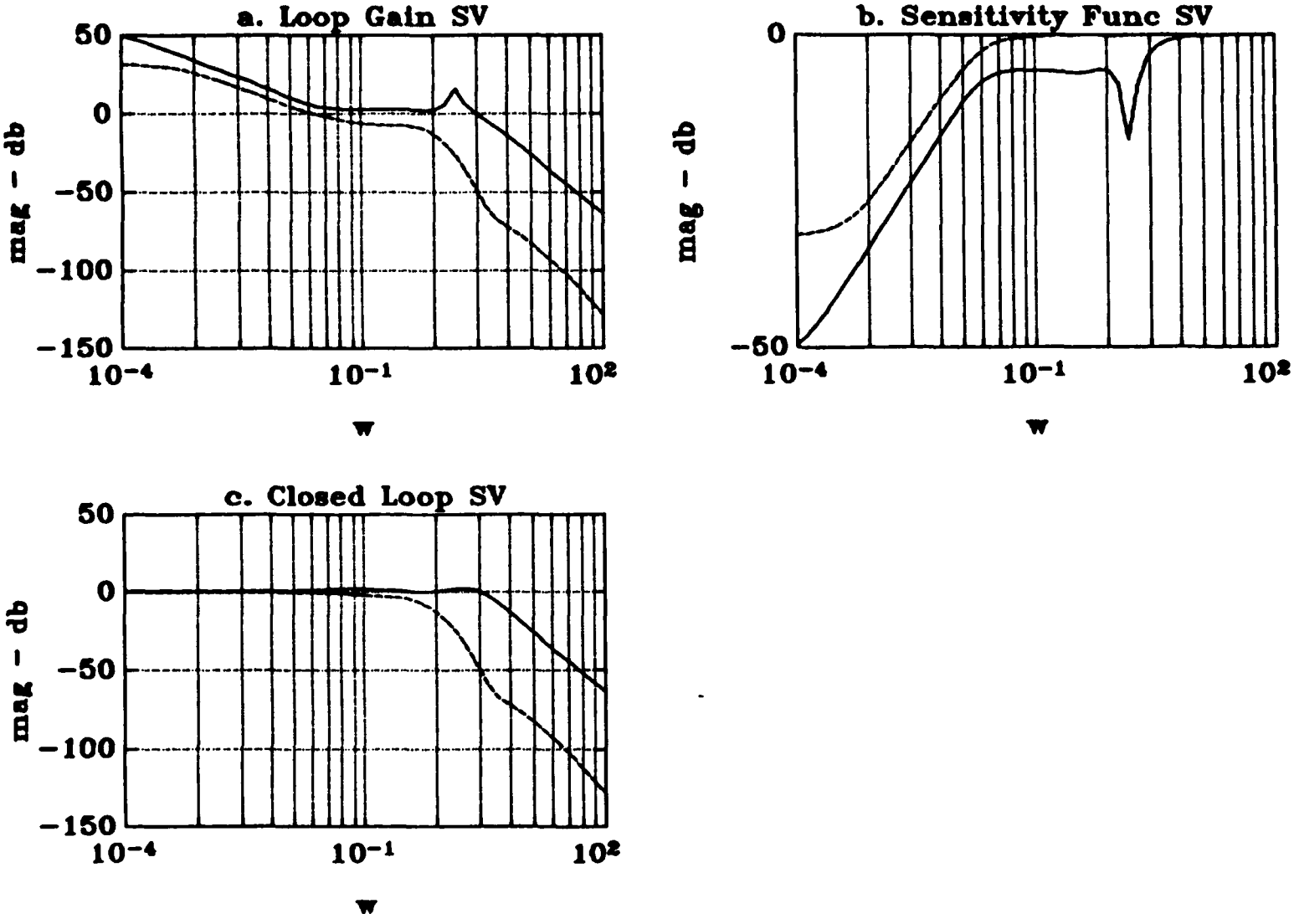

Fig. 5.8a.- c. Flt Cond 084 Singular Value Plots for H2 Ctrl

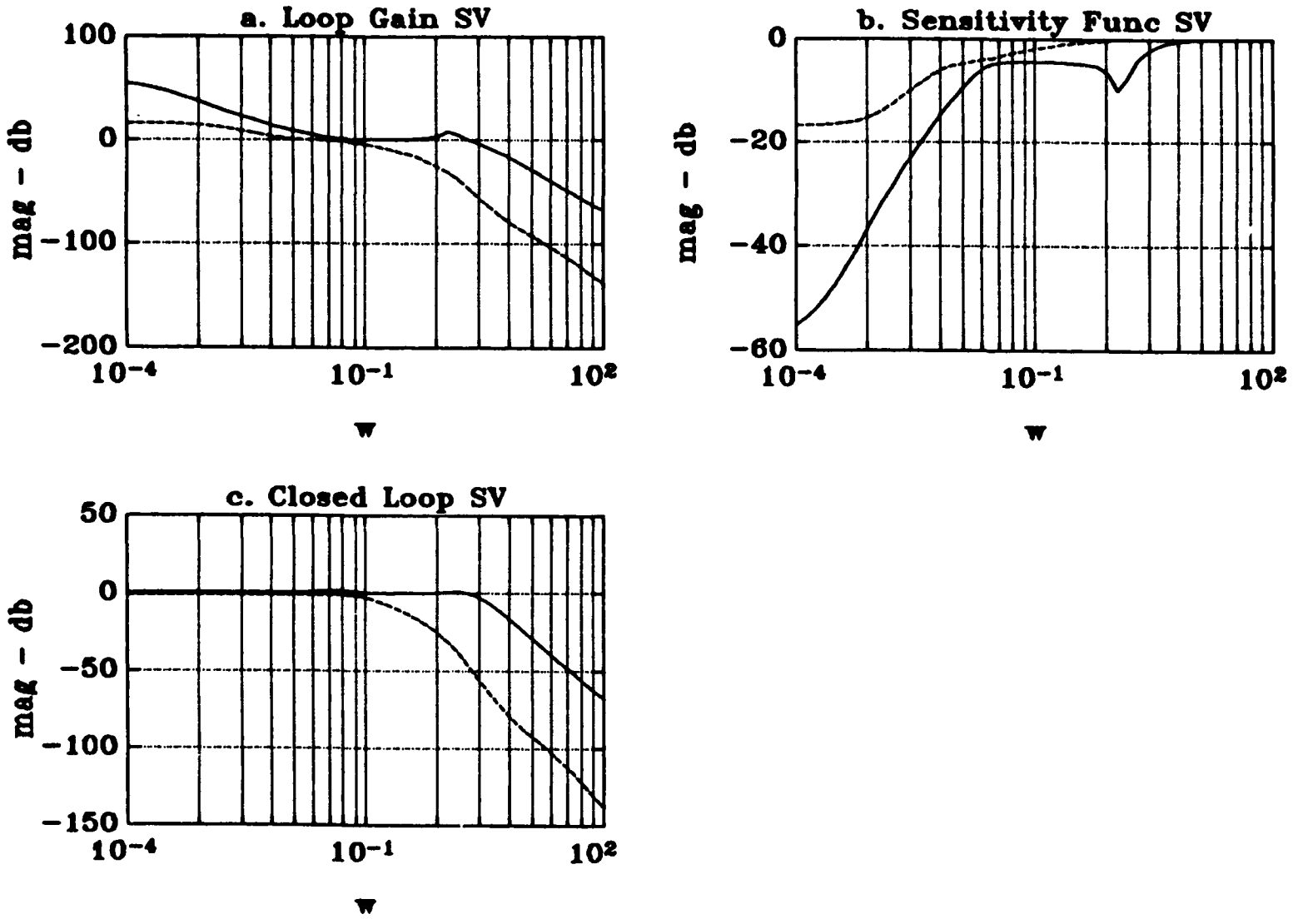

Fig. 5.9a.- c. Flt Cond 033 Singular Value Plots for H2 Ctrl

Flight Condition 084, had a gamma of 67 and a spectral radius of 0.38. Similar problems were encountered for Flight Condition 033. The controller designed for this case had a gamma and rho of 77 and 0.47, respectively. The modified weights allowed gamma to be reduced and the optimum H∞ norm to be approached, but not close enough to achieve desirable results. The maximum H∞ norm for T_{ed} was calculated to be about 0.85. More discussion about the reasons for some of the results obtained will follow in the next section.

The final designs using H∞ optimization yielded results that met the specifications for the nominal flight conditions. The time plots for the two cases are shown in Figures 5.10 and 5.11. The tracking and response of the system was acceptable. The control surface activity was within the specified limits. The damping for all modes was greater than 0.4 and the dominant mode damping was greater than 0.6. The roll angles and normal acceleration were well within the limits.

The singular value plots for the H∞ designs for Flight Condition 084 and Flight Condition 033 are shown in Figures 5.12 and 5.13. The loop gain minimum singular values show that the system does not have adequate gain at low frequency which implies the system will not be robust to parameter variations. The bandwidth of the system is also very low.

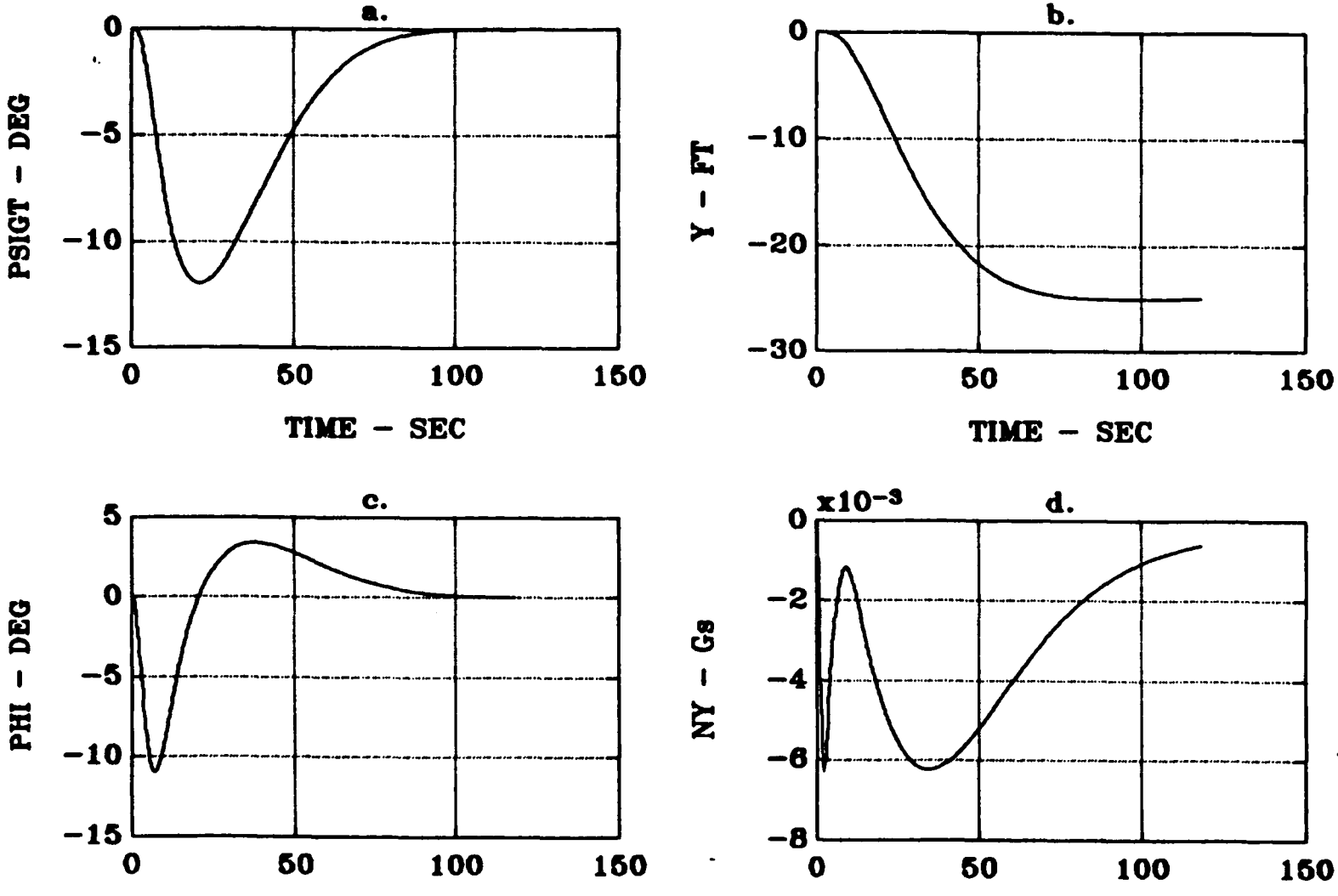

Fig. 5.10a.- d. Flt Cond 084 Time Response for H∞ Ctrl

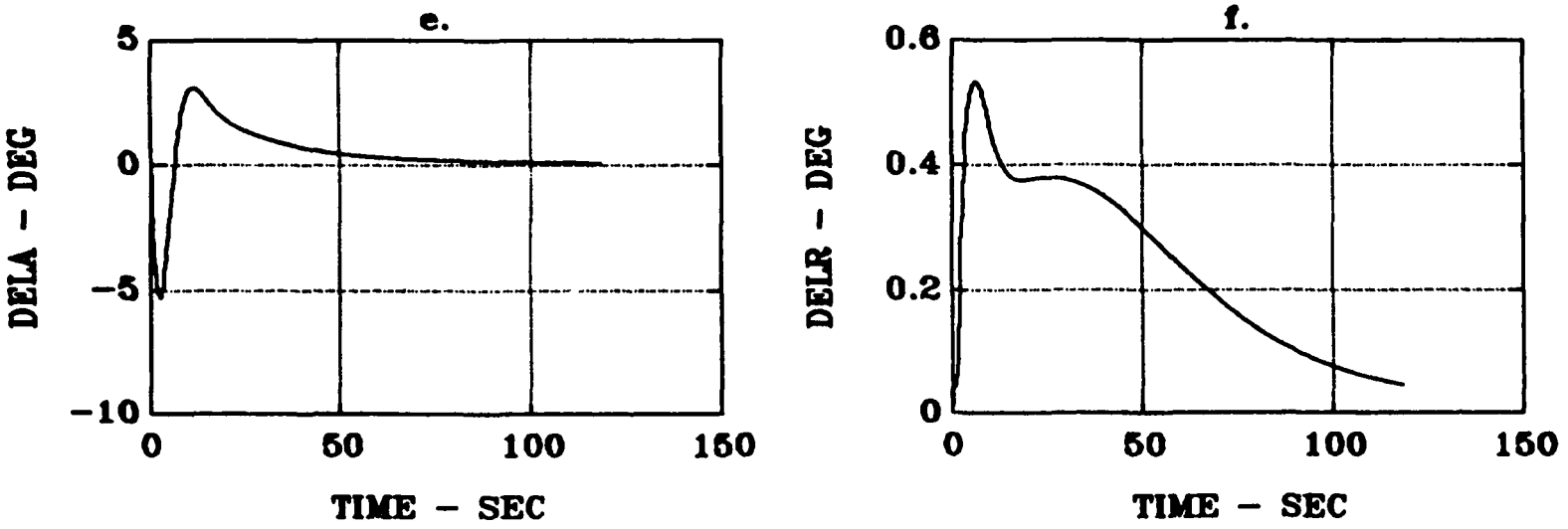

Fig. 5.10e.- f. Flt Cond 084 Time Response for H∞ Ctrl

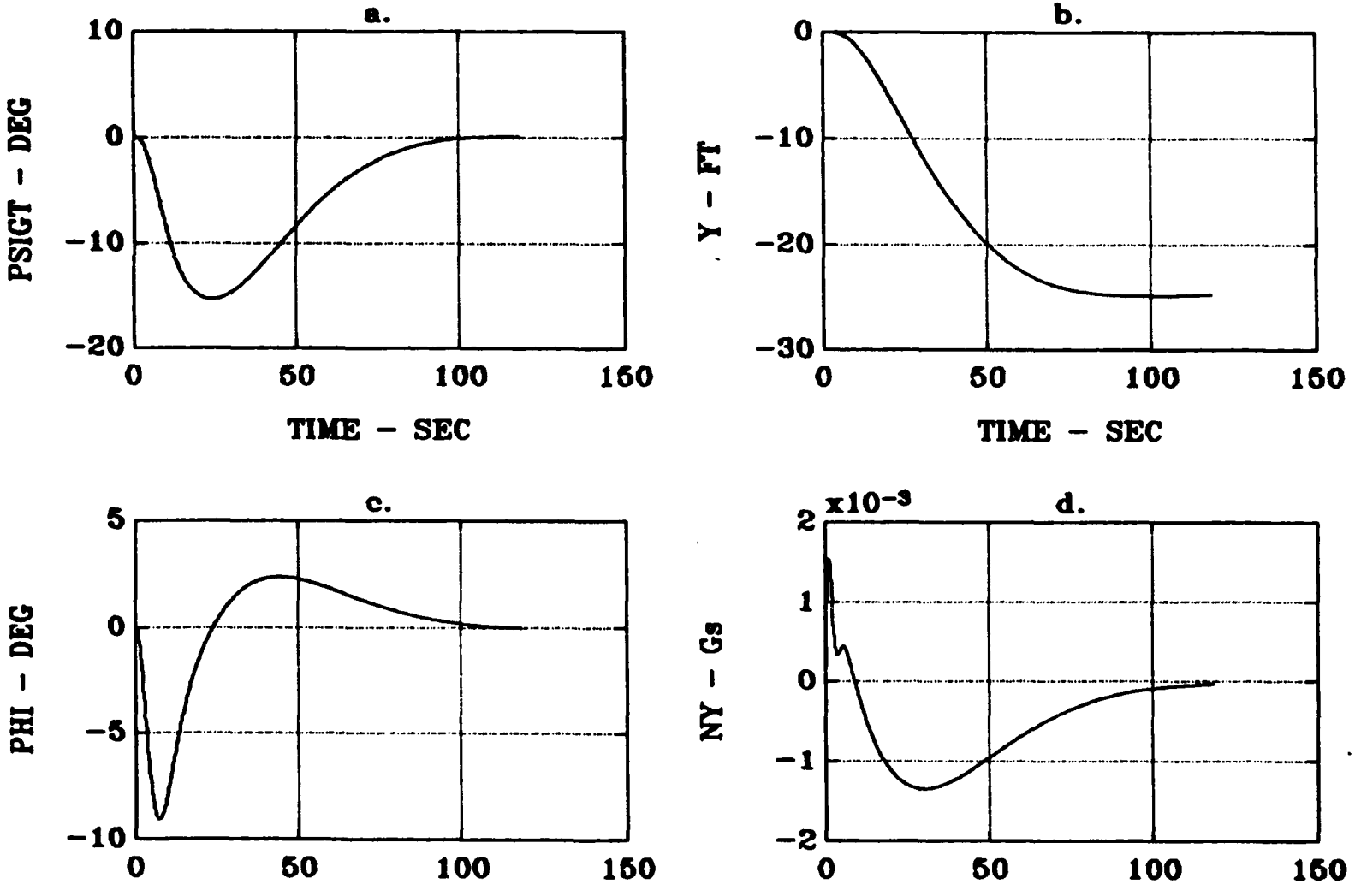

Fig. 5.11a.- d. Flt Cond 033 Time Response for H∞ Ctrl

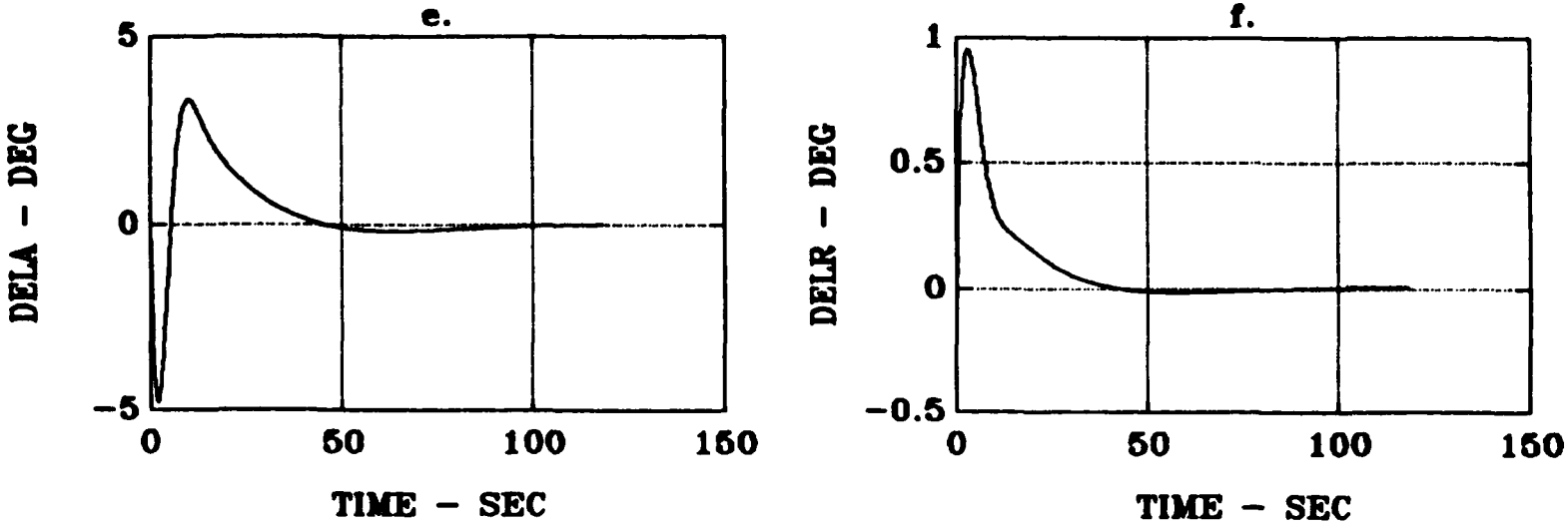

Fig. 5.11e.- f. Flt Cond 033 Time Response for H∞ Ctrl

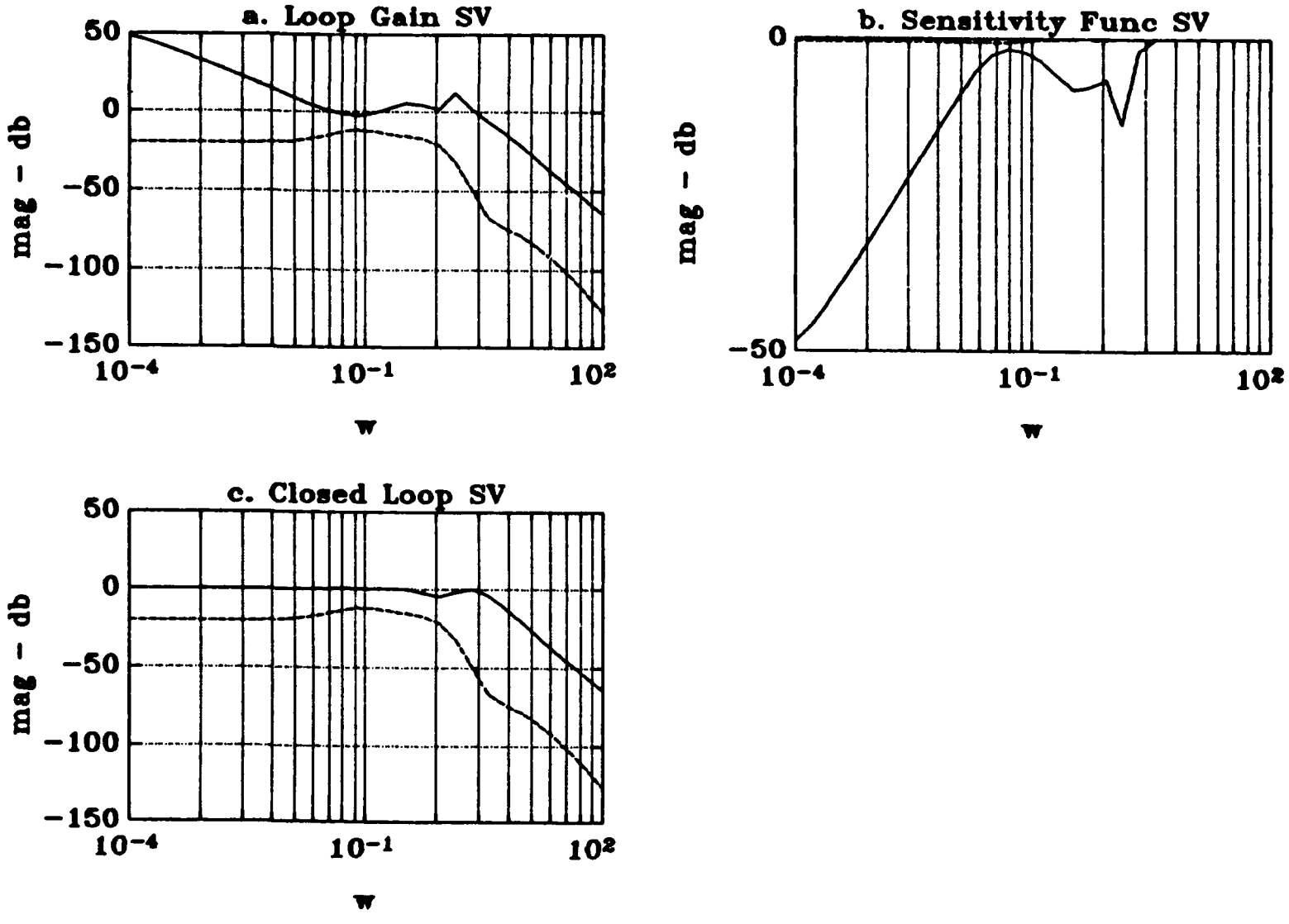

Fig. 5.12a.- c. Flt Cond 084 Singular Value Plots for H∞ Ctrl

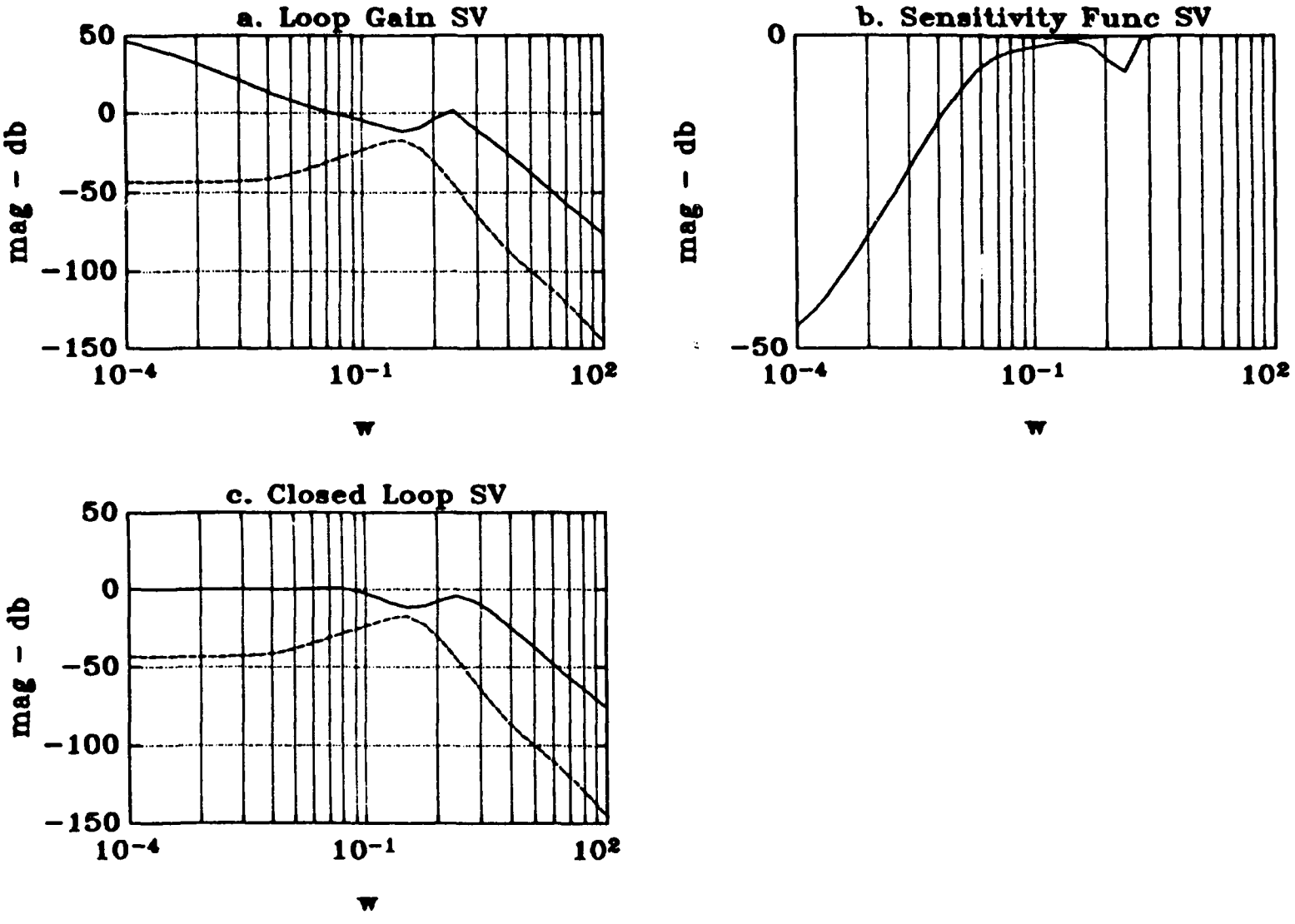

Fig. 5.13a.- c. Flt Cond 033 Singular Value Plots for H∞ Ctrl

VI. Results

6.1 Closed Loop Simulation Results

The closed loop simulation was run using the controllers developed using the H2 and H∞ control theory. The H2 compensator developed for Flight Condition 084 was used as the controller for flight conditions 004, 020, 036, 052, 068, 084, and 100, the fast approach flight conditions. The H2 compensator designed for Flight Condition 033 was used in a closed loop simulation for flight conditions 001, 017, 033, 049, 065, 081, and 097, the slow approach flight conditions. The time plots for the H2 simulation results are shown in Figures 6.1-6.12.

The simulation results for the off nominal conditions were varied. Flight Conditions 001 and 004 had an unstable pole. Looking at the time history plots for these two cases, it is clearly evident that Flight Condition 001 is unstable. The same is not true for Flight Condition 004. The time constant for the unstable mode is very large and does not show up over the duration of time plotted. All other flight conditions were stable and had a damping ratio of greater than 0.6 for the dominant mode. Flight Conditions 065 through 100, with the exception of 084, had modes with a damping ratio of less than 0.4. The lowest damped mode for these cases was 0.27.

The steady state tracking accuracies were also varied.

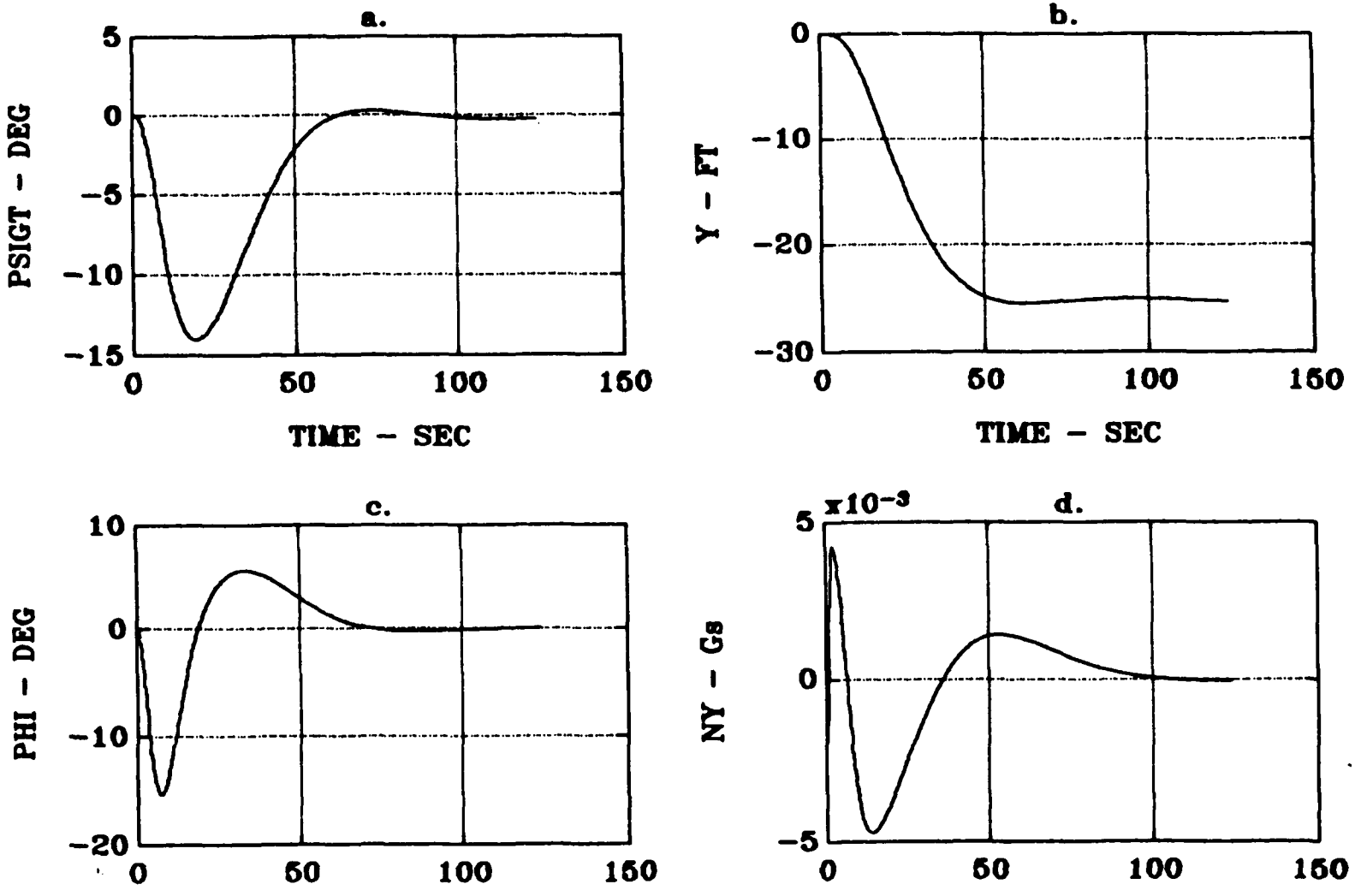

Fig. 6.1a.- d. Flt Cond 004 Time Response for H2 Ctrl

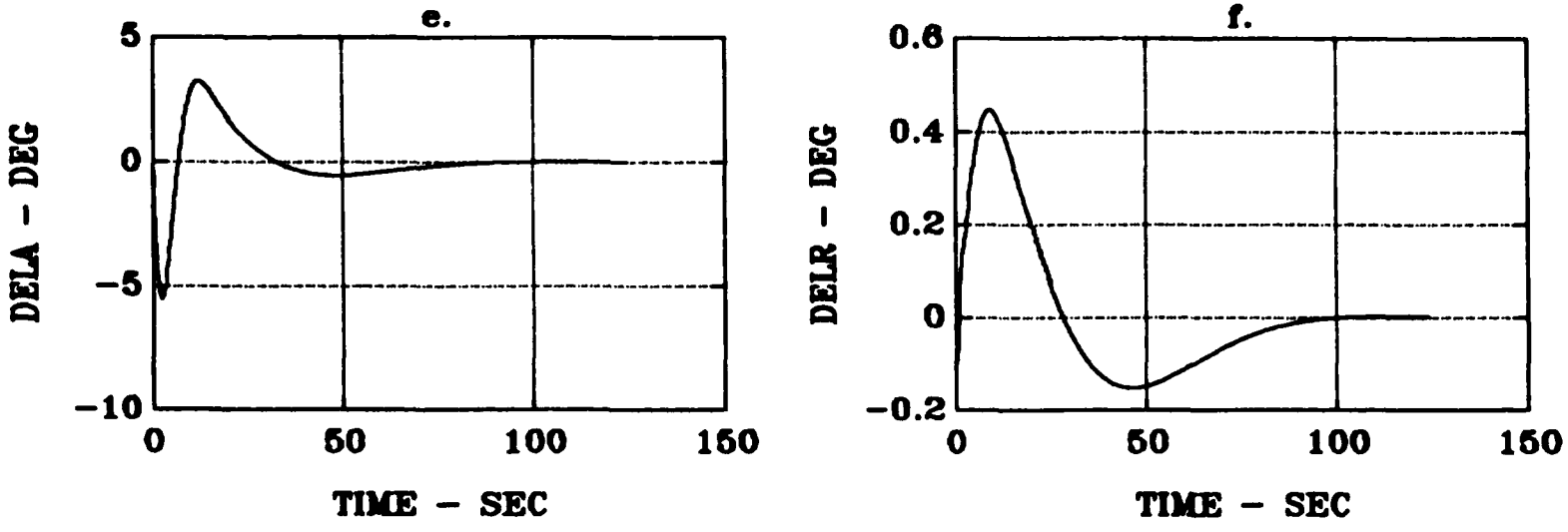

Fig. 6.1e.- f. Flt Cond 004 Time Response for H2 Ctrl

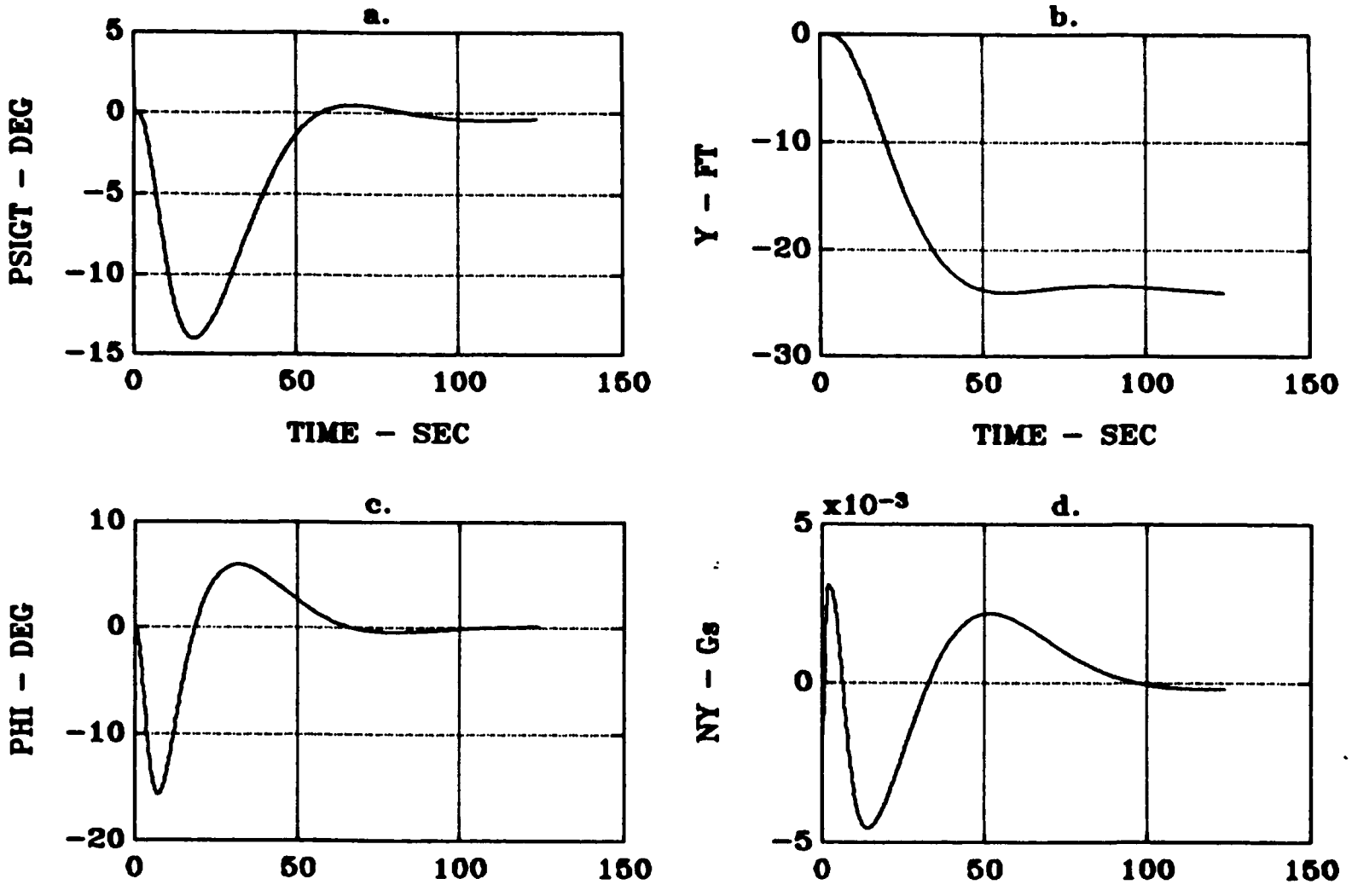

Fig. 6.2a.- d. Flt Cond 020 Time Response for H2 Ctrl

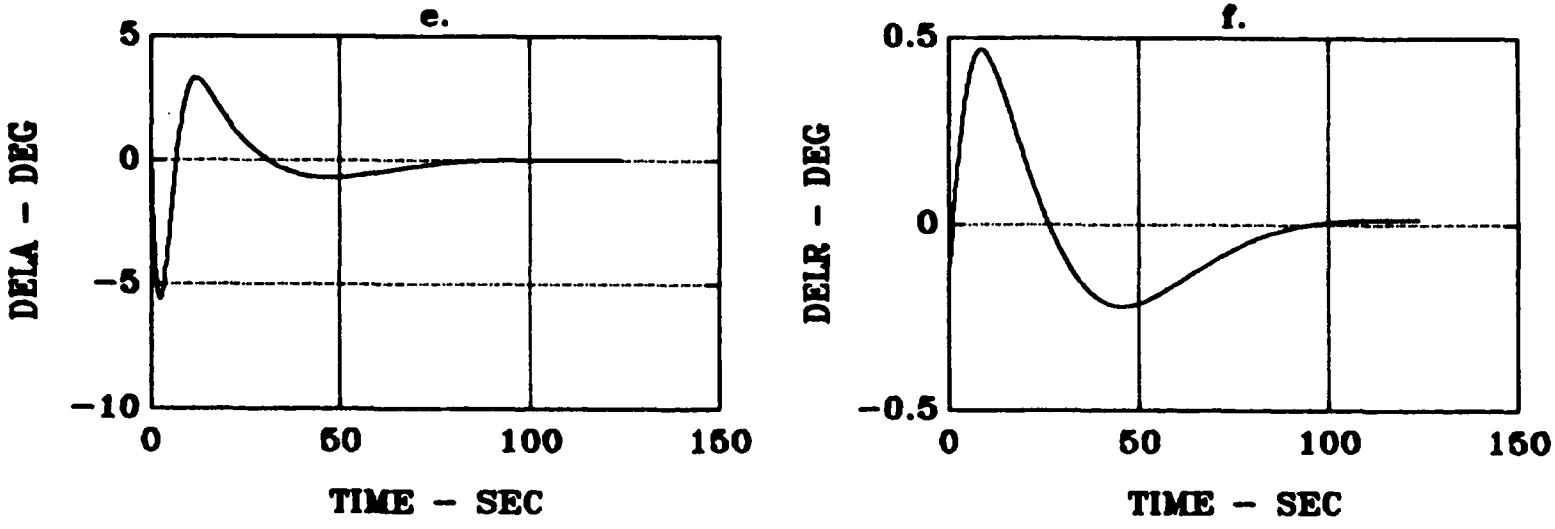

Fig. 6.2e.- f. Flt Cond 020 Time Response for H2 Ctrl

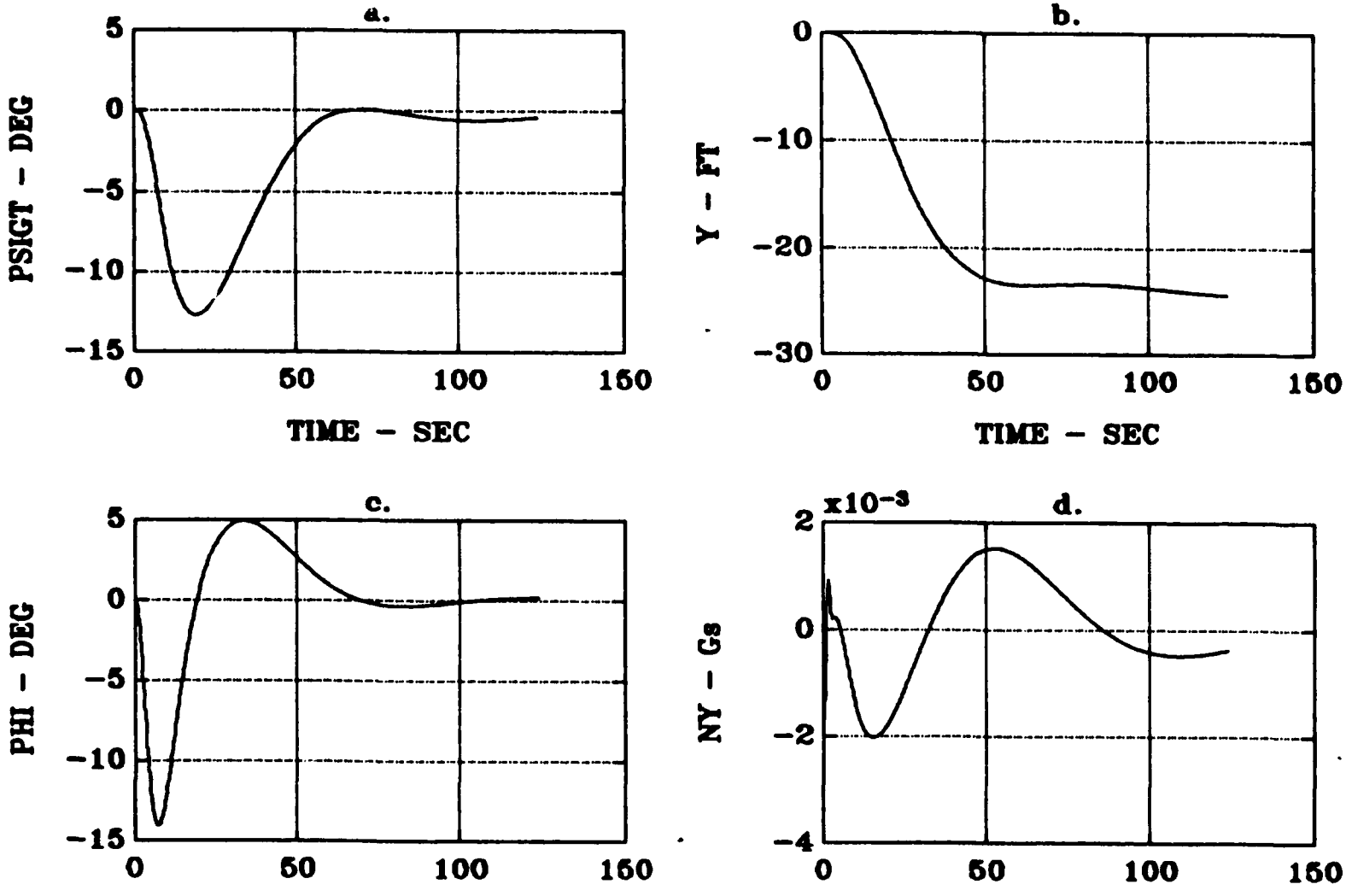

Fig. 6.3a.- d. Flt Cond 036 Time Response for H2 Ctrl

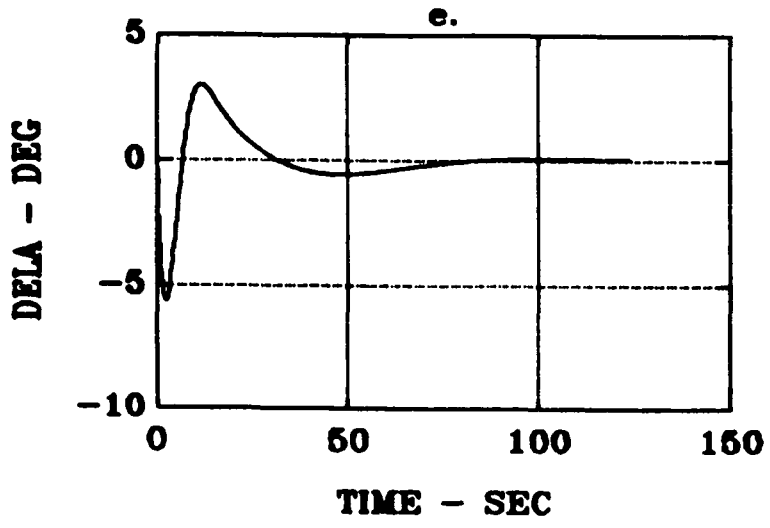

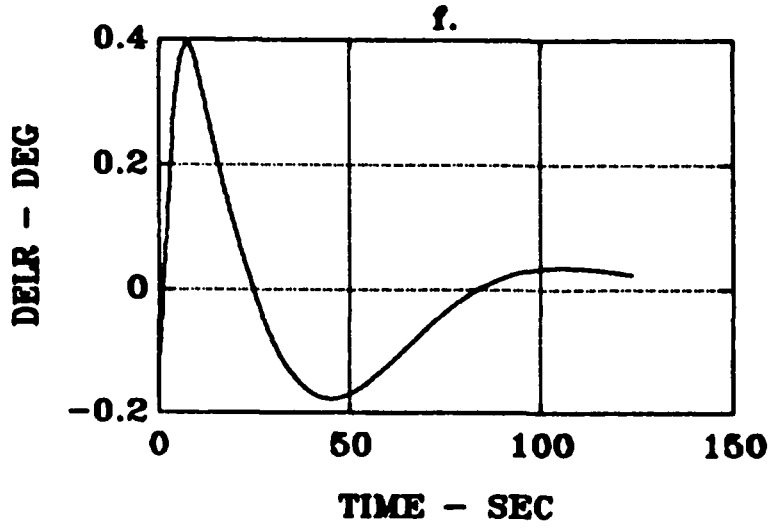

Fig. 6.3e.- f. Flt Cond 036 Time Response for H2 Ctrl

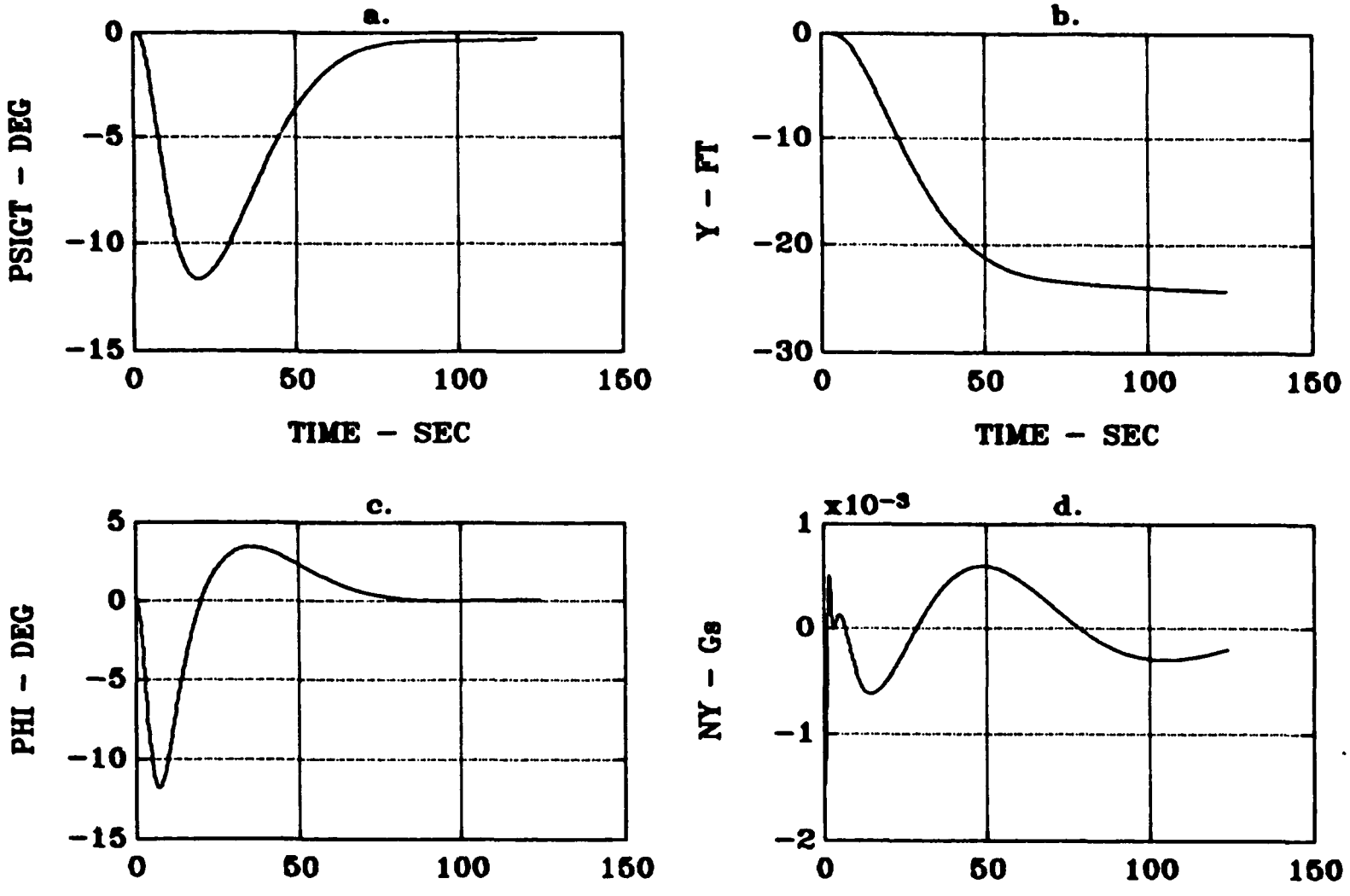

Fig. 6.4a.- d. Flt Cond 052 Time Response for H2 Ctrl

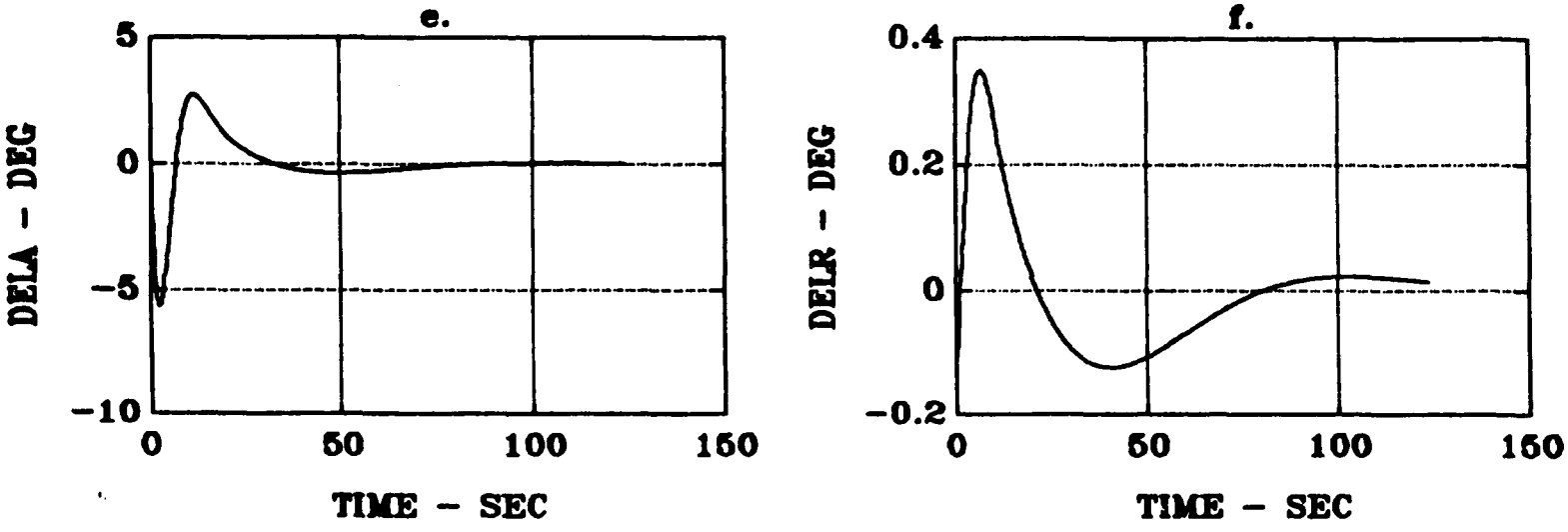

Fig. 6.4e.- f. Flt Cond 052 Time Response for H2 Ctrl

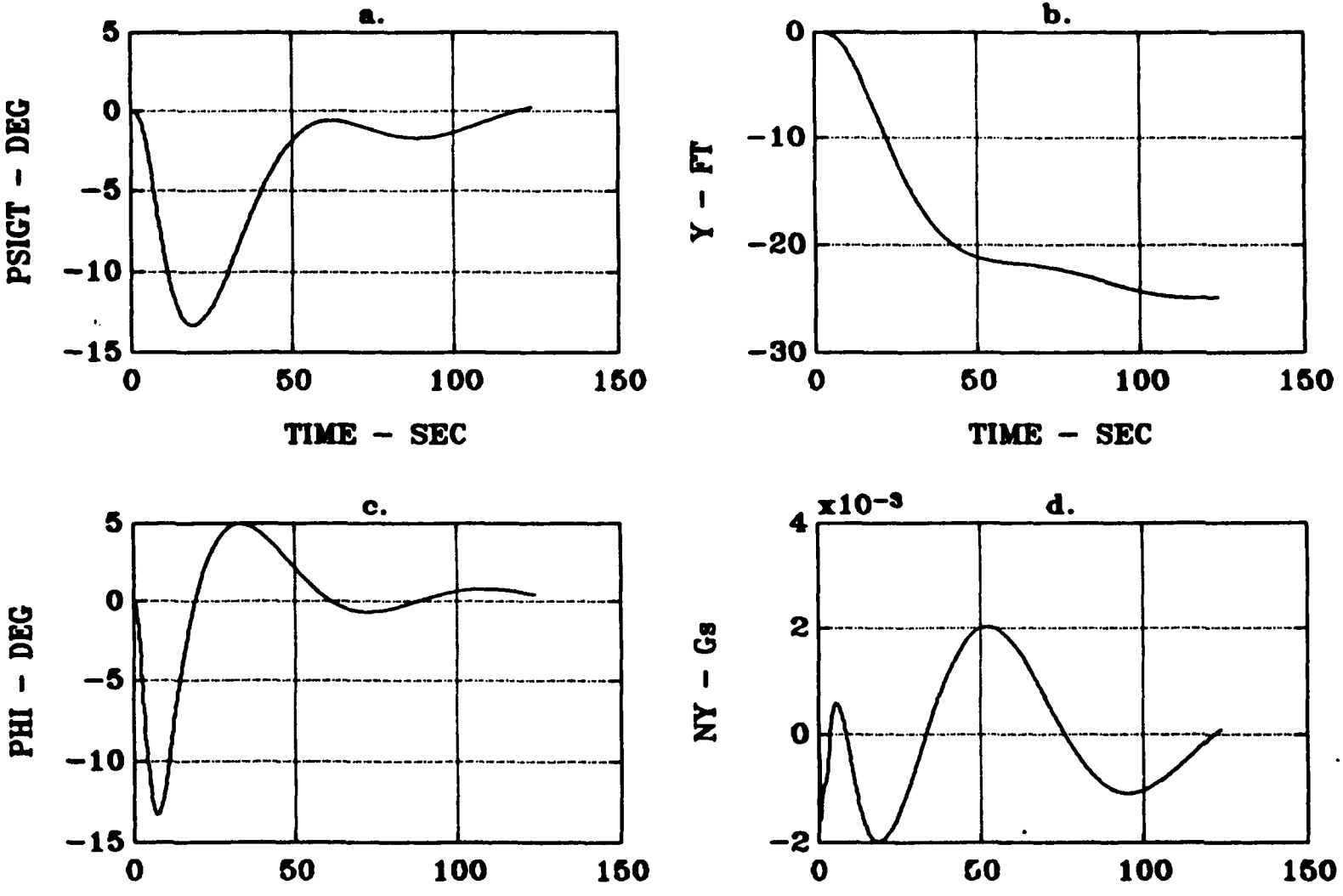

Fig. 6.5a.- d. Flt Cond 068 Time Response for H2 Ctrl

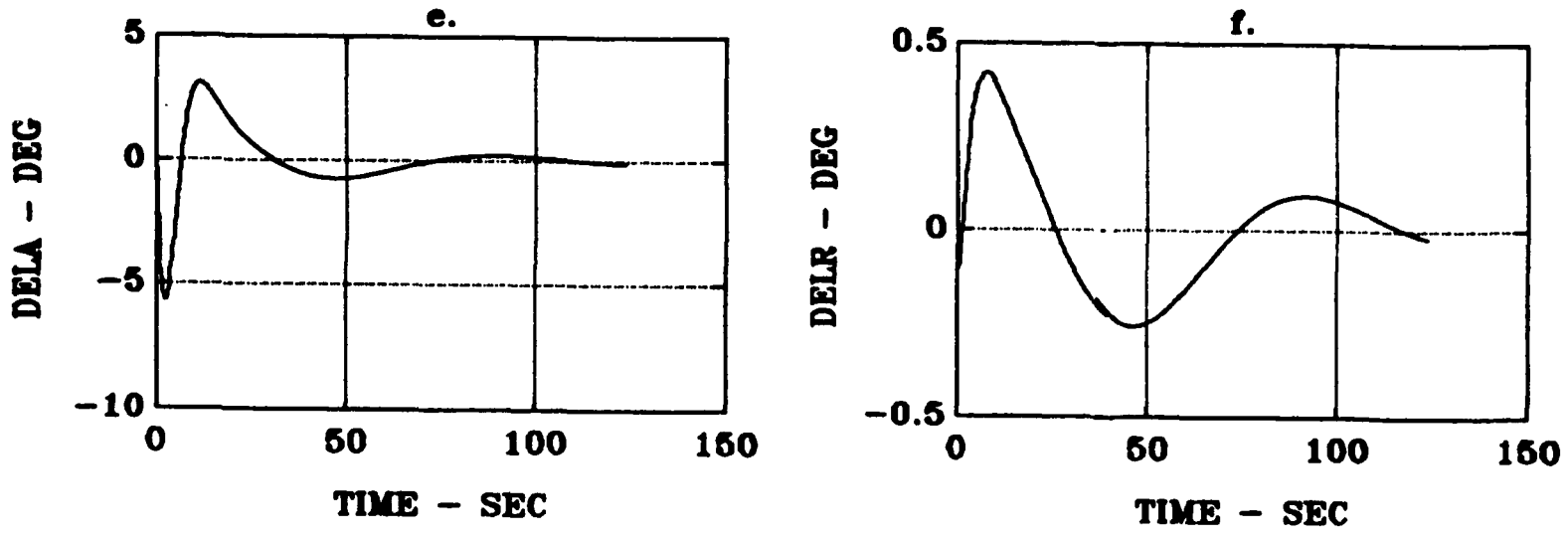

Fig. 6.5e.- f. Flt Cond 068 Time Response for H2 Ctrl

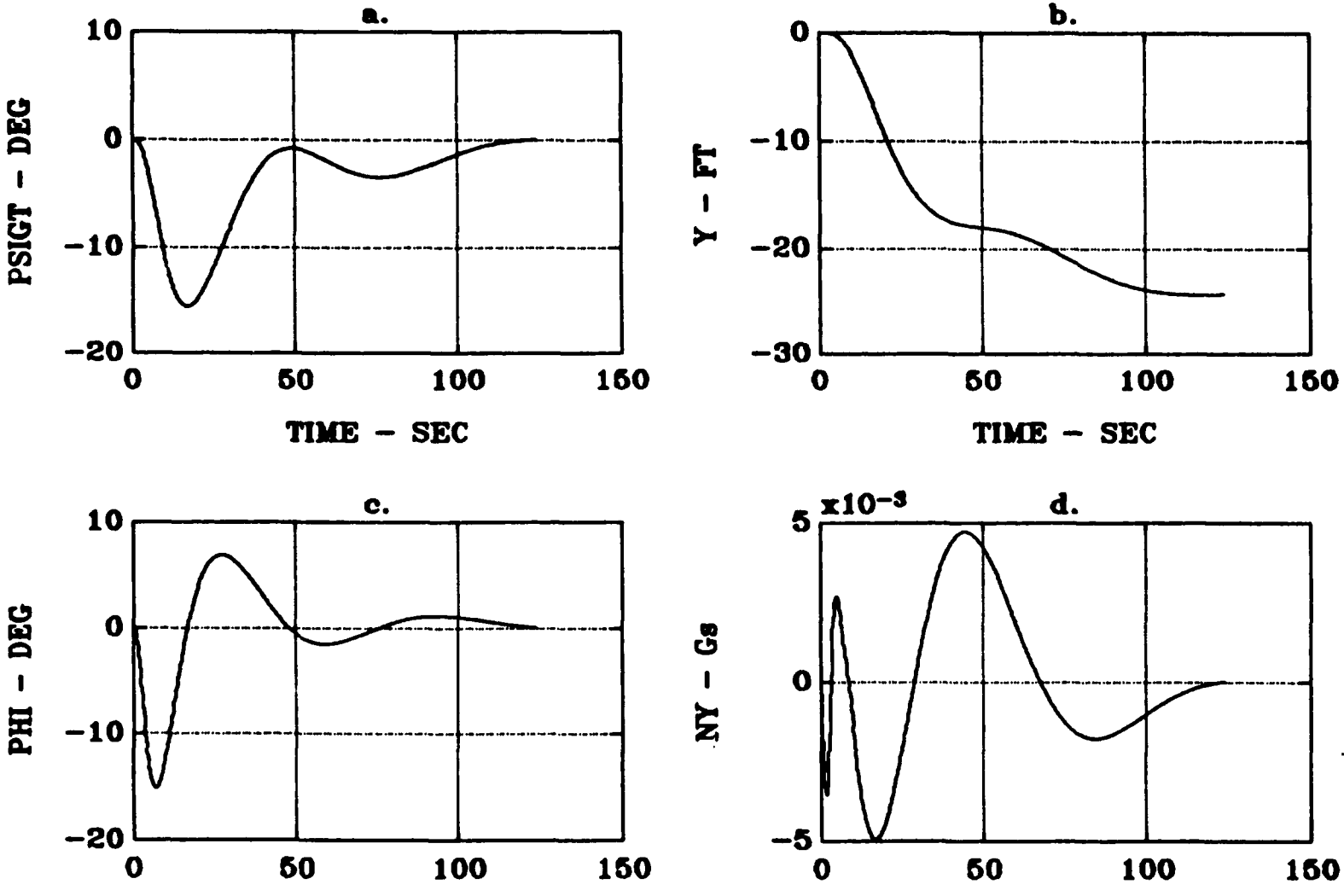

Fig. 6.6a.- d. Flt Cond 100 Time Response for H2 Ctrl

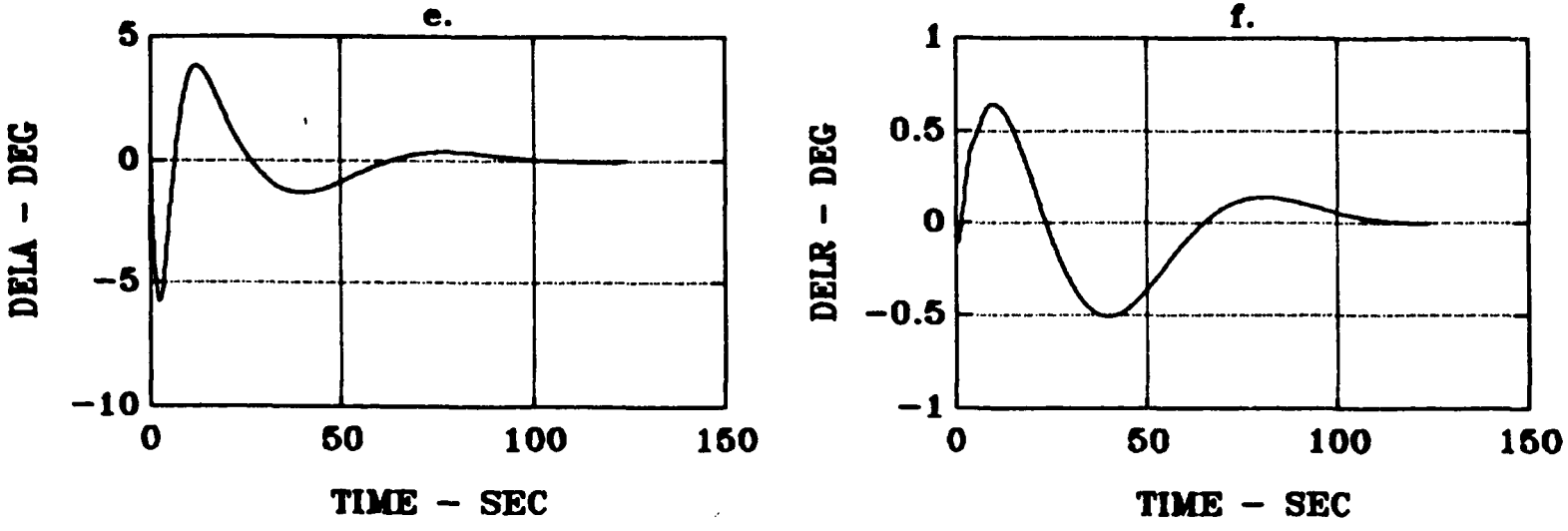

Fig. 6.6e.- f. Flt Cond 100 Time Response for H2 Ctrl

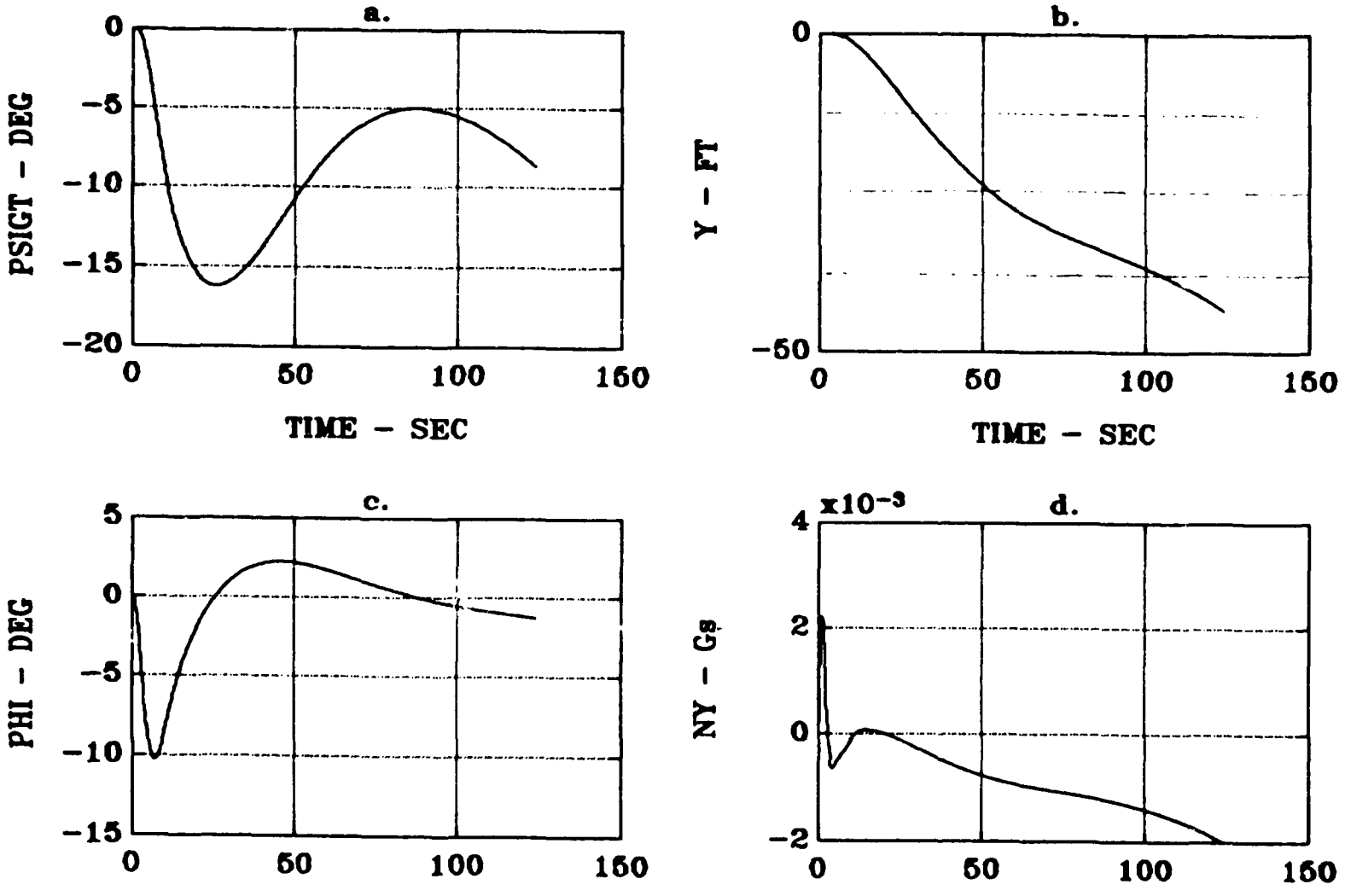

Fig. 6.7a.- d. Flt Cond 001 Time Response for H2 Ctrl

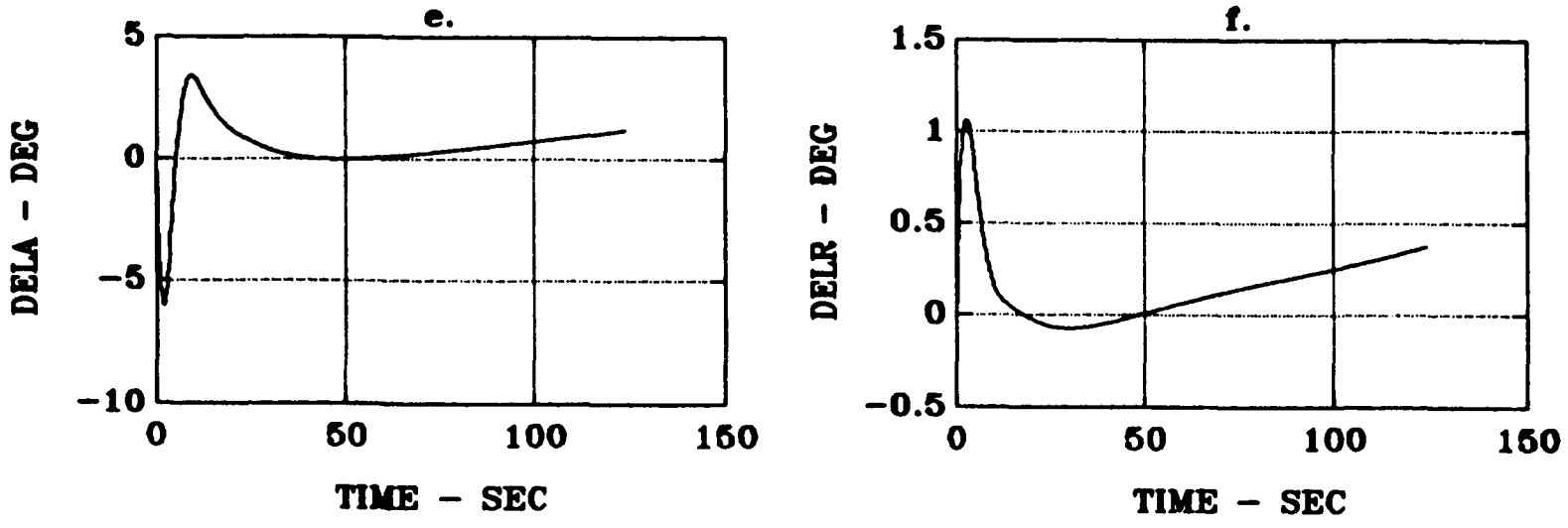

Fig. 6.7e.- f. Flt Cond 001 Time Response for H2 Ctrl

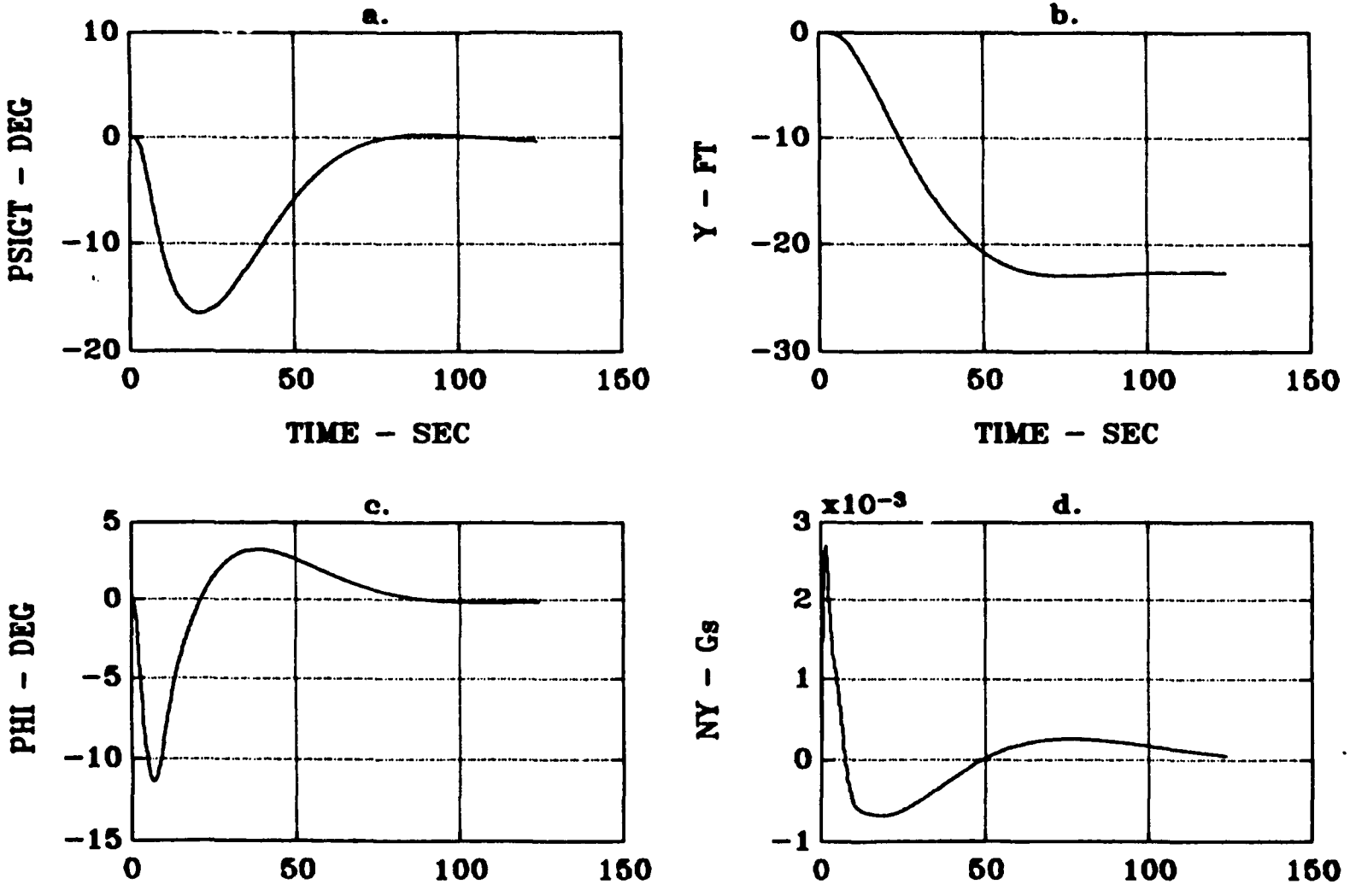

Fig. 6.8a.- d. Flt Cond 017 Time Response for H2 Ctrl

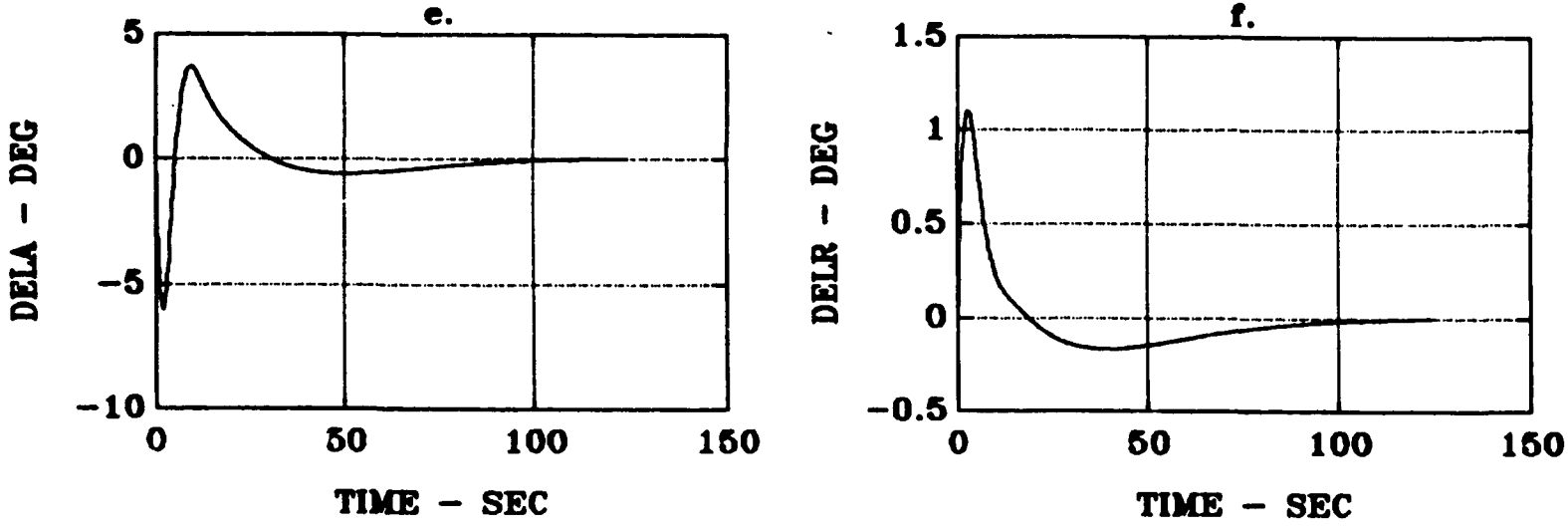

Fig. 6.8e.- f. Flt Cond 017 Time Response for H2 Ctrl

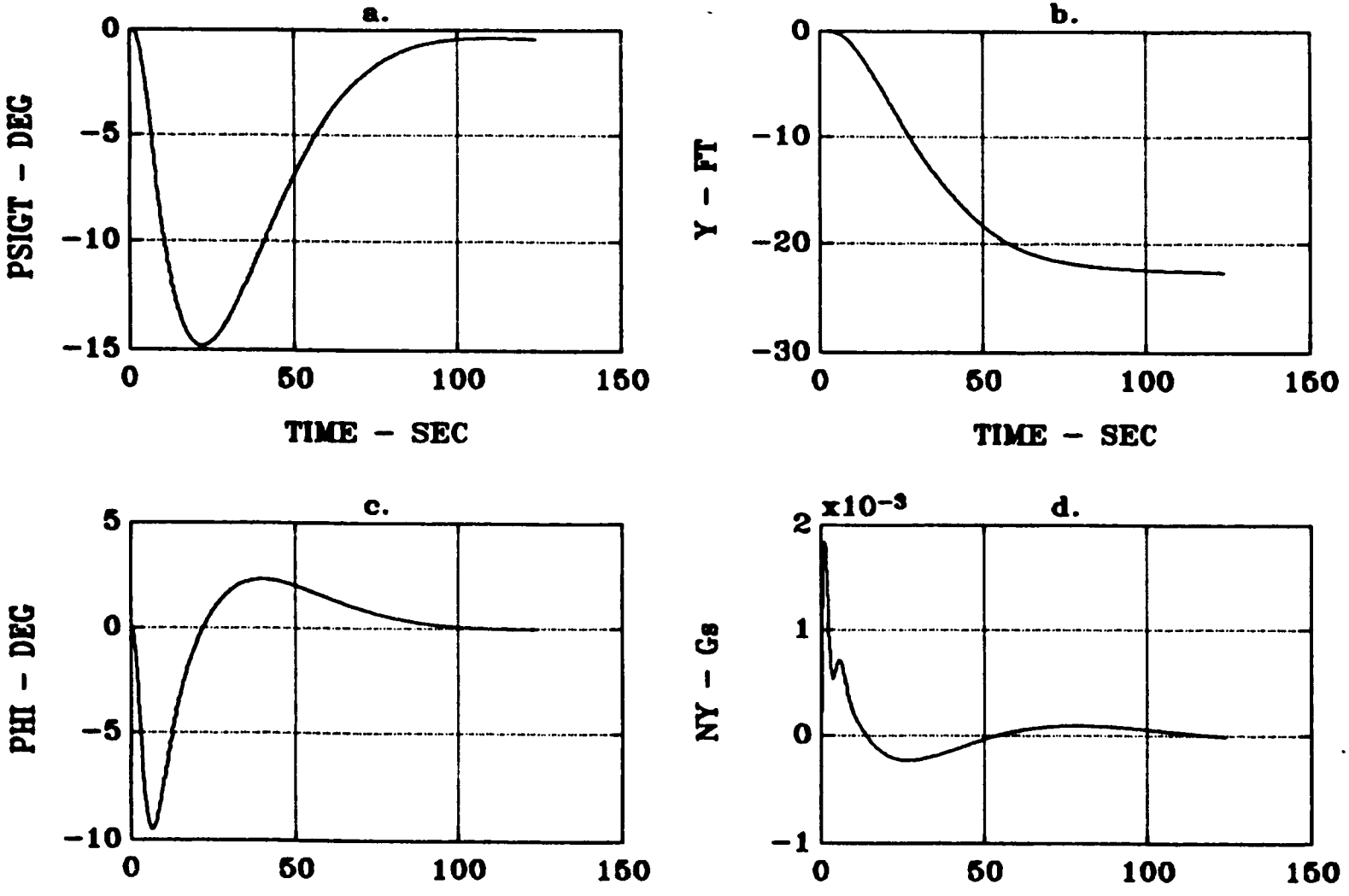

Fig. 6.9a.- d. Flt Cond 049 Time Response for H2 Ctrl

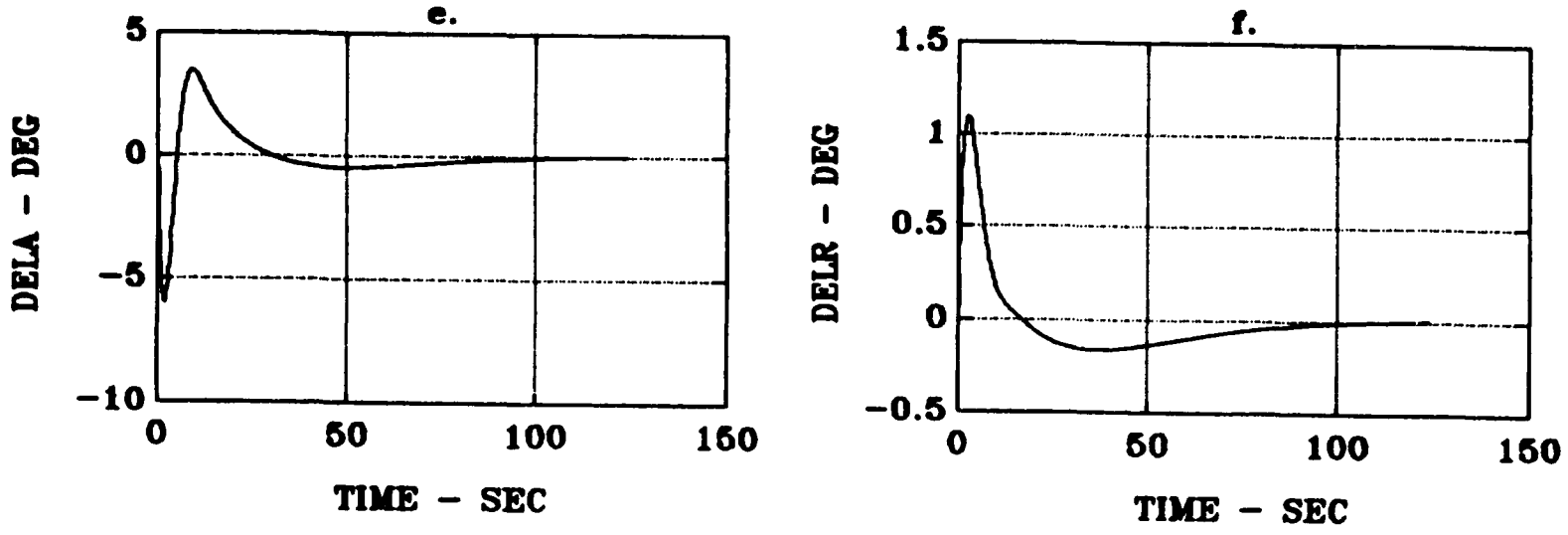

Fig. 6.9e.- f. Flt Cond 049 Time Response for H2 Ctrl

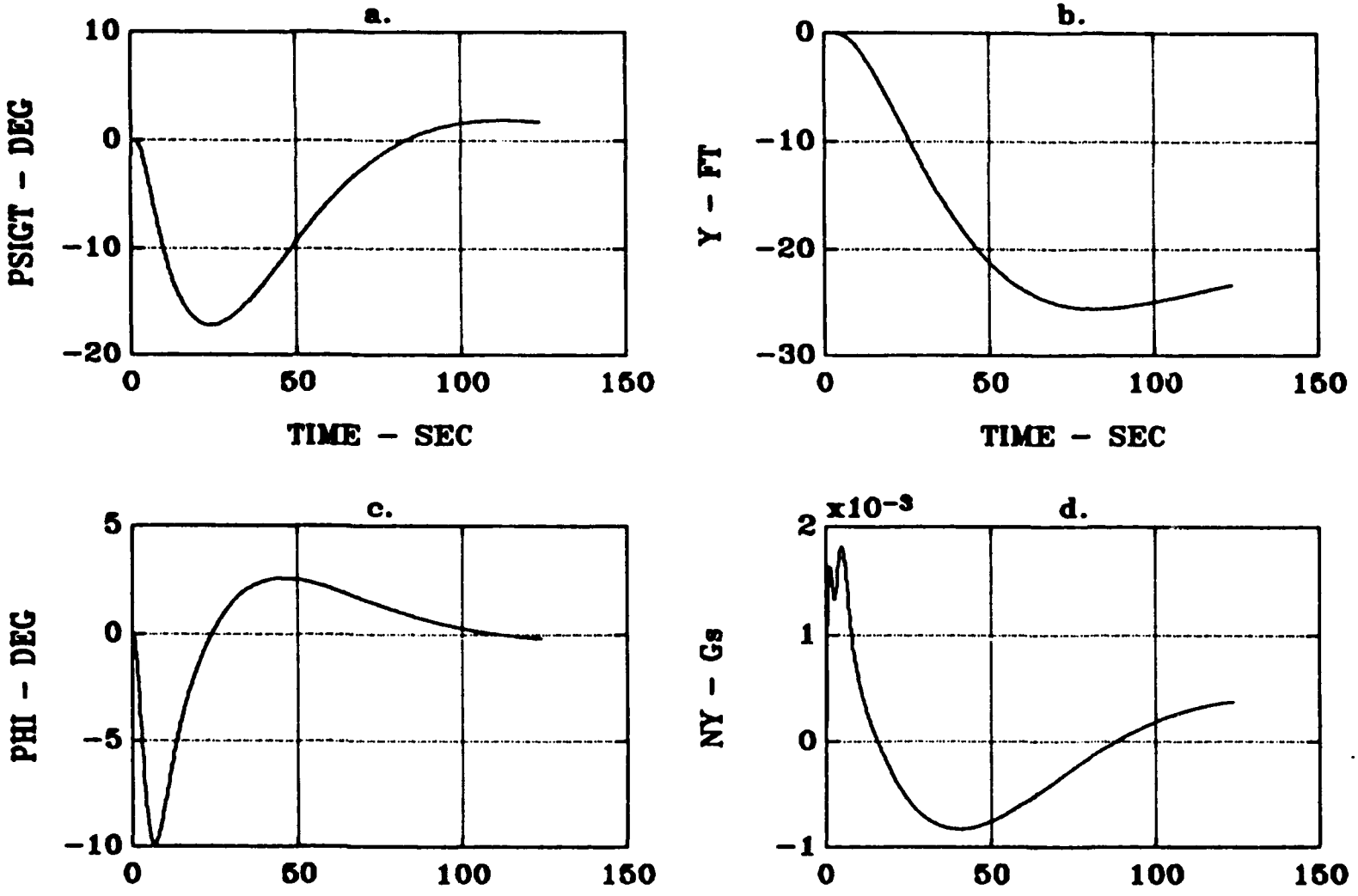

Fig. 6.10a.- d. Flt Cond 065 Time Response for H2 Ctrl

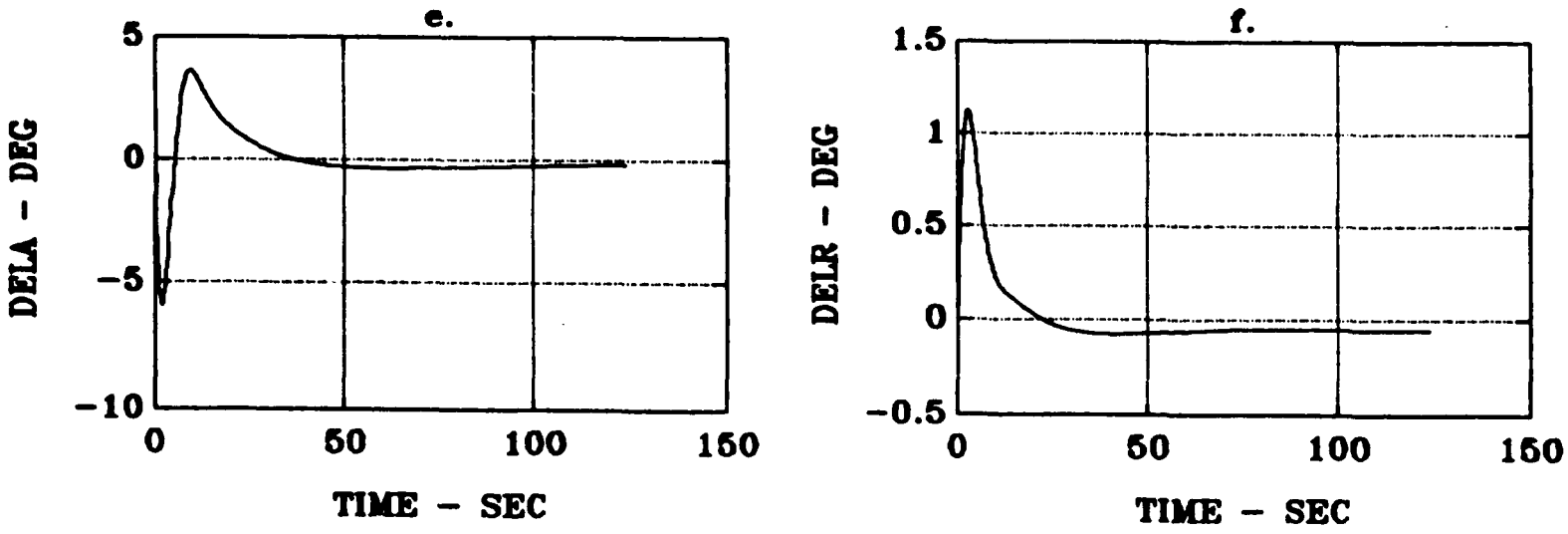

Fig. 6.10e.- f. Flt Cond 065 Time Response for H2 Ctrl

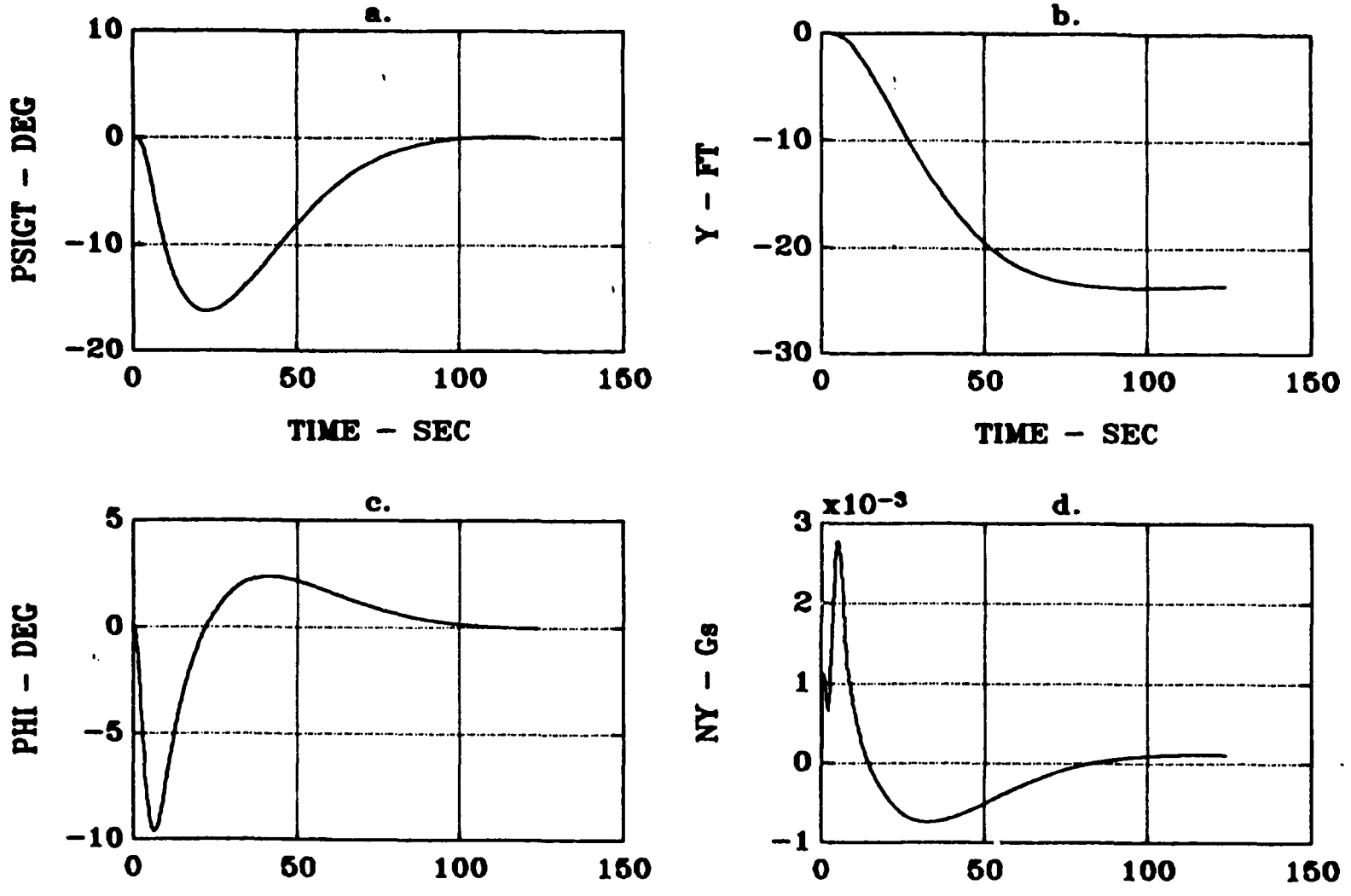

Fig. 6.11a.- d. Flt Cond 081 Time Response for H2 Ctrl

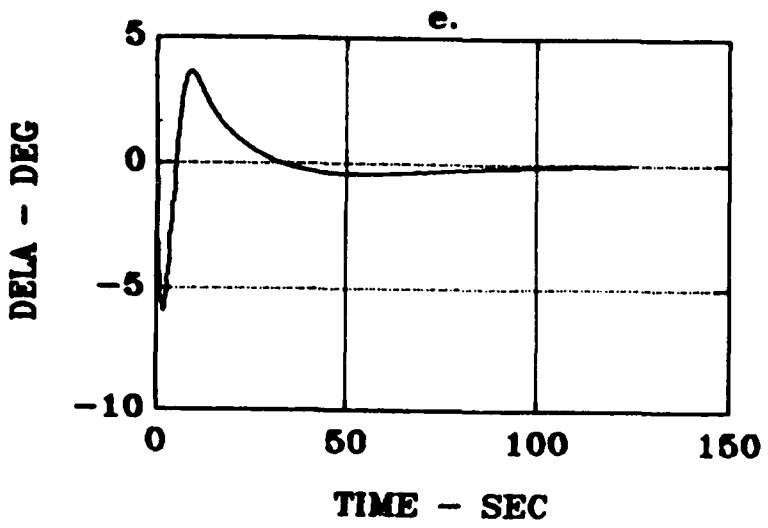

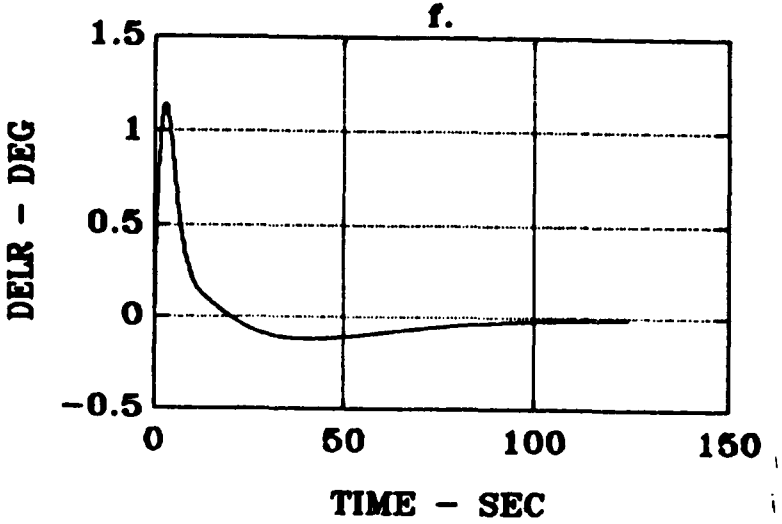

Fig. 6.11e.- f. Flt Cond 081 Time Response for H2 Ctrl

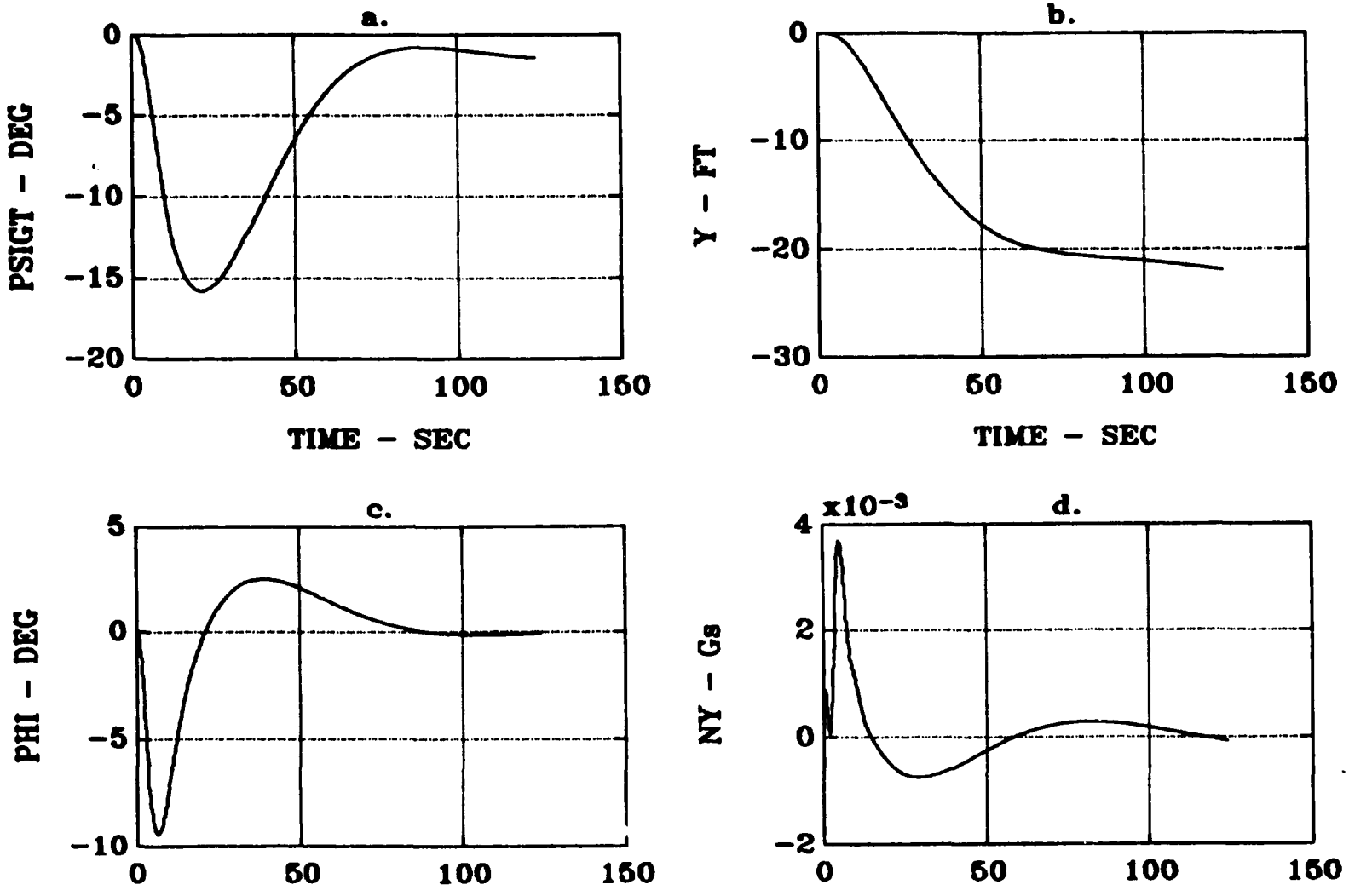

Fig. 6.12a.- d. Flt Cond 097 Time Response for H2 Ctrl

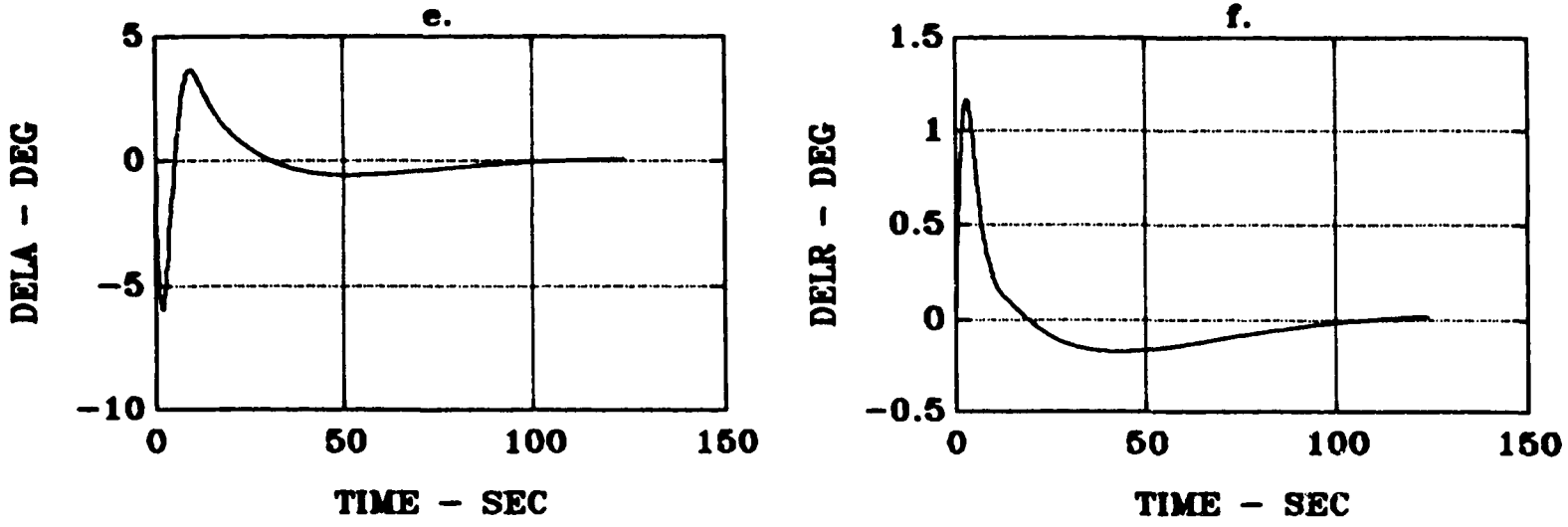

Fig. 6.12e.- f. Flt Cond 097 Time Response for H2 Ctrl

The fast approach flight conditions tracked reasonably well. Several of the cases had not achieved zero steady state tracking accuracies during the desired time interval. The slow approach cases took even longer in approaching the desired steady state values.

The control surface activity was well within the specifications. The angular positions and rates were within ±15 degrees and the ±30 deg/sec, respectively. The bank angle never exceeded about ±17 degrees. The lateral acceleration never exceeded 0.01 g's.

The H∞ results were not as favorable when the compensators designed for Flight Conditions 033 and 084 were used in the closed loop simulation for the other flight conditions. The results for the fast approach flight conditions yielded an unstable mode in all cases except for Flight condition 004. The results for the slow approach data had an unstable mode in all cases.

6.2 Discussion of Results

The performance for the controllers developed did not achieve the performance desired. Originally, the goal was to design one controller using H2 and H∞ control theory that would meet the performance, stability, and robustness requirements. It was found that the velocity dependence of the performance required the data to be grouped into two sets of data. It was hoped that controllers could then be developed that would yield acceptable results. The intent

was then to compare the results of the H2 and H∞ results.

The H2 and H∞ control theory did yield acceptable results for the nominal cases for which the compensators were designed. All specifications were met for the nominal fast and slow approach flight conditions.

The H2 compensators did yield better performance when used in the off nominal cases. This was expected since the loop gain for the H2 designs was higher therefore implying better performance. Adequate loop gains still could not be achieved for either compensator with H2 or H∞ control theory.

It was noted earlier that the controllability and observability matrices were poorly conditioned. The requirements for H2 and H∞ control theory are that the (A,B1) and the (A,C1) matrices be stabilizable and detectable for H2 and controllable and observable for H∞. The poor conditioning of these matrices obviously resulted in numerical problems, since these requirements were violated.

The effects were clearly noticeable when designing the H∞ controllers. The weights used for the H2 design did not work for the H∞ design. The value of gamma required in the gamma iteration yielded an H∞ controller that was very close to the H2 controller. This occurred because as gamma approaches a large number, the H∞ equations reduce to the H2 equations. There was also some noticable effects when the weights were changed. As the weights were changed, checking the controllability and observability matrices revealed that

the conditioning, while still very poor, was improving. The condition number was reduced by 10 orders of magnitude by adjusting the weights. As mentioned before, the results were that the value of gamma could be reduced and the spectral radius increased.

The poor conditioning of the plant may have been responsible for not being able to achieve good control response. An analysis of the plant conditioning revealed it was poor. In (1:586), it is stated that " the plant condition number provides a quantitative means for assessing the degree of difficulty in achieving good control." In addition, the comment is made that to obtain a good loop shape (high gain at low frequency), while ensuring robust stability, the plant must be well conditioned.

The selection of weights was very difficult. The process was highly iterative. The process of selecting weights, checking the singular value plots, and looking at the time response plots was very time consuming. The weights selected affected the response dramatically. Even with all this ability to shape the response, the final selection of weights did not yield the desired performance.

VII. Conclusions and Recommendations

7.1 Summary and Conclusions

The objective of this thesis was to design a lateral autopilot for a transport aircraft using H2 and H∞ control theory. The autopilot was to be robust with respect to variations in flight conditions.

After background information was covered in Chapter 1, the H2 and H∞ control theory was covered. Important aspects of multivariable control theory were also discussed. The standard problem formulation was identified.

In Chapter 3 the problem was stated. The data provided included the state space representations of fourteen flight conditions in addition to specifications on performance, robustness, and control activity.

This data was then taken and formulated into the standard problem or the small gain problem. Once in this form, an iterative method of design techniques was used in developing a controllers using H2 and H∞ theory.

In Chapter 5, the controller development was covered and the performance for the nominal cases was given. Then in Chapter 6, the controllers developed for the nominal cases were used in a closed loop simulation and evaluated over fourteen flight conditions.

The controllers developed using the H2 control theory provided the best performance and stability robustness for

the flight conditions tested. While these controllers provided some measure of stability and performance robustness, they still did not achieve the desired results. The ill conditioning of the plant may have limited the achievable results.

The H∞ controllers did not stabilize the off nominal conditions. The (A,B1) and (A,C1) matrices being uncontrollable and unobservable numerically is the apparent reason for the poor performance of the H∞ controllers. This led to numerical problems as evidenced by the destabilizing controllers. The optimal H∞ solution could not be approached. The minimum value of gamma that could be used was well above the optimum value.

The controllers obtained using H∞ control theory were different from the H2 controllers, but they were not optimum. Due to the numerical errors in the calculations, it is unclear exactly how to characterize them.

The weight selection provided a large amount of flexibility in shaping the system response, but the desired system response and robustness were not achieved. An extensive iterative process of weight selection was accomplished. The results given were the best obtained. It is thought that, because of the extensive search, the required performance may not be achievable from weight selection alone for this problem setup.

7.2 Recommendations

The problem synthesis and weight selection consumed the majority of the effort. The process of setting up the problem is very undefined but is also very important. This problem as given had a poorly conditioned plant. The outputs chosen resulted in very low loop gains for the open loop system. A different set of outputs can yield a plant that is better conditioned. A look at using state feedback showed a considerable improvement in the open loop system. This approach was not used since β could not be measured.

If the plant conditioning can be eliminated as a concern, the numerical problems encountered while using H∞ control theory may disappear or improve. If the numerical difficulty associated with H∞ control theory is still present, it would be beneficial to quantify what the numerical limits on the conditioning of the controllability and observability matrices are that defines when a system is uncontrollable and unobservable numerically.

This leaves the area of weight selection. The selection of a weighting strategy is very important. This is closely tied in with the problem setup. The problem as setup had weighting filters on the inputs and error signals. As mentioned previously, the weights also contributed to the numerical problems. In trying to achieve the desired loop shapes, the weight selection caused the conditioning of the

controllability and observability matrices of (A,B1) and (A,C1) to be poor, respectively.

The process of weight selection is highly iterative and time consuming. A more structured way of choosing weights is needed.

Appendix A: Lateral State Space Data

The following data is the state space models for the fourteen flight conditions for the Boeing 737 aircraft. The data is presented as it was given. The states are

$$x = [\ \beta \quad p \quad \phi \quad r \quad \psi \quad y\ ]^T$$

The outputs are

$$y = [\ \dot{\beta} \quad n_y \quad \dot{r} \quad \psi_{gt}\ ]$$

The inputs to the system are

$$u = [\ \delta_a \quad \delta_r \quad \beta_g\ ]$$

The flight conditions are 001, 004, 017, 020, 033, 036, 049, 052, 065, 068, 081, 084, 097, and 100. The A,B C, and D matrices are listed by letter and flight condition number.

A001	-0.1481	0.1984	0.1355	-0.9699	0	0
	-5.3738	-2.0194	-0.0025	0.6359	0	0
	0	1.0000	0	0.1990	0	0
	0.7480	-0.1671	-0.0023	-0.1937	0	0
	0	0	0	1.0196	-0.0001	0
	4.0649	0	-0.7932	0	4.0649	-0.0002
B001	0.0019	0.0474	0.1481			
	0.8651	0.9043	5.3738			
	0	0	0			
	0.0531	-0.7397	-0.7480			
	0	0	0			
	0	0	0			
C001	-0.1481	0.1984	0.1355	-0.9699	0	0
	-0.0187	0.0004	0	0.0014	0	0
	0.7480	-0.1671	-0.0023	-0.1937	0	0
	1.0000	0	-0.1951	0	1.0000	0
D001	0.0019	0.0474	0.1481			
	0.0002	0.0060	0.0187			
	0.0531	-0.7397	-0.7480			
	0	0	0			
A004	-0.2130	0.0645	0.0906	-0.9866	0	0
	-10.5010	-3.0712	-0.0086	0.6389	0	0
	0	1.0000	0	0.0654	0	0
	2.0574	-0.1849	-0.0031	-0.2825	0	0
	0	0	0	1.0021	-0.0001	0
	6.1857	0	-0.4035	0	6.1857	-0.0002
B004	0.0035	0.0686	0.2130			
	2.3464	2.2789	10.5010			
	0	0	0			
	0.1241	-1.6316	-2.0574			
	0	0	0			
	0	0	0			
C004	-0.2130	0.0645	0.0906	-0.9866	0	0
	-0.0410	-0.0001	0	0.0022	0	0
	2.0574	-0.1849	-0.0031	-0.2825	0	0
	1.0000	0	-0.0652	0	1.0000	0
D004	0.0035	0.0686	0.2130			
	0.0007	0.0132	0.0410			
	0.1241	-1.6316	-2.0574			
	0	0	0			

A017	-0.1392	0.1894	0.1440	-0.9714	0	0
	-4.9704	-1.9664	-0.0020	0.7383	0	0
	0	1.0000	0	0.1907	0	0
	0.6439	-0.1689	-0.0026	-0.1771	0	0
	0	0	0	1.0180	-0.0001	0
	3.8291	0	-0.7171	0	3.8291	-0.0002
B017	0.0010	0.0448	0.1392			
	0.9928	0.8127	4.9704			
	0	0	0			
	0.0843	-0.6606	-0.6439			
	0	0	0			
	0	0	0			
C017	-0.1392	0.1894	0.1440	-0.9714	0	0
	-0.0166	0.0003	0	0.0013	0	0
	0.6439	-0.1689	-0.0026	-0.1771	0	0
	1.0000	0	-0.1873	0	1.0000	0
D017	0.0010	0.0448	0.1392			
	0.0001	0.0053	0.0166			
	0.0843	-0.6606	-0.6439			
	0	0	0			
A020	-0.2135	0.0398	0.0907	-0.9878	0	0
	-10.4604	-3.2899	-0.0088	0.7375	0	0
	0	1.0000	0	0.0423	0	0
	2.1236	-0.1767	-0.0042	-0.2651	0	0
	0	0	0	1.0009	-0.0001	0
	6.1857	0	-0.2615	0	6.1857	-0.0002
B020	0.0024	0.0686	0.2135			
	2.3831	2.3279	10.4604			
	0	0	0			
	0.1444	-1.6426	-2.1236			
	0	0	0			
	0	0	0			
C020	-0.2135	0.0398	0.0907	-0.9878	0	0
	-0.0410	-0.0005	0	0.0022	0	0
	2.1236	-0.1767	-0.0042	-0.2651	0	0
	1.0000	0	-0.0423	0	1.0000	0
D020	0.0024	0.0686	0.2135			
	0.0005	0.0132	0.0410			
	0.1444	-1.6426	-2.1236			
	0	0	0			

A033	-0.1342	0.1977	0.1497	-0.9707	0	0
	-4.6784	-2.1477	-0.0038	0.8306	0	0
	0	1.0000	0	0.1950	0	0
	0.5226	-0.1951	-0.0012	-0.1905	0	0
	0	0	0	1.0188	-0.0001	0
	3.6819	0	-0.7044	0	3.6819	-0.0002
B033	0.0005	0.0432	0.1342			
	0.9542	0.7603	4.6784			
	0	0	0			
	0.0855	-0.6293	-0.5226			
	0	0	0			
	0	0	0			
C033	-0.1342	0.1977	0.1497	-0.9707	0	0
	-0.0154	0.0007	0	0.0012	0	0
	0.5226	-0.1951	-0.0012	-0.1905	0	0
	1.0000	0	-0.1913	0	1.0000	0
D033	0.0005	0.0432	0.1342			
	0.0001	0.0049	0.0154			
	0.0855	-0.6293	-0.5226			
	0	0	0			
A036	-0.2137	0.0309	0.0907	-0.9891	0	0
	-9.4091	-3.7688	-0.0108	0.8289	0	0
	0	1.0000	0	0.0311	0	0
	2.1602	-0.1993	-0.0057	-0.2476	0	0
	0	0	0	1.0005	-0.0001	0
	6.1857	0	-0.1923	0	6.1857	-0.0002
B036	0.0019	0.0686	0.2137			
	2.3575	2.3503	9.4091			
	0	0	0			
	0.1523	-1.6656	-2.1602			
	0	0	0			
	0	0	0			
C036	-0.2137	0.0309	0.0907	-0.9891	0	0
	-0.0411	-0.0000	0	0.0020	0	0
	2.1602	-0.1993	-0.0057	-0.2476	0	0
	1.0000	0	-0.0311	0	1.0000	0
D036	0.0019	0.0686	0.2137			
	0.0004	0.0132	0.0411			
	0.1523	-1.6656	-2.1602			
	0	0	0			

A049	-0.1355	0.1866	0.1537	-0.9737	0	0
	-4.5050	-2.3097	-0.0039	0.7497	0	0
	0	1.0000	0	0.1826	0	0
	0.4975	-0.2190	-0.0008	-0.1918	0	0
	0	0	0	1.0165	-0.0001	0
	3.5935	0	-0.6455	0	3.5935	-0.0002
B049	0.0003	0.0422	0.1355			
	0.9720	0.7344	4.5050			
	0	0	0			
	0.0896	-0.6034	-0.4975			
	0	0	0			
	0	0	0			
C049	-0.1355	0.1866	0.1537	-0.9737	0	0
	-0.0151	0.0008	0	0.0011	0	0
	0.4975	-0.2190	-0.0008	-0.1918	0	0
	1.0000	0	-0.1796	0	1.0000	0
D049	0.0003	0.0422	0.1355			
	0.0000	0.0047	0.0151			
	0.0896	-0.6034	-0.4975			
	0	0	0			
A052	-0.2139	0.0232	0.0977	-0.9899	0	0
	-8.1563	-3.7618	-0.0110	0.7173	0	0
	0	1.0000	0	0.0225	0	0
	1.9229	-0.2004	-0.0051	-0.2365	0	0
	0	0	0	1.0003	-0.0001	0
	5.7438	0	-0.1292	0	5.7438	-0.0002
B052	0.0014	0.0648	0.2139			
	1.9950	2.0730	8.1563			
	0	0	0			
	0.1338	-1.4570	-1.9229			
	0	0	0			
	0	0	0			
C052	-0.2139	0.0232	0.0977	-0.9899	0	0
	-0.0382	0.0001	0	0.0018	0	0
	1.9229	-0.2004	-0.0051	-0.2365	0	0
	1.0000	0	-0.0225	0	1.0000	0
D052	0.0014	0.0648	0.2139			
	0.0002	0.0116	0.0382			
	0.1338	-1.4570	-1.9229			
	0	0	0			

A065	-0.1308	0.1779	0.1592	-0.9768	0	0
	-4.5147	-2.1408	-0.0023	0.9537	0	0
	0	1.0000	0	0.1723	0	0
	0.5158	-0.2069	-0.0011	-0.1594	0	0
	0	0	0	1.0147	-0.0001	0
	3.4757	0	-0.5902	0	3.4757	-0.0002
B065	0.0002	0.0409	0.1308			
	0.9389	0.6949	4.5147			
	0	0	0			
	0.0867	-0.5673	-0.5158			
	0	0	0			
	0	0	0			
C065	-0.1308	0.1779	0.1592	-0.9768	0	0
	-0.0141	0.0009	0	0.0009	0	0
	0.5158	-0.2069	-0.0011	-0.1594	0	0
	1.0000	0	-0.1698	0	1.0000	0
D065	0.0002	0.0409	0.1308			
	0.0000	0.0044	0.0141			
	0.0867	-0.5673	-0.5158			
	0	0	0			
A068	-0.2093	0.0008	0.1003	-0.9910	0	0
	-7.4918	-3.4403	-0.0052	0.9763	0	0
	0	1.0000	0	-0.0013	0	0
	2.0306	-0.1696	-0.0051	-0.2089	0	0
	0	0	0	1.0000	-0.0001	0
	5.5965	0	0.0072	0	5.5965	-0.0002
B068	0.0013	0.0633	0.2093			
	2.0111	2.0120	7.4918			
	0	0	0			
	0.1304	-1.3927	-2.0306			
	0	0	0			
	0	0	0			
C068	-0.2093	0.0008	0.1003	-0.9910	0	0
	-0.0364	0.0004	0	0.0016	0	0
	2.0306	-0.1696	-0.0051	-0.2089	0	0
	1.0000	0	0.0013	0	1.0000	0
D068	0.0013	0.0633	0.2093			
	0.0002	0.0110	0.0364			
	0.1304	-1.3927	-2.0306			
	0	0	0			

A081	-0.1441	0.1484	0.1627	-0.9830	0	0
	-4.6721	-2.1018	-0.0008	0.9807	0	0
	0	1.0000	0	0.1403	0	0
	0.4422	-0.2068	-0.0023	-0.1538	0	0
	0	0	0	1.0098	-0.0001	0
	3.4168	0	-0.4748	0	3.4168	-0.0002
B081	0.0002	0.0402	0.1441			
	0.9445	0.6894	4.6721			
	0	0	0			
	0.0876	-0.5491	-0.4422			
	0	0	0			
	0	0	0			
C081	-0.1441	0.1484	0.1627	-0.9830	0	0
	-0.0153	0.0010	0	0.0008	0	0
	0.4422	-0.2068	-0.0023	-0.1538	0	0
	1.0000	0	-0.1390	0	1.0000	0
D081	0.0002	0.0402	0.1441			
	0.0000	0.0043	0.0153			
	0.0876	-0.5491	-0.4422			
	0	0	0			
A084	-0.2350	-0.0337	0.1030	-0.9912	0	0
	-8.0207	-3.2912	-0.0054	0.9187	0	0
	0	1.0000	0	-0.0352	0	0
	1.8108	-0.1275	-0.0045	-0.2228	0	0
	0	0	0	1.0006	-0.0001	0
	5.4492	0	0.1917	0	5.4492	-0.0002
B084	0.0014	0.0618	0.2350			
	1.5471	1.9663	8.0207			
	0	0	0			
	0.1094	-1.3270	-1.8108			
	0	0	0			
	0	0	0			
C084	-0.2350	-0.0337	0.1030	-0.9912	0	0
	-0.0398	0.0002	0	0.0014	0	0
	1.8108	-0.1275	-0.0045	-0.2228	0	0
	1.0000	0	0.0352	0	1.0000	0
D084	0.0014	0.0618	0.2350			
	0.0002	0.0105	0.0398			
	0.1094	-1.3270	-1.8108			
	0	0	0			

A097	-0.1413	0.1216	0.1677	-0.9892	0	0
	-4.4734	-2.0836	-0.0005	1.0067	0	0
	0	1.0000	0	0.1109	0	0
	0.5101	-0.2114	-0.0042	-0.1307	0	0
	0	0	0	1.0061	-0.0001	0
	3.3284	0	-0.3669	0	3.3284	-0.0002
B097	-0.0001	0.0392	0.1413			
	0.9606	0.6702	4.4734			
	0	0	0			
	0.0904	-0.5217	-0.5101			
	0	0	0			
	0	0	0			
C097	-0.1413	0.1216	0.1677	-0.9892	0	0
	-0.0146	0.0012	0	0.0005	0	0
	0.5101	-0.2114	-0.0042	-0.1307	0	0
	1.0000	0	-0.1102	0	1.0000	0
D097	-0.0001	0.0392	0.1413			
	-0.0000	0.0041	0.0146			
	0.0904	-0.5217	-0.5101			
	0	0	0			
A100	-0.2165	-0.0394	0.1120	-0.9926	0	0
	-7.6192	-2.9495	-0.0052	0.9048	0	0
	0	1.0000	0	-0.0434	0	0
	1.5893	-0.1280	-0.0053	-0.1806	0	0
	0	0	0	1.0009	-0.0001	0
	5.0075	0	0.2169	0	5.0075	-0.0002
B100	0.0009	0.0573	0.2165			
	2.0303	1.6786	7.6192			
	0	0	0			
	0.1310	-1.1371	-1.5893			
	0	0	0			
	0	0	0			
C100	-0.2165	-0.0394	0.1120	-0.9926	0	0
	-0.0337	0.0006	0	0.0010	0	0
	1.5893	-0.1280	-0.0053	-0.1806	0	0
	1.0000	0	0.0433	0	1.0000	0
D100	0.0009	0.0573	0.2165			
	0.0001	0.0089	0.0337			
	0.1310	-1.1371	-1.5893			
	0	0	0			

Appendix B: MATLAB User Written Routines

```
% routine dow1
% builds a1,b1,c1,d1
% inputs: w1a4-w1a5,w1b4-w1b5,w1k4-w1k5
% outputs: a1,b1,c1,d1
%
% W1 on each channels 4,5 is of the form k*(s+b)/(s+a)
% W1 on 1-2 is unity
num4=w1k4*[1 w1a4];
num5=w1k5*[1 w1a5];
den4=[1 w1b4];
den5=[1 w1b5];
a1=zeros(2,2);
b1=zeros(2,4);
c1=zeros(4,2);
d1=zeros(4,4);
d1(1,1)=1;
d1(2,2)=1;
[a,b,c,d]=tf2ss(num4,den4);
a1(1,1)=a;
b1(1,3)=b;
c1(3,1)=c;
d1(3,3)=d;
clear a b c d;
[a,b,c,d]=tf2ss(num5,den5);
a1(2,2)=a;
b1(2,4)=b;
c1(4,2)=c;
d1(4,4)=d;
clear a b c d num4 num5 den4 den5
```

```
% forms weight We on outputs betadot,Ny,psigt, and y.

% inputs: wek1-wek5 wea1-wea5 web1-web5 vec1&vec3

% outputs: matrices ae be ce

% routine dowe
% We for betadot and ny is We = k*a/(s+b)
% We for psigt and y is We = k*(s+a)/(s+b)(s+c)
% weight on betadot
num=wek1*wea1;
den=[1 web1];
[a,b,c,d]=tf2ss(num,den);
ae(1,1)=a;
be(1,1)=b;
ce(1,1)=c;
clear num den a b c
% weight on Ny
num=wek2 * wea2;
den=[1 web2];
[a,b,c,d]=tf2ss(num,den);
ae(2,2)=a;
be(2,2)=b;
ce(2,2)=c;
clear num den a b c
% weight on psigt
num= wek4*[1 wea4];
den=[1 (web4+vec4) web4*vec4];
[a,b,c,d]=tf2ss(num,den);
ae(3:4,3:4)=a;
be(3:4,3)=b;
ce(3,3:4)=c;
clear num den a b c
% weight on y
num= wek5*[1 wea5];
den=[1 (web5+vec5) web5*vec5];
[a,b,c,d]=tf2ss(num,den);
ae(5:6,5:6)=a;
be(5:6,4)=b;
ce(4,5:6)=c;
clear num den a b c
```

```
% routine dowe
% forms weight We on outputs betadot,Ny,psigt, and y.
% inputs: wek1-wek5 wea1-wea5 web1-web5 wec1&wec3
% outputs: matrices ae be ce
% We for betadot and ny is We = k*a/(s+b)
% We for psigt and y is We = k*(s+a)/(s+b)(s+c)
% weight on betadot
num=wek1*wea1;
den=[1 web1];
[a,b,c,d]=tf2ss(num,den);
ae(1,1)=a;
be(1,1)=b;
ce(1,1)=c;
clear num den a b c
% weight on Ny
num=wek2 * wea2;
den=[1 web2];
[a,b,c,d]=tf2ss(num,den);
ae(2,2)=a;
be(2,2)=b;
ce(2,2)=c;
clear num den a b c
% weight on psigt
num= wek4*[1 wea4];
den=[1 (web4+wec4) web4*wec4];
[a,b,c,d]=tf2ss(num,den);
ae(3:4,3:4)=a;
be(3:4,3)=b;
ce(3,3:4)=c;
clear num den a b c
% weight on y
num= wek5*[1 wea5];
den=[1 (web5+wec5) web5*wec5];
[a,b,c,d]=tf2ss(num,den);
ae(5:6,5:6)=a;
be(5:6,4)=b;
ce(4,5:6)=c;
clear num den a b c
```

```
% routine doabcd
% builds A B1 B2 C1 C2 D11 D12 D21 D22 matrices
% nsa - # states in the plant
% ns1 - # states in W1
% nse - # states in WE
% nd1,nd2,nd3 - # exogenous inputs
% nu - # of control inputs to plant
% ne - # of controlled inputs
% nog - # of plant outputs
% rhoda,rhodr - penalties on control inputs
nsa=8;
ns1=2;
nse=6;
nd1=4;
nd2=1;
nd3=4;
nu=2;
ne1=4;
ne2=2;
nog=4;
rhodadr=[rhoda 0;0 rhodr];
% make A
A = [a084             zeros(nsa,ns1)  zeros(nsa,nse);
     zeros(ns1,nsa)   a1              zeros(ns1,nse);
    -be*c084          be*c1           ae            ];
% make B1
B1 = [zeros(nsa,nd1) bg084           zeros(nsa,nd3);
      b1             zeros(ns1,nd2)  zeros(ns1,nd3);
      be*d1         -be*dg084       -be*d3         ];
% make B2
B2 = [b084          ;
      zeros(ns1 nu) ;
      zeros(nse,nu)];
% make C1
C1 = [zeros(ne1,nsa)  zeros(ne1,ns1)  ce              ;
      zeros(ne2,nsa)  zeros(ne2,ns1)  zeros(ne2,nse)];
% make D11
D11 = [zeros(ne1,nd1) zeros(ne1,nd2) zeros(ne1,nd3);
       zeros(ne2,nd1) zeros(ne2,nd2) zeros(ne2,nd3)];
% make D12
D12 = [zeros(ne1,nu)  ;
       rhodadr*eye(2)];
% make C2
C2 = [-c084 c1 zeros(nog,nse)];
% make D21
D21 = [d1 -dg084 -d3];
% make D22
D22 = [zeros(nog,nu)];
```

```
% routine close
% closes loop with plant and compensator
% nd1,nd2,nd3 - inputs to closed loop system
% no - outputs of closed loop system
% nsc - # of states in the compensator
% a,b,c,d - closed loop system matrices
nd1=4;
nd2=1;
nd3=4;
no=4;
nsc=16;
% make a
a = [ a084          b084*ccp;
     -bcp*c084      acp     ];
% make b
b = [zeros(nsa,nd1)   bg084          zeros(nsa,nd3);
     bcp              -bcp*dg084     -bcp*d3        ];
% make c
c = [c084   zeros(no,nsc)];
% make d
d = [zeros(no,nd1)  dg084  d3];
```

```
% routine rh2084
% builds matrices for computation of H2 compensator
% calculates compensator, close loop, and runs simulation
% plots states and outputs of system
dowe;
dowl;
abcd084;
h2lqg;
close084;
cleanup
pack
[y,x]=lsim(a,b,c,d,u,t,x0);x=x(:,1:8);
plot(t,x(:,1));grid;ylabel('beta');xlabel('time - sec');pause
plot(t,x(:,2));grid;ylabel('p');xlabel('time - sec');pause
plot(t,x(:,3));grid;ylabel('phi');xlabel('time - sec');pause
plot(t,x(:,4));grid;ylabel('r');xlabel('time - sec');pause
plot(t,x(:,5));grid;ylabel('psi');xlabel('time - sec');pause
plot(t,x(:,6));grid;ylabel('y');xlabel('time - sec');pause
plot(t,x(:,7));grid;ylabel('dela');xlabel('time - sec');pause
plot(t,x(:,8));grid;ylabel('delr');xlabel('time - sec');pause
plot(t,y(:,1));grid;ylabel('beta dot');xlabel('time - sec');pause
plot(t,y(:,2));grid;ylabel('ny');xlabel('time - sec');pause
plot(t,y(:,3));grid;ylabel('psigt');xlabel('time - sec');pause
plot(t,y(:,4));grid;ylabel('y');xlabel('time - sec');pause
save xytemp x y a b c d acp bcp ccp dcp t
```

```
% routine pltw1p
% plots the bode plot of the input weight on psigt
num=w1k4*[1 w1a4];den=[1 w1b4];pltbode;grid;
ylabel('mag W1(PSIGT) - db')
xlabel('FREQ - rad/sec')


% routine pltbode
% plots the Bode plot of a transfer function
[mag,p]=bode(num,den,freq);mag=20*log10(mag);semilogx(freq,mag)
grid


% routine svplts
% plots the loop gain singular value plot, the sensitivity
% function singular value plot, and the complementary
% sensitivity singular value plot
[a,b,c,d]=series(acp,bcp,ccp,dcp,a084,b084,c084,d084);
svgk=sigma(a,b,c,d,1,w);
svgk=20*log10(svgk);
svgk=svgk(1:2,:);
svs=sigma(a,b,c,d,3,w);
svs=-20*log10(svs);
[a,b,c,d]=feedbk(a,b,c,d,2);
svcl=sigma(a,b,c,d,1,w);
svcl=20*log10(svcl);
svcl=svcl(1:2,:);
semilogx(w,svgk);grid;
title('Loop Gain SV');pause;
semilogx(w,svs);grid;
title('Sensitivity Func SV');pause;
semilogx(w,svcl);grid;
title('Closed Loop SV')
save svtemp w svgk svcl svs
```

Bibliography

1. "Controller Design Techniques for Localizer Capture and Track for a Transport Aircraft," Proceedings of the 1989 American Control Conference," 585-620. Pittsburg, PA, June, 1989.

2. Doyle, J. C., K. Glover, P. Khargonekar, and B. Francis. "State-Space Solution to Standard H2 and H∞ Control Problems," IEEE Transactions on Automatic Control, Vol. 34, No. 8, August, 1989.

3. Francis, B. A. "A Course in H∞ Control Theory," Lecture Notes in Control and Information Systems. Edited by M. Thoma and A. Wyner. Berlin: Springer-Verlag, 1987.

4. Ridgely, D. B. and Banda, S. Introduction to Robust Multivariable Control. AFWAL-TR-85-3102. February, 1986.

5. Ridgely, D. B., Class handout in H2/H∞ seminar, A Summary of the H2 and H∞ Equations, School of Engineering, Air Force Institute of Technology (AU), Wright Patterson AFB OH, May 89.

6. Roskam, Jan. Airplane Flight Dynamics and Automatic Controls. Kansas: Roskam Aviation and Engineering Corporation, 1982.

Vita

Captain Randy L. Robinson [redacted]. He graduated from Walker High School in Jasper in 1978. He attended the University of Alabama and received the degree of Bachelor of Science in Aerospace Engineering in May 1983. During his last year at Alabama, he entered the USAF through the College Senior Engineering Program (CSEP). Upon graduation, he received his commission in the USAF by attending Officer Training School. He was assigned to the Advanced Medium Range Air-to-Air Missile (AMRAAM) Program at Eglin AFB, Florida as a missile performance engineer from August 1983 through May 1988. While at Eglin, he received a Masters of Science in Systems Analysis from the University of West Florida. He entered the Air Force Institute of Technology School of Engineering in June 1988.

[redacted]

SECURITY CLASSIFICATION OF THIS PAGE

REPORT DOCUMENTATION PAGE

Form Approved
OMB No. 0704-0188

1a. REPORT SECURITY CLASSIFICATION UNCLASSIFIED	1b. RESTRICTIVE MARKINGS
2a. SECURITY CLASSIFICATION AUTHORITY	3. DISTRIBUTION/AVAILABILITY OF REPORT Approved for public release; distribution unlimited
2b. DECLASSIFICATION/DOWNGRADING SCHEDULE	
4. PERFORMING ORGANIZATION REPORT NUMBER(S) AFIT/GAE/ENY/89D-30	5. MONITORING ORGANIZATION REPORT NUMBER(S)
6a. NAME OF PERFORMING ORGANIZATION School of Engineering 6b. OFFICE SYMBOL (If applicable) AFIT/ENY	7a. NAME OF MONITORING ORGANIZATION
6c. ADDRESS (City, State, and ZIP Code) Air Force Institute of Technology Wright-Patterson AFB, Ohio 45433	7b. ADDRESS (City, State, and ZIP Code)
8a. NAME OF FUNDING/SPONSORING ORGANIZATION Flight Dynamics Lab 8b. OFFICE SYMBOL (If applicable) WRDC/FIGC	9. PROCUREMENT INSTRUMENT IDENTIFICATION NUMBER
8c. ADDRESS (City, State, and ZIP Code) Wright-Patterson AFB, Ohio 45433	10. SOURCE OF FUNDING NUMBERS PROGRAM ELEMENT NO. / PROJECT NO. / TASK NO / WORK UNIT ACCESSION NO.

11. TITLE (Include Security Classification)
Robustness Evaluation Of H2 and H∞ Control Theory as Applied to a Transport Aircraft

12. PERSONAL AUTHOR(S)
Randy L. Robinson, M.S., Capt, USAF

13a. TYPE OF REPORT	13b. TIME COVERED	14. DATE OF REPORT (Year, Month, Day)	15. PAGE COUNT
Thesis	FROM _____ TO _____	1990 March	118

16. SUPPLEMENTARY NOTATION

17. COSATI CODES			18. SUBJECT TERMS (Continue on reverse if necessary and identify by block number)
FIELD	GROUP	SUB-GROUP	Multivariable Control; Robust Control, H2 Control Theory H∞ Control Theory

19. ABSTRACT (Continue on reverse if necessary and identify by block number)

The purpose of this study was to evaluate the performance and stability robustness of a lateral autopilot designed for a transport aircraft using H2 and H∞ control theory. The intent was to design a controller that met performance and robustness specifications over a range of flight conditions. First, a control structure to be used in designing the autopilot was developed. Once this was accomplished, it was formulated into the small gain problem. Controllers were then developed using H2 and H∞ control theory. The final task involved evaluating the controllers developed in a closed loop simulation.

20. DISTRIBUTION/AVAILABILITY OF ABSTRACT	21. ABSTRACT SECURITY CLASSIFICATION
☒ UNCLASSIFIED/UNLIMITED ☐ SAME AS RPT. ☐ DTIC USERS	UNCLASSIFIED
22a. NAME OF RESPONSIBLE INDIVIDUAL Capt D. Brett Ridgely, Aero Instr.	22b. TELEPHONE (Include Area Code) (513) 255-9917 22c. OFFICE SYMBOL AFIT/ENY

DD Form 1473, JUN 86 *Previous editions are obsolete.* SECURITY CLASSIFICATION OF THIS PAGE

UNCLASSIFIED